ADVERTIMENT. La consulta d'aquesta tesi queda condicionada a l'acceptació de les següents condicions d'ús: La difusió d'aquesta tesi per mitjà del servei TDX (www.tesisenxarxa.net) ha estat autoritzada pels titulars dels drets de propietat intel·lectual únicament per a usos privats emmarcats en activitats d'investigació i docència. No s'autoritza la seva reproducció amb finalitats de lucre ni la seva difusió i posada a disposició des d'un lloc aliè al servei TDX. No s'autoritza la presentació del seu contingut en una finestra o marc aliè a TDX (framing). Aquesta reserva de drets afecta tant al resum de presentació de la tesi com als seus continguts. En la utilització o cita de parts de la tesi és obligat indicar el nom de la persona autora.

ADVERTENCIA. La consulta de esta tesis queda condicionada a la aceptación de las siguientes condiciones de uso: La difusión de esta tesis por medio del servicio TDR (www.tesisenred.net) ha sido autorizada por los titulares de los derechos de propiedad intelectual únicamente para usos privados enmarcados en actividades de investigación y docencia. No se autoriza su reproducción con finalidades de lucro ni su difusión y puesta a disposición desde un sitio ajeno al servicio TDR. No se autoriza la presentación de su contenido en una ventana o marco ajeno a TDR (framing). Esta reserva de derechos afecta tanto al resumen de presentación de la tesis como a sus contenidos. En la utilización o cita de partes de la tesis es obligado indicar el nombre de la persona autora.

WARNING. On having consulted this thesis you're accepting the following use conditions: Spreading this thesis by the TDX (www.tesisenxarxa.net) service has been authorized by the titular of the intellectual property rights only for private uses placed in investigation and teaching activities. Reproduction with lucrative aims is not authorized neither its spreading and availability from a site foreign to the TDX service. Introducing its content in a window or frame foreign to the TDX service is not authorized (framing). This rights affect to the presentation summary of the thesis as well as to its contents. In the using or citation of parts of the thesis it's obliged to indicate the name of the author

UNIVERSITAT POLITÈCNICA DE CATALUNYA (UPC)
Programa de Doctorat en Enginyeria Ambiental

INSTITUT DE DIAGNOSI AMBIENTAL I ESTUDIS DE L'AIGUA (IDAEA)
Consejo Superior de Investigaciones Científicas (CSIC)

CHARACTERIZATION OF HYDROLOGICAL PROCESSES IN A MEDITERRANEAN MOUNTAIN RESEARCH CATCHMENT BY COMBINING DISTRIBUTED HYDROLOGICAL MEASUREMENTS AND ENVIRONMENTAL TRACERS

Doctoral Thesis

Maria Roig Planasdemunt

To be elegible for the Doctor degree

Supervised by:

Dr. Jérôme Latron and Dra. Pilar Llorens Garcia

Tutor:

Dra. Lucila Candela Lledó

Barcelona, June 2016

This study has been conducted at the Surface Hydrology and Erosion group of the Institute of Environmental Assessment and Water Research (IDAEA)-Spanish National Research Council (CSIC)

Author
Maria Roig Planasdemunt
Supervised by
Jérôme Latron and Pilar Llorens Garcia

Design and edited by
Maria Roig Planasdemunt
Photography
Maria Roig Planasdemunt
Defended in
Universitat Politècnica de Catalunya. Barcelona
Printed by
Soluciones Tecnologicas Blackcolor, S.L.

A la meva gran família,
a les meves amigues,
i a tu, per llegir-me

“Quality is much better than quantity.
One home run is much better than two doubles.”

Steve Jobs

AGRAÏMENTS

Hi ha hagut molts factors que han condicionat aquesta tesi. Però el factor humà ha demostrat ésser l'essencial. Per això, a totes les persones que hi han contribuït, les anomeni o no, moltes gràcies!

En primer lloc m'agradaria donar les gràcies al meus directors de tesi, en Jérôme Latron i la Pilar Llorens. Gràcies per obrir-me les portes de la hidrologia. Gràcies als vostres consells i correccions, hem dut a terme una tesi de qualitat, de la qual n'estic molt orgullosa.

Vull continuar agraint a en Francesc Gallart la seva fascinació contagiosa pel coneixement.

Durant la tesi han estat diversos els companys que han anat passant pel grup d'Hidrologia Superficial i Erosió - la Nuria, en Pablo, en Mariano, en Carles, en Xavi, l'Antonio, i l'Elisenda- a tots vosaltres, gràcies pels ànims i l'ajuda. A en Pablo i la Nuria els vull agrair especialment la seva gran qualitat humana. Tots han estat bons companys i m'han recolzat, tant en la proximitat com en la distància, tant al camp com al despatx, han contribuït a que jo "fes ciència". Hi ha hagut tantes anècdotes i aventures compartides que han fet molt amena aquesta tesi!

Vull recordar les passes pel laboratori: els catàlegs de compres, el renta-ampolles manual, les volumetries, etc. Allí vaig aprendre que una bona mesura requereix d'una bona calibració; gràcies, Alejandro Blanco. També, i d'una manera molt especial, voldria agrair a la Mercè Cabanes i en Rafael Bartrolí la seva professionalitat al laboratori i el seu sentit de l'humor. Malgrat que, he de confessar, que he pogut utilitzar pocs traçadors ambientals. Així és la ciència, mai sabràs què et farà servei. Vull agrair a la Mireia Oromí la seva professionalitat amb el Picarro L2120-i i les respostes ràpides a les meves consultes. No em vull oblidar del meu regal, que es diu Cristina; sense la seva ajuda amb les volumetries jo encara estaria al laboratori.

Gràcies també als centres de recerca de Luxemburg i Nova Zelanda per haver facilitat les meves estades, sense elles, la tesi no seria el que és. Mes chers collègues du List (Luxembourg), je vous remercie de m'avoir accueillie au Luxembourg, cela m'a permis de découvrir de nouvelles techniques que mi sont utiles dans le cadre de mes recherches. Gràcies especialment a la Núria Martínez. La teva paciència i el "canya-canya" van fer que tornés a casa encara més fascinada per la hidrologia. And I won't forget the colleagues of GNS Science (New Zealand): thank you for sharing with me your knowledge about water age modelling and showing me the "kiwi life".

I would like to express my especial gratitude and thanks to the external reviewers, Dr. Laurent Pfister and Dr. Mike Stewart, for sharing their knowledge and expertise in this study.

També vull agrair a totes les persones del grup de recerca d'Hidrologia Subterrània del CSIC-UPC la seva companyia durant l'eterna recta final de la tesi. Pels dinars de carmanyola i les bromes al passadís.

Vull agrair l'ajuda del personal tècnic i administratiu del CSIC i la Universitat Politècnica de Catalunya a l'hora de resoldre els documents "burrocràtics".

A les amigues i amics de tota la vida, les de la carrera, els de les estades a l'estranger i d'altres que ja fa anys que escolten les meves "batalletes" pel CSIC, que llegeixen "abstracts" i *gaudeixen* dels assajos per els congressos. Per acabar, vull agrair el suport incondicional de la meva gran família, a la que em sento tan orgullosa de pertànyer. Els "breaks" dels dimecres a casa els cosins. Les sobretaules amb els oncles, tietes i cosins. Els debats amb els germans i el saber que sempre hi són. A la gran matriarca de la família, ella és el meu referent d'esforç, energia i tossuderia. I sobretot als meus pares, per lo molt m'estimen, em valoren i em donen. Gràcies per recordar-me que primer sóc jo i després la feina.

He tingut el suport econòmic d'una beca FPI del Ministerio de Economía y Competitividad (MINECO) (BES-2011-045862), dues ajudes per estades breus del MINECO i finalment la prestació per desocupació. La meva recerca ha estat finançada per dos projectes de recerca de MINECO: 'RespHiMed. Aproximaciones combinadas para el estudio de la estacionalidad de la respuesta hidrológica en un ambiente mediterráneo en un contexto de cambio global' (CGL2010-18374) i el 'EcoHyMed. Ecohidrología de cuencas mediterráneas de cabecera. Conexiones entre vegetación y respuesta hidrológica en un contexto de cambio global' (CGL2013-43418). Les conques d'investigació de Vallcebre treballen amb el suport de la xarxa RESEL en acord entre el CSIC i DGCONA.

ABSTRACT

The main objective of this thesis is to characterize hydrological processes in a Mediterranean mountain catchment, by combining distributed hydrological measurements and environmental tracers in order to improve the understanding of catchment hydrological function.

During the period 2009-2013 hydrological data were collected from the Vallcebre Research Catchments, monitored since 1996 by the Surface Hydrology and Erosion group of the IDAEA-CSIC. Data include, in addition to rainfall and discharge measurements, distributed hydrological measurements and environmental tracers (both geochemical and isotope ones) at different time scales (seasonal to event scale).

With this information, this study first investigates the spatial and temporal variability of the depth to water table during rainfall-runoff events. The results show that the depth to water table did not rise uniformly throughout the catchment during rainfall-runoff events. The spatial variability of depth to water table was mainly controlled by location characteristics, especially the piezometer distance from the stream, which influenced the distribution of wetness conditions within the catchment. The wetness conditions in turn affected the timing of the water table response, as well as the magnitude of the streamflow response. Spatio-temporal water table variability during floods varied, depending on the catchment's antecedent wetness conditions. Under dry conditions, higher spatio-temporal variability of the depth to water table and slower groundwater response were observed during the entire event. In dry conditions, runoff was generated essentially by groundwater contribution in near-stream locations. In contrast, during intermediate conditions and especially during wet conditions, the spatio-temporal variability of the depth to water table throughout the flood event was lower and response times were shorter, generating a larger hydrological response.

Dissolved organic carbon (DOC) concentration dynamics in different hydrological compartments were also analysed (rainfall, soil water, groundwater and stream water) at different time scales (seasonal to event scale). The results show some seasonality in rainwater and soil water DOC concentrations, while no clear seasonality was found in stream water and groundwater, where DOC dynamics were strongly related to discharge and water table variations. During storm events, DOC concentrations increased systematically in stream water. In addition, for storm events with several discharge peaks, the slope of the discharge/DOC concentration relationship was higher for the first peak. The increase in stream water DOC concentration during floods suggested a relevant contribution of soil water, as well as the existence of stream water DOC sources near or in the stream bed. The rather similar dynamics of stream water DOC concentration in all floods contrasted with the diversity of hydrological

processes observed. This raises the question of the origin of the rapid DOC increase found and the validity of the use of DOC as a tracer.

Finally, water mean transit time (MTT) was calculated in different hydrological compartments of the catchment, using stable isotopes (δ18O and δ2H) and tritium. The use of δ18O signal variations in rainfall and in the sampled hydrological compartments showed some limitations on water age calculation in the catchment studied: it only indicated that MTT was greater than two years. The use of a new methodology (TEPMGLUE) to calculate MTT using tritium allowed consideration of different sources of uncertainty in water age determination, as well as evaluation of the benefit of using samples of different ages and of differing analytical quality. The results showed similar MTT calculations, whether including only the water samples taken in the 1990s or using all samples (1996-1998 and 2013). However, when calculating MTT with only high analytical quality samples taken in 2013, two different MTTs were obtained. The MTT results showed that, in the Vallcebre catchments, well water was the youngest, followed by stream and spring water. The study also showed the relevance of the rainfall tritium input function to MTT calculations. Finally, results showed that topography did not affect MTT spatial distribution, whereas geological settings did.

The results of this thesis provide additional information about how the hydrology of the Vallcebre Research Catchments functions. They also suggest some interesting future research lines.

RESUM

L'objectiu de la tesi doctoral és millorar la caracterització dels processos hidrològics de les conques mediterrànies de muntanya utilitzant mesures hidrològiques distribuïdes i traçadors ambientals, amb la finalitat de comprendre'n el funcionament hidrològic.

Durant el període 2009-2013 es van recollir dades hidrològiques de les conques d'investigació de Vallcebre, monitoritzades des de 1996 pel grup d'Hidrologia Superficial i Erosió del IDAEA-CSIC. Les dades inclouen, a més a més de registres de precipitacions i cabal, mesures hidrològiques distribuïdes i de dades de traçadors ambientals (geoquímics i isotòpics) a diferents escales temporals (estacional i d'esdeveniment).

A partir d'aquesta informació s'ha analitzat, en primer lloc, la dinàmica espaciotemporal del nivell freàtic durant els episodis de pluja. Els resultats mostren que, durant aquests episodis, el nivell freàtic no reacciona de manera homogènia a tota la conca. La variabilitat espaial del nivell freàtic està molt afectada per les característiques de la localització de cada piezòmetre, especialment la distància al torrent, que té un paper essencial en la distribució de les condicions d'humitat de la conca. Aquestes condicions d'humitat, a la vegada, afecten al temps de resposta del nivell freàtic i a la magnitud de la resposta hidrològica. Segons les condicions d'humitat de la conca, la variabilitat espaciotemporal del nivell freàtic durant esdeveniments és diferent. En condicions seques, la variabilitat espaciotemporal del nivell freàtic és alta al llarg de tot l'esdeveniment. L'escolament es genera principalment per la contribució de les àrees que estan a prop del torrent. En canvi, en condicions de transició i especialment en condicions d'humitat, la variabilitat espaciotemporal del nivell freàtic és menor i respon de forma més ràpida, i produeix una resposta hidrològica major a escala de conca.

Tot seguit, s'ha analitzat la dinàmica de la concentració de carboni orgànic dissolt (DOC) en diferents compartiments hidrològics (aigua de pluja, aigua del sòl, aigua subterrània i aigua del torrent) i a diferents escales temporals (estacional i d'esdeveniment). Els resultats mostren una variació estacional de la concentració de DOC a l'aigua de pluja i a la del sòl; però no s'aprecia aquesta estacionalitat a l'aigua subterrània i a la del torrent, a causa de que la concentració de DOC als dos compartiments està relacionada amb la dinàmica del nivell freàtic i la del cabal. A escala d'esdeveniment s'observa un augment sistemàtic de la concentració de DOC al torrent. A més a més, en els esdeveniments de diversos pics de cabal el pendent de la relació cabal/concentració de DOC sempre és major al primer pic. Aquest augment de la concentració de DOC al cabal durant els esdeveniments suggereix una contribució rellevant de l'aigua del sòl, però també l'existència de fonts de DOC pròximes al torrent o del mateix llit del torrent. D'altra banda, la relativa semblança de la dinàmica del DOC en el torrent durant esdeveniments

de diferent magnitud i amb processos hidrològics contrastats molt diferents, planteja la qüestió de l'origen de l'augment de DOC i el seu possible ús com a traçador.

Per últim, s'ha realitzat el càlcul del temps mitjà de trànsit (MTT) de l'aigua als diferents compartiments hidrològics de la conca utilitzant, primer, els isòtops estables ($\delta^{18}O$ i $\delta^{2}H$), i segon, el triti. L'ús de la variació del senyal isotòpic del $\delta^{18}O$ a l'aigua de pluja i a diferents compartiments d'aigua mostrejats presenta limitacions a la conca d'estudi; únicament permet demostrar que el MTT de les aigües és major de dos anys. L'ús d'una nova metodologia (TEPMGLUE) per calcular el MTT, utilitzant el triti, permet considerar diferents fonts d'incertesa i avaluar l'ús de mostres d'edats diferents i de diferent precisió analítica. Els resultats revelen que s'obtenen valors de MTT similars, tant utilitzant mostres dels anys noranta, com totes les mostres disponibles (1996-1998 i 2013). En canvi, quan únicament es calcula el MTT utilitzant les mostres del 2013 s'obtenen dos valors de MTT molt diferents. Els resultats de l'estudi també mostren que a les conques de Vallcebre l'aigua més jove és la dels pous, seguida de l'aigua del torrents i la de les fonts. L'estudi també demostra el paper rellevant de la funció d'entrada de triti amb la pluja per calcular el MTT. Per últim, els resultats suggereixen que la topografia no afecta la distribució espaial del MTT de la conca, però sí la geologia.

Tots els resultats d'aquesta tesi aporten informació addicional sobre el funcionament hidrològic de les conques de Vallcebre, i a més a més suggereixen noves línies d'investigació.

RESUMEN

El objetivo de esta tesis doctoral es mejorar la caracterización de los procesos hidrológicos de las cuencas Mediterráneas de montaña, utilizando mediciones hidrológicas distribuidas y trazadores ambientales, con la finalidad de comprender mejor su funcionamiento hidrológico.

Durante el período 2009-2013 se recogieron datos hidrológicos de las cuencas de investigación de Vallcebre, monitorizadas desde 1996 por el grupo de Hidrología Superficial y Erosión del IDAEA-CSIC. Los datos incluyen, además del registro de precipitaciones y caudales, mediciones hidrológicas distribuidas y datos de trazadores ambientales (geoquímicos e isotópicos) a diferentes escalas temporales (estacional y de crecida).

Con esta información, se ha analizado en primer lugar la dinámica espacio-temporal del nivel freático durante las crecidas. Los resultados muestran que durante las crecidas el nivel freático no reacciona de forma homogénea en toda la cuenca. La variabilidad espacial del nivel freático está muy afectada por las características de la localización de cada piezómetro, especialmente la distancia al cauce que tiene un papel esencial en la distribución de las condiciones de humedad de la cuenca. Estas condiciones de humedad, a su vez, afectan al tiempo de respuesta del nivel freático y a la magnitud de la respuesta hidrológica. Según las condiciones de humedad de la cuenca la variabilidad espacio-temporal del nivel freático durante la crecida es diferente. En condiciones secas la variabilidad espacio-temporal del nivel freático es alta a lo largo de toda la crecida. En estas condiciones, la escorrentía se genera principalmente por la contribución de las áreas próximas al cauce. En cambio, en condiciones de transición y especialmente en condiciones húmedas, la variabilidad espacio-temporal del nivel freático es menor y su respuesta es mas rápida, produciendo una mayor respuesta hidrológica en la cuenca.

Seguidamente, se ha analizado la dinámica de la concentración del carbono orgánico disuelto (DOC) en diferentes compartimentos (agua de lluvia, agua del suelo, agua subterránea y agua del cauce) a diferentes escalas temporales (estacional y de crecida). Los resultados indican una variación estacional de la concentración de DOC en el agua de lluvia y en la del suelo. Sin embargo, no se aprecia esta estacionalidad en el agua subterránea y en la del cauce, debido a que la concentración de DOC en estos compartimentos está relacionada con la dinámica del nivel freático y del caudal. Durante las crecidas se observa un aumento sistemático de la concentración de DOC en el cauce. Además en las crecidas con varios picos de caudal el pendiente de la relación caudal/concentración de DOC es siempre mayor en el primer pico. El aumento de la concentración de DOC en el cauce durante las crecidas sugiere una contribución relevante del agua del suelo, pero también la existencia de fuentes de DOC próximas al cauce o en el mismo lecho. La relativa similitud de la dinámica del DOC en el cauce durante eventos de

distinta magnitud y con procesos hidrológicos contrastados muy distintos, plantea la cuestión del origen del aumento de DOC y su posible utilización como trazador.

Por último, se ha realizado el cálculo del tiempo medio de transito (MTT) del agua, en diferentes compartimentos hidrológicos de la cuenca utilizando, primero, isótopos estables ($\delta^{18}O$ y $\delta^{2}H$), y después el tritio. El uso de la variación de la señal isotópica del $\delta^{18}O$ en el agua de lluvia y en los diferentes compartimentos de agua muestreados muestra sus limitaciones en la cuenca de estudio; solo permite demostrar que el MTT es mayor de dos años. El uso de una nueva metodología (TEPMGLUE) para calcular el MTT usando el tritio, permite considerar diferentes fuentes de incertidumbre y evaluar el uso de muestras de edades diferentes y con distinta precisión analítica. Los resultados revelan que se obtienen valores de MTT similares, tanto utilizando muestras de los años noventa, como todas las muestras disponibles (1996-1998 y 2013). Sin embargo, cuando se calcula el MTT utilizando solo muestras del 2013 se obtienen dos valores de MTT muy distintos. Los resultados de MTT muestran que en las cuencas de Vallcebre el agua es más jóven en los pozos, seguida del agua de los cauces y la de las fuentes. El estudio también demuestra el papel relevante de la función de entrada de tritio en la lluvia para el cálculo del MTT. Por último, los resultados sugieren que la topografía no afecta la distribución espacial del MTT en la cuenca, pero sí la geología.

Todos los resultados de esta tesis aportan información adicional sobre el funcionamiento hidrológico de las cuencas de Vallcebre, además sugieren nuevas líneas de investigación.

CONTENTS

AGRAÏMENTS I

ABSTRACT III

RESUM V

RESUMEN VII

CONTENTS IX

LIST OF FIGURES XIII

LIST OF TABLES XVII

CHAPTER 1

1 INTRODUCTION 1

1.1 Combining hydrometric data and environmental tracers 1

1.2 The hydrology of Mediterranean catchments 3

1.3 The Vallcebre Research Catchment 5

1.4 Objectives of the study 7

1.5 Thesis structure 8

CHAPTER 2

2 SPATIAL AND TEMPORAL VARIABILITY OF DEPTH TO WATER TABLE DURING RAINFALL-RUNOFF EVENTS 9

2.1 Introduction 9

2.2 Methods 11

2.2.1 Study site 11

2.2.2 Hydrometric monitoring 12

2.2.3 Characteristics of piezometer locations 13

2.2.4 Analysis of rainfall-runoff events 13

2.3 Results 14

2.3.1 Locations and water table response characteristics 14

2.3.2 Relationship between water table response and location characteristics 15

2.3.3 Water table response characteristics during rainfall-runoff events 18

2.3.4 Analysis of continuous water table dynamics during floods 21

2.4 Discussion 27

2.4.1 Influence of location characteristics on depth to water table spatial variability 27

2.4.2 Influence of location characteristics on water table response 28
2.4.3 Water table response during rainfall-runoff events 28
2.4.4 Influence of antecedent wetness conditions 29
2.5 Conclusions 31

CHAPTER 3

3 SEASONAL AND STORMFLOW DYNAMICS OF DISSOLVED ORGANIC CARBON 33

3.1 Introduction 33
3.2 Methods 35
3.2.1 Study site 35
3.2.2 Hydrometric monitoring 36
3.2.3 DOC water sampling and laboratory analyses 37
3.2.4 Data analyses 38
3.3 Results 39
3.3.1 DOC dynamics throughout the year 39
3.3.2 DOC dynamics in the stream during rainfall–runoff events 44
3.4 Discussion 48
3.4.1 Seasonal patterns of DOC 48
3.4.2 DOC dynamics in stream water during rainfall–runoff events 51
3.5 Conclusions 53

CHAPTER 4

4 MEAN TRANSIT TIME ESTIMATION USING STABLE ISOTOPES AND TRITIUM 55

4.1 Introduction 55
4.2 Methods 57
4.2.1 Study area 57
4.2.2 Location characteristics 58
4.2.3 Hydrological data 58
4.2.4 Water sampling 59
4.2.5 MTT estimation using oxygen 18 and deuterium 61
4.2.6 MTT estimation using tritium 62
4.3 Results 65
4.3.1 Temporal variation of ^{2}H and ^{18}O 65
4.3.2 Estimation of mean residence time using stable isotopes 67
4.3.3 Estimation of mean transit time using tritium 68

4.4 Discussion 78
4.4.1 Temporal variation of stable isotopes 78
4.4.2 Estimation of mean residence time using stable isotopes 78
4.4.3 Estimation of mean transit time using tritium 79
4.4.4 Choice of the input function and of the methodology 79
4.4.5 Water ages distribution in the Cal Rodó catchment 80
4.5 Conclusions 81

CHAPTER 5

5 GENERAL CONCLUSIONS 83

REFERENCES 87

LIST OF ACRONYMS 105

APPENDIX A. PHOTOGRAPHIC SUPPORTING INFORMATION 107

APPENDIX B. COMPLEMENTARY INFORMATION OF CHAPTER 2 111

APPENDIX C. COMPLEMENTARY INFORMATION OF CHAPTER 3 119

APPENDIX D. COMPLEMENTARY INFORMATION OF CHAPTER 4 125

LIST OF PUBLICATIONS 131

ABOUT THE AUTHOR 135

LIST OF FIGURES

Fig. 1.1 Map of the Cal Rodó catchment and of the Can Vila, Ca l'Isard and Santa Magdalena sub-catchments. Only the monitoring design used in the present study (July 2009 to July 2013) is shown. Land uses were digitized from a high-resolution orthophoto (ICC, 2012); and the stream network is taken from Latron (2003). 5

Fig. 1.2 Pictures of the types of landscapes found in the Vallcebre Research Catchments. Source: M.Roig-Planasdemunt 6

Fig. 2.1 Map of the Can Vila catchment, showing the monitoring design. 12

Fig. 2.2 Median and quartiles (25% and 75%) of (a) pre-event depth to water table, (b) water table increase, (c) response time, (d) time to peak, (e) time lag between water table peak and discharge peak at each piezometer location for the 19 observed rainfall-runoff events, (f) distance from the stream and (g) Topographic Wetness Index at each piezometer location. (Piezometers are ranked according to their WT_i value). 16

Fig. 2.3 Relationship between the median pre-event depth to water table at each piezometer location and (a) the distance from the stream, (b) the Topographic Wetness Index and (c) the elevation above the stream. Black dots are the median values and bars correspond to quartiles (25% and 75%). Significance:**p < 0.01; *p < 0.05; ns p > 0.05. 17

Fig. 2.4 Relationship between the median pre-event depth to water table at each piezometer location and (a) response time, (b) time to peak and (c) time lag between water table peak and discharge peak. Black dots are the median values and bars correspond to quartiles (25% and 75%). Significance:**p < 0.01; *p < 0.05; ns p > 0.05. 18

Fig. 2.5 Characteristics of the 19 rainfall-runoff events analysed. Pre-event discharge (Q_b) is shown on the x-axis; and rainfall on the y-axis. Dot size is proportional to the storm runoff coefficient (C_s) and the grey scale indicates rainfall intensity. Numbers refer to events analysed in Fig. 2.8. 19

Fig. 2.6 (a) Pre-event discharge (Q_b) and (b) storm runoff coefficient (C_s) of the 19 rainfall-runoff events analysed. Median and quartiles (25% and 75%) of (c) pre-event depth to water table, (d) water table increase, (e) response time, (f) time to peak and (g) time lag between water table peak and discharge peak for each rainfall-runoff event at all piezometer locations. Rainfall-runoff events are ranked according to their storm runoff coefficient (C_s) value. 20

Fig. 2.7 Relationship between the pre-event depth to water table and (a) pre-event discharge and (b) storm runoff coefficient. (c) Relationship between water table increase and storm

runoff coefficient. Black dots are the median values and bars correspond to quartiles (25% and 75%). Significance:**p < 0.01; *p < 0.05; ns p > 0.05. 21

Fig. 2.8 (a) Rainfall and discharge and (b) depth to water table at the 13 piezometer locations, observed during three floods with different antecedent wetness conditions. (c) Relationship between the mean depth to water table and its standard deviation (red dots correspond to the time of peak discharge). (d) Relationship between the mean depth to water table and discharge (one hour time step). 25

Fig. 3.1 Map of the Can Vila catchment, showing locations of the main instruments and of the sampling sites. 38

Fig. 3.2 Temporal dynamic of DOC concentration in rainwater during the study period (May 2011 to July 2013). White dots correspond to the concentrations of 5mm rainfall increment samples. Black dots correspond to the mean concentration of a rainfall event. The solid line is a running average. The colour scale on the x axis represents the dormant period, vegetative period, dry period and wetting-up period (see text). 39

Fig. 3.3 Temporal dynamic (May 2011 to July 2013) of (a) soil temperature, (b) soil water content and DOC concentration in soil water (LCV01), (c) depth to water table and DOC concentration in groundwater (ZCV08) and (d) daily mean discharge at the outlet and DOC concentration in stream water. White dots correspond to samples DOC concentrations and black solid lines to running averages (three values). Numbers refer to floods sampled (see Table 3.2). The colour scale on the x axis represents the dormant period, vegetative period, dry period and wetting-up period (see text). 42

Fig. 3.4 Relationship between discharge measured at the outlet of the catchment and the DOC concentration in stream water. Two different dynamics are observable below and above a threshold of 20 L s^{-1} km^{-2}, roughly defining flood conditions. 43

Fig. 3.5 (a) Relationship between DOC concentration in groundwater (Z_{CV08}) and stream water. (b) Relationship between mean daily values of depth to water table (Z_{CV08}) and discharge measured at the outlet of the catchment. White dots correspond to days when groundwater and stream were sampled for DOC. 44

Fig. 3.6 (a) Discharge and DOC concentration in stream water during the two flood peaks of the 30 April 2012 event. (b) Relationship between discharge and DOC concentration in stream water throughout the event. (b) is the slope of the linear regressionbetween discharge and DOC concentration. 46

Fig. 3.7 Relationship between discharge and DOC concentration in stream water during dormant, vegetative and wetting-up periods. All data for the first and second peaks of floods observed during each of the periods were adjusted. (b is the slope of the linear regression between discharge and DOC concentration). 47

Fig. 3.8 a) Discharge and DOC concentration in stream water during three floods observed during dormant, vegetative and wetting-up periods. (b) Relationship between discharge and DOC concentration in stream water during the event. (c) Soil water content (SWC at 0–90 cm depth) and depth to the water table (piezometers ZCV08 and ZCV35) during the event. (d) Relationship between the depth to the water table at ZCV08 and DOC concentration in stream water during the event. (e) Relationship between the soil water content (0–90 cm) and DOC concentration in stream water during the event. In (b), (d) and (e), arrows indicate the directions of the hysteresis for each flood peak. 49

Fig. 4.1 Map of the Cal Rodó catchment and subcatchments (Can Vila and Ca l'Isard) showing the geological characteristics, the stream network, the monitoring design, and the sampling locations (springs, streams and wells. 59

Fig. 4.2 Temporal sequences of monthly rainfall tritium concentration, monthly rainfall tritium concentration after applying the scaled factor of 0.82 and the yearly input function after applying the scaled factor and the recharge equation. 63

Fig. 4.3(a) Likelihood weighted cumulative density function for two normal distributions and (b) a bimodal distributions. 65

Fig. 4.4 Temporal dynamics of $\delta^{18}O$ and $\delta^{2}H$ signal in (a) rainfall, stream (b)water (St4), (c) spring water (Sp12) and (d) groundwater (Gw18) during the study period (May 2011 to July 2013) at baseflow conditions. Black dots correspond to $\delta^{18}O$ while grey dots correspond to $\delta^{2}H$. Note the change of Y scale between rainfall graph and the other graphs. 66

Fig. 4.5 Relationship between $\delta^{18}O$ and $\delta^{2}H$ signal in stream water (St4), spring water (Sp12) and groundwater (Gw18) throughout the study period (see Fig. 4.1 for sampling locations). The solid line plots the Local Meteoric Water Line (LMWL) obtained from rainfall samples (weekly data) whereas the dashed one the Global Meteoric Water Line (GMWL). 67

Fig. 4.6 $\delta^{18}O$ goodness-of fit (standard deviation) obtained with the Exponential Piston Model for different f and MTT for (a) stream water, (b) spring water and (c) groundwater. 67

Fig. 4.7 (a) Likelihood weighted cumulative density function (lwcdf) for the four studied locations, considering all the tritium samples (1990s and 2013). (b) Weighted mean and [0.05-0.95] confidence intervals of estimated MTT for the same locations. 69

Fig. 4.8 Normal Q-Q plots comparing the observed MTT distribution and the expected normal distribution in St1 (a), St4 (b), Sp 12 (c) and Gw18 (d). 69

Fig. 4.9 (a) Likelihood weighted cumulative density function, (lwcdf) for the four studied locations, obtained considering only the 1990s samples (five samples). (b) Weighted mean and [0.05-0.95] confidence intervals of the estimated MTT for the same studied locations. 70

Fig. 4.10 (a) Likelihood weighted cumulative density function (lwcdf) for the four studied locations, obtained considering only the 2013 samples. (b) Weighted mean and [0.05-0.95]

confidence intervals of the MTT two possible solutions (see text) for the same studied locations. 71

Fig. 4.11 MTT estimated in thethree springs, twelve streams and six wells of Cal Rodó catchment. The black dots are the weighted MTT and [0.05-0.95] confidence intervals estimated in the present study. The white dots and black squares are the MTT estimated by Herrmann et al., (1999) using the EM model and the dispersion model, respectively.....72

Fig. 4.12 MTT estimated in thethree springs, twelve streams and six wells of Cal Rodó catchment. The black dots are the weighted MTT and [0.05-0.95] confidence intervals estimated in the present study. The white dots and black squares are the MTT estimated by Herrmann et al. (1999) using the EM model and the dispersion model, respectively.....73

Fig. 4.13 Comparison between the weighted mean of MTT estimated in this study, using the EPM , and those in Herrmann et al. (1999) using (a) the Dispersion model and (b) the Exponential model.....73

Fig. 4.14 (a) Relationship between the MTT and the Topographic Wetness Index of the 21 locations (springs, streams and wells). (b) Relationship between the MTT and the slope. Dots are the weighted mean MTT and bar the [0.05-0.95] confidence intervals.....76

Fig. 4.15 Map of the Cal Rodó catchment and sub-catchments (Can Vila and Ca l'Isard) showing the weighted MTT ± weighted standard deviation of the the springs (star), streams (circle) and wells (triangle) estimated from samples taken in the nineties. The geological characteristics of the catchment are also shown. 77

LIST OF TABLES

Table 1.1 Hydrological studies in Mediterranean research catchments. The studies are classified according to the methodology used. The studies carried out at the Vallcebre research catchments are not included. 4

Table 2.1 Characteristics of piezometer locations. 13

Table 2.2 Spearman rank correlation coefficient between location characteristics (elevation above the stream, distance from the stream and Topographic Wetness Index (TWI)) and the median pre-event depth to water table (WT_i). 17

Table 2.3 Spearman rank correlation coefficient between depths to water table variables (i.e. median pre-event depth to water table (WT_i), median water table increase ($WT_{increase}$)) and timing variables (i.e. median time response ($t_{response}$), median time to peak (t_{peak}) and median time lag between water table peak and discharge peak ($t_{peak-peak}$)) at each piezometer location. 18

Table 2.4 Spearman rank correlation coefficient between the median pre-event depth to water table (WT_i), variables characterizing the water table response (median water table increase ($WT_{increase}$), median response time ($t_{response}$), median time to peak (t_{peak}) and median time lag between water table peak and discharge peak ($t_{peak-peak}$)) and rainfall-runoff event characteristics (pre-event discharge (Q_b) and storm runoff coefficient (C_s)). 21

Table 2.5 Characteristics of the rainfall-runoff events analysed in this study. 26

Table 3.1 Mean DOC concentration (mg L^{-1}, ± standard error) measured in rainwater, soil water, groundwater and stream water over the whole study period and during the dormant, vegetative, dry and wetting-up periods (n is the number of samples analysed). 41

Table 3.2 Characteristics of the rainfall–runoff events sampled during the study period....45

Table 4.1 Results of MTT estimation using the EPM model and considering all the tritium samples. CI = confidence interval. σ = Standard deviation. 68

Table 4.2 Results of MTT estimation using the EPM model and considering only the 2013 samples. CI = confidence interval. σ = Standard deviation. 71

Table 4.3 Results of MTT estimation using the EPM model and considering only the 1990s samples. CI = confidence interval. σ = Standard deviation. 74

Table 4.4 Probability of being different between pairs of `lwcdf´ of stream sampling locations using the randomisation test (see Fig. 4.1 for the localization of the sampling locations). 75

Table 4.5 Probability of being different between pairs of `lwcdf´ of the springs sampling locations using the randomisation test. 75

Table 4.6 Probability of being different between pairs of `lwcdf´ of the shallow groundwater sampling locations using the randomisation test. 76

CHAPTER 1

INTRODUCTION

1 INTRODUCTION

This section includes a general overview of hydrological studies at the catchment scale, with special emphasis on Mediterranean catchments. The overview focuses on the use of hydrometric approaches and environmental tracers for understanding factors and processes that control catchment hydrological response and runoff generation.

As water is a scarce and essential resource for life, its sustainable management is of crucial importance. For this reason, water is of significant scientific interest in itself. In addition, knowledge of the hydrological pathways by which water moves through the catchment is important for our hydrological, geochemical and ecological understanding.

The volume of water that arrives and flows in a stream comes from either direct precipitation on the flowpath or surface, subsurface and groundwater flow. Musy and Higy (2010) define (i) runoff or overland flow as the flow over the surface of the ground occurring after a storm, (ii) subsurface flow as the water that moves in the top layers of the soil that have been partially or totally saturated and (iii) groundwater flow as the water that infiltrates and then finds its way into the groundwater. Hydrologists also usually differentiate between soil water (unsaturated zone) from soil surface down to the upper limit of the water table and groundwater (saturated zone) (Custodio and Llamas, 2001).

The characterization of dominant runoff processes is not an easy task, especially when such processes occur below the soil surface. In consequence, while surface runoff processes, such as infiltration or saturation excess overland flow, have often been well identified, processes occurring below the surface are still not properly understood (Beven, 1989).

Several factors condition catchment hydrology, such as: i) the catchment's characteristics (e.g. topography, geology, soil type, vegetation type, land use, catchment size, etc.); ii) atmospheric forcing and climate; and iii) the antecedent hydrological conditions of the catchment.

1.1 Combining hydrometric data and environmental tracers

Hydrological studies at the catchment scale seek to identify and understand processes and factors affecting runoff generation, among other questions.

In recent decades, geochemical and isotopic methods have been combined with classic hydrometric approaches to identify the processes and factors governing catchment hydrology (see Hooper, 2001; Lischeid, 2008; Klaus and McDonnell, 2013). These combinations have proved a reliable tool for understanding hydrological mechanisms. They explain, among other things: how and where is water stored in a catchment? for how long? how is water mixed

between the different hydrological compartments? how does subsurface water distribution vary spatially and temporally? and how and when is runoff generated?

The use of hydrometric data

Hydrological studies are mainly based on hydrometric data, which usually include rainfall and discharge. However, as many hydrological processes occur below the soil surface, rainfall and discharge data do not sufficiently explain the processes and factors controlling runoff generation (Beven, 1991). For this reason, some pioneering studies began to monitor piezometric data measured at a few locations, in addition to discharge measurements (Hursh and Brater, 1941). The later incorporation of soil water content measurements, in hydrological studies at the catchment scale, demonstrated the important role of these variables in controlling catchment scale processes (e.g. Sklash and Farvolden, 1976; Myrabø, 1997; Bárdossy and Lehmann, 1998).

The improvement and affordability of sensors, as well as better data logging and storage technologies, have made it easier to record hydrological data continuously and at different locations, providing a high amount of hydrometric information at different time scales from catchments worldwide. A clear example is the use of large sets of probes to monitor variables with high spatio-temporal variability, such as piezometric level or soil water content (e.g. Anderson and Burt, 1977; Myrabø, 1997; Western and Blöschl, 1999; Freer et al., 2002; Seibert et al., 2003).

The use of environmental tracers

Environmental tracers such as geochemical tracers or isotopes have been widely used in catchment hydrology (see Kendal and McDonnell, 1998; Hooper, 2001; Lischeid, 2008; Leibundgut et al., 2009 and references therein). On the one hand, they have proved a reliable tool for investigating runoff generation during storm events, by providing information on the spatial origin of water and on the contribution of different water sources. On the other hand, tracers have helped to calculate water's mean transit time (MTT), i.e. the time water spends travelling subsurface through a catchment to the stream network (see a review in McGuire and McDonnell, 2006).

The spatial origin of water, during rainfall-runoff events, can be studied by means of geochemical tracers when different hydrological compartments have different geochemical characteristics (Kirchner, 2003; Lischeid, 2008). For instance, the concentrations of dissolved organic carbon (DOC) can be used to identify the contribution of water compartments with a high organic matter content (e.g. Ladouche et al., 2001; Carey and Quinton, 2005; Morel et al., 2009).

Conversely, water isotopes ($\delta^{2}H$ and $\delta^{18}O$) allow calculation of the relative contributions within the hydrograph of rainfall (sometimes referred to as new or event water) and of water

stored in the catchment before the onset of a hydrological event (sometimes referred to as old water or pre-event water) (Burns et al., 2001; Klaus and McDonnell, 2013). Isotopes have several advantages over geochemical tracers, as they can only be altered by mixing with isotopically different waters (Sklash et al., 1976) and there is no potential interaction between minerals and interstitial water, such as there is for geochemical tracers (Kennedy et al., 1986; Buttle, 1994).

Water's MTT is usually assessed by several tracers: $\delta^{18}O$ (DeWalle et al., 1997), radioisotopes (Maloszewski and Zuber, 1982; Stewart and Fahey, 2010) or by a combination of tracers (Dincer et al., 1970; Uhlenbrook et al., 2002; Green et al., 2014; McCallum et al., 2014). δ18O is more suitable for dating waters younger than 4-5 years, while tritium is generally used to calculate water ages up to 100 years, because its decay covers several half-lives (McGuire and McDonnell, 2006; Stewart et al., 2007; Stewart et al., 2010).

Numerous studies have combined multiple tracers to identify the processes and factors governing catchment hydrology (e.g. Uhlenbrook et al., 2002; McGlynn and McDonnell, 2003b; Joerin et al., 2005). In addition, recently, other tracers or water properties have been used for hydrological purposes. For example, diatoms have been used to quantify the spatial sources of runoff (Pfister et al., 2009; Martinez-Carreras et al., 2015) or thermal imagery techniques (Pfister et al., 2010; Schuetz and Weiler, 2011) have been used to detect groundwater inflows to the stream and water mixing areas.

1.2 The hydrology of Mediterranean catchments

Most of the hydrological studies of the last 50 years have examined humid and temperate regions. Mediterranean regions, which are the context of this study, have received less attention, despite the Mediterranean being one of the most vulnerable regions of Europe in terms of water resources, due to its sensitivity to Global Change (European Environment Agency, 2012).

Mediterranean climate regions, which lie between 30º and 45º latitude, are located around the Mediterranean itself and in coastal areas of California, South America, South Africa and South and Western Australia. Mediterranean climate is characterized by strong intra and interannual precipitation variability (Woodward, 2009) and by strong climatic seasonality, with drought periods. For these reasons, Mediterranean regions are characterized by unevenly distributed water resources that mainly depend on runoff generated in mountain areas. Therefore, the study of the hydrology of Mediterranean mountain areas is especially important as a strategic aspect of water resource management (Viviroli et al., 2007) and may help anticipate hydrological consequences of global change. García-Ruiz et al. (2011) analysed future climate change scenarios in Mediterranean regions and stressed the need to improve water management, water pricing and water recycling policies, in order to ensure water supply.

Table 1.1 gives a non-exhaustive inventory of hydrological studies of Mediterranean research catchments. These studies are classified according to the methodology used (hydrometric, geochemical and isotopic).

Table 1.1 Hydrological studies in Mediterranean research catchments. The studies are classified according to the methodology used. The studies carried out at the Vallcebre research catchments are not included.

Data	Catchment	Location	Reference
Hydrometric	TM9	Catalonia. Spain	Àvila, 1987
	-	Victoria. Australia	Burch et al., 1987
	Wights	Perth. Australia	Ruprecht and Schofield, 1989
	Rimbaud	Var. France	Lavabre et al.,1993
	Réal Collobrier	Var. France	Gaillard et al., 1995
	Maurets	Var. France	Taha et al., 1997; Grésillon and Taha, 1998
	Roujan	Languedoc-Roussillon. France	Linde et al., 2007
	San Salvador, Arnás and Araguás	Aragón. Spain	Lana-Renault et al., 2007, 2014; García-Ruíz et al., 2008; Serrano Muela, 2013
	Guadalperalón	Extremadura. Spain	Ceballos and Schnabel, 1998; Schnabel and Mateos Rodríguez, 2000
Geochemical	Rimbaud	Var. France	Travi et al., 1994
	Maurets	Var. France	Marc et al., 1995
	Roujan	Hérault. France	Ribolzi et al., 2000
	Riera Major	Catalonia. Spain	Butturini and Sabater, 2000
	Mont-Lozère	Cevennes. France	Marc et al., 2001
	Mokelumne	Sierra Nevada. California	Holloway and Dahlgren, 2001
	Fuirosos	Catalonia. Spain	Bernal et al., 2002, 2005; Vázquez et al., 2007
	Can Vila, Riera Major and Fuirosos	Catalonia. Spain	Butturini et al., 2006, 2008
	Hérault	Hérault. France	Petelet-Giraud and Negrel, 2007
	Draix	Alpes de Haute Provence, France	Crass et al., 2007
	La Tordera	Catalonia. Spain	Von Schiller et al., 2008
Isotopic	Cannone	Corsica. France	Loÿe-Pilot, 1990
	Montseny, Prades	Catalonia. Spain	Neal et al., 1992
	La Sapine, Les Cloutasses and La Latte	Lozère. France	Durand et al., 1993
	Rimbaud	Var. France	Travi et al., 1994
	Maurets	Var. France	Marc et al., 1995
	Mont-Lozère	Cevennes. France	Marc et al., 2001
	Draix	Alpes de Haute Provence, France	Crass et al., 2007

1.3 The Vallcebre Research Catchment

The Vallcebre Research Catchments, where this study has been conducted, is located at the headwaters of the Llobregat River, on the southern margin of the Pyrenees, NE Spain (42°12' N, 1°49' E). This research area, managed by the Surface Hydrology and Erosion group (IDAEA-CSIC), was selected in the late eighties to analyse the hydrological consequences of land abandonment and the sediment yield from badland areas (Latron et al., 2010a).

The research area consists of two catchment clusters: Cal Rodó and Cal Parisa. The main cluster (Cal Rodó, 4.17 km^2) was sub-divided into three sub-catchments: Can Vila (0.56 km^2), Ca l'Isard (1.32 km^2) and Santa Magdalena (0.53 km^2) (Fig. 1.1).

This study focuses mainly on the Can Vila catchment, whose characteristics (i.e. topography, geology, land use, soil type, vegetation type, etc.) are described in the methodology of each chapter of the thesis.

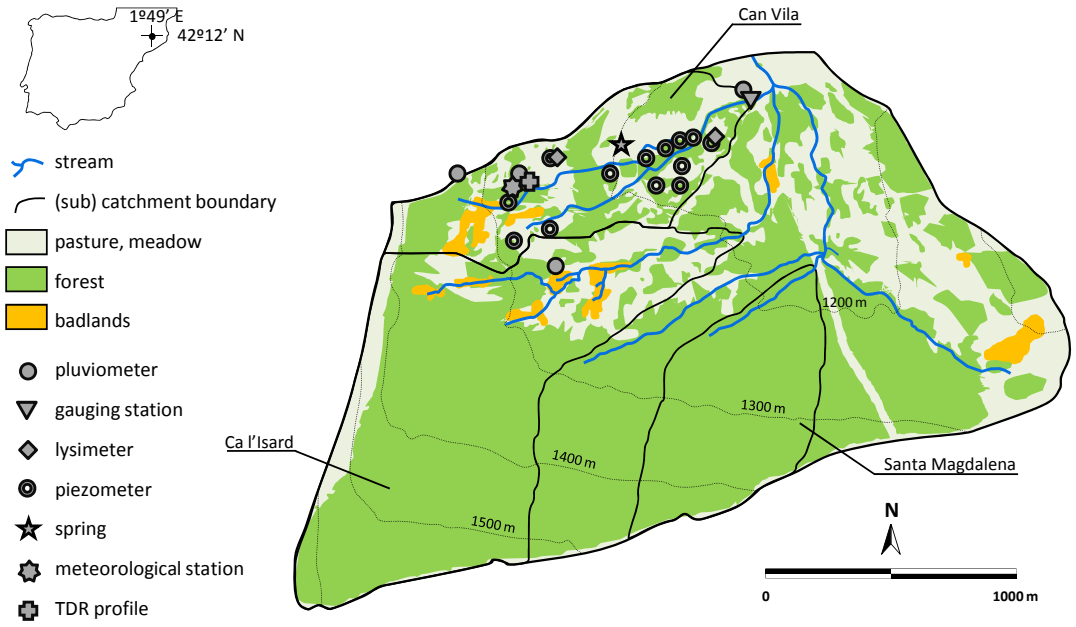

Fig. 1.1 Map of the Cal Rodó catchment and of the Can Vila, Ca l'Isard and Santa Magdalena sub-catchments. Only the monitoring design used in the present study (July 2009 to July 2013) is shown. Land uses were digitized from a high-resolution orthophoto (ICC, 2012); and the stream network is taken from Latron (2003).

Fig. 1.2 Pictures of the types of landscapes found in the Vallcebre Research Catchments. Source: M.Roig-Planasdemunt

A complete overview of the general hydrological findings in the Vallcebre research area can be found in Llorens and Gallart (1992), Llorens et al. (1992, 2010a), Gallart et al. (1994, 1997, 2002, 2005a, 2010, 2014), Latron (2003), Latron et al. (2003, 2008, 2009, 2010a, 2010b, 2014), Latron and Gallart (2007, 2008) and García-Estringana et al. (2012).

In addition, more specific studies, though not directly discussed here, have been performed in the research area, such as: investigations of sediment dynamics and transport (Gallart et al., 1998, 2005b, 2014; Regüés and Gallart, 2004; Regüés et al., 1995, 2000; Llorens, 1997; Soler et al., 2007, 2008), hydrological modelling (Anderton et al., 2002a and b; Gallart et al., 2007, 2008; Martínez-Carreras et al., 2007; Ruiz-Pérez et al., 2015) and ecohydrology (Llorens et al., 1997,

2003, 2010a, 2010b, 2011, 2013, 2014; Poyatos et al., 2005, 2008; Muzylo et al., 2012a and b; Molina et al., 2014).

These studies, conducted over the last 25 years, have contributed to improving the understanding of hydrological processes in the research area, and shed light on the hydrology of Mediterranean catchments.

More specifically, and directly related with the subjects of the present paper, Latron and Gallart (2007, 2008) and Latron et al. (2008) included information on the depth to water table to explain runoff generation processes in Can Vila catchment. However, in these papers the spatial variability of the depth to water table was not analysed. Likewise, Herrmann et al. (1999) used environmental tracers (δ18O and tritium) to calculate MTT in the Vallcebre catchments, but the uncertainty of MTT calculation was not considered.

1.4 Objectives of the study

Within this framework, and following the research lines of the Surface Hydrology and Erosion group of the Institute of Environmental Assessment and Water Research (IDAEA)-Spanish National Research Council (CSIC), the main objective of this thesis is the characterization of hydrological processes in a Mediterranean mountain catchment by combining distributed hydrological measurements and environmental tracers.

To achieve this target, the thesis is divided into three objectives:

- To investigate the spatio-temporal dynamics of depth to water table during storm events.
- To analyse dissolved organic carbon (DOC) concentration dynamics in different water compartments (rainfall, soil water, groundwater and stream water) through the year and during storm events.
- To calculate water mean transit time (MTT) in different water compartments (stream, springs and wells).

The thesis aims to contribute to the clarification of the following questions:

Does the depth to water table vary temporally and spatially during storm events? Is the depth to water table affected by catchment location characteristics? Do antecedent wetness conditions affect shallow groundwater dynamics and streamflow response?

Does DOC in rainfall, soil water, groundwater and stream water follow any pattern during the year? Are the DOC dynamics during storm events similar throughout the year? Is DOC a useful tracer of water origin in the Vallcebre research catchments?

How old is the water in the streams, springs and wells of the Cal Rodó catchment? Does water MTT vary spatially in the catchment? What results are obtained when applying an

uncertainty analysis of MTT calculations, using tritium and different sampling designs? Are these results similar to those obtained by Herrmann et al. (1999)?

1.5 Thesis structure

The thesis consists of five chapters, including the Introduction (Chapter One) and Conclusions (Chapter Five).

Chapter Two studies the spatio-temporal dynamics of depth to water table during storm events in the Can Vila catchment. It examines the effect of location characteristics on the spatial and temporal distribution of depth to water table. The roles of antecedent wetness conditions in water table response and streamflow response are also analysed.

Chapter Three focuses on the study of the seasonal and storm dynamics of dissolved organic carbon (DOC) at the Can Vila catchment. This chapter characterizes DOC dynamics in the different hydrological compartments and analyses the factors affecting them. DOC dynamics during storm events and the factors that control DOC's delivery to the stream are also evaluated.

Chapter Four calculates water mean transit time in the streams, springs and wells of the Cal Rodó catchment by using stable isotopes and tritium. It includes a complete uncertainty analysis of MTT calculations, using tritium and different sampling designs. The results are compared with the results obtained by Herrmann et al. (1999) and MTT spatial variability is examined.

CHAPTER 2

SPATIAL AND TEMPORAL VARIABILITY OF DEPTH TO WATER TABLE DURING RAINFALL-RUNOFF EVENTS IN A MEDITERRANEAN MOUNTAIN CATCHMENT (VALLCEBRE, EASTERN PYRENEES)

to be submitted in Journal of Hydrology

Maria Roig-Planasdemunt[1], Pilar Llorens[1], Jérôme Latron[1]

[1] Institute of Environmental Assessment and Water Research (IDAEA), CSIC

2 SPATIAL AND TEMPORAL VARIABILITY OF DEPTH TO WATER TABLE DURING RAINFALL-RUNOFF EVENTS

2.1 Introduction

Groundwater dynamics are key to control of streamflow dynamics and runoff generation processes. Therefore, the study of shallow groundwater dynamics, and their controlling factors, is essential to the understanding of the hydrological functioning of a catchment. The improvement and affordability of sensors have made it much easier to record data on depth to water table continuously at different locations. Recent studies based on distributed water table measurements have demonstrated that depth to water table does not respond homogeneously to rainfall in humid regions (e.g. Haugt and van Meerveld, 2011; Rodhe and Seibert, 2011). Most studies observed a marked spatial-temporal variability of water table dynamics, related to location characteristics such as bedrock topography (e.g. Freer et al., 2002; Van Meerveld et al., 2015), soil properties (Bachmair and Weiler, 2012), distance to the stream (Seibert et al., 2003; Kuraś et al., 2008; McMillan and Srinivasan, 2015) and former agricultural activities that changed local topography and soil properties (Lana Renault et al., 2014). In recent studies, the topography wetness index (Beven and Kirkby, 1979) and the distance to the stream have proved good predictors of water table dynamics. Jordan (1994) and Rinderer et al. (2016) observed that the depth to water table was close to the soil surface in areas of the catchment with high values on the topographic wetness index. Other studies showed that areas with persistent water table and fast water table responses were the areas near the stream channel (Peters et al., 2003; Detty and McGuire, 2010). In fact, at locations at similar distances from the stream, water table levels correlate closely (Seibert et al., 2003).

Different antecedent wetness conditions also affect water table responses (Bachmair et al., 2012). For example, Penna et al. (2014) observed that, the shallower the depth to water table, the faster and more extended the groundwater response. Penna et al. (2011) also observed that during small storms in dry antecedent conditions the low amount of stormflow was mainly produced by contributions from riparian zones, whereas during wet antecedent conditions, the hillslope contribution was dominant.

Finally, since the spatio-temporal variability of the water table depth has a strong influence on streamflow dynamics, the relationship between streamflow and water table responses has been studied in a great number of catchments worldwide (e.g. Myrabø, 1997; Seibert et al., 2003; Kuraś et al., 2008; Latron and Gallart, 2008). Results show that, in general, piezometers close to the stream have the strongest correlation with discharge (Haugt and van Meerveld, 2011) and that different correlations depend on location (Kendall et al., 1999) or on catchment

wetness conditions (Lana-Renault et al., 2007). Seasonal differences in the relationship between runoff response and water table dynamics are also often found (e.g. Bachmair et al., 2012).

Despite the number of studies of the spatio-temporal variability of the depth to water table on the small catchment scale, relatively few studies have focused specifically on the variability of the groundwater response during rainfall-runoff events. Based on observations at 90 wells, Bachmair et al. (2012) found that the wells activated during events varied between events. Penna et al. (2014) analysed the relationship between the mean water table depth and the standard deviation during rainfall-runoff events, in order to study spatial variability. More recently, Rinderer et al. (2016) investigated the topographic controls and the effects of rainfall and wetness antecedent conditions on the water table timing response during rainfall-runoff events.

Most of these investigations were carried out in humid temperate catchments (with mean annual precipitation usually above 1,000 mm y^{-1}). Water table dynamics have received less attention in Mediterranean regions, which is the context of this study. In the south of France, Gaillard et al. (1995) combined water table and soil water potential with soil water content data to study the runoff generation processes. Grésillon and Taha (1998) found close correlation between stream flow and piezometric levels near the stream. Taha et al. (1997) tested a hydrological model using water table measurements. Also in the south of France, Linde et al. (2007) calculated the spatial variations of water table by using self-potential and piezometric data. In the Spanish Pyrenees, Lana-Renault et al. (2007) studied the streamflow and water table response of several rainfall-runoff events. More recently, Lana-Renault et al. (2014) investigated in greater detail the spatio-temporal fluctuations of the water table by measuring at five locations in the same catchment.

In the Vallcebre research catchments, water table data from one location have been used to test hydrological models (Gallart et al., 2007) and to investigate runoff generation processes (Latron and Gallart, 2008). However, as only a couple of sites were monitored in these studies, the spatial variability of the depth to water table could not be examined. The aim of this study is to make use of the distributed water table information available in the Vallcebre research catchments since 2009 to investigate the spatial and temporal distribution of depth to water table during rainfall-runoff events in a Mediterranean mountain area. Therefore, its objectives were: (a) to examine the effect of location characteristics on the spatial and temporal distribution of depth to water table; (b) to examine the effect of shallow groundwater dynamics on streamflow; and (c) to analyse the role of antecedent wetness conditions on shallow groundwater dynamics during rainfall-runoff events.

2.2 Methods

2.2.1 Study site

All the data presented in this study were collected from the Can Vila research catchment (0.56 km^2), located in the Vallcebre research area (Latron et al., 2010a) at the headwaters of the Llobregat River, on the southern margin of the Pyrenees, northeast Spain (42°12'N, 1°49'E). The Vallcebre research area, managed by the Surface Hydrology and Erosion group (IDAEA-CSIC), was selected in early 1990 to analyse the hydrological consequences of land abandonment and the hydrological and sediment yield behaviour of badlands areas.

In the Can Vila catchment (Fig. 2.1), elevations range from 1,458 to 1,115 m above sea level, and slope gradients are moderate, with a mean value of 25.6% (Latron and Gallart, 2007). The topographic wetness index ranges from 6.1 to 10.2 (Beven and Kirkby, 1979). Soils that have developed over red clayey smectite-rich mudrocks are predominantly of silt-loam texture. Topsoil is rich in organic matter (on average 4.1% from 0 to 55 cm below the ground surface) and well-structured, with high infiltration capacity, although hydraulic conductivity decreases rapidly with depth (Rubio et al., 2008). Before and during the 19th century most of the hill-slopes of the catchment were deforested and terraced for agricultural purposes. They were abandoned during the second half of the 20th century. As a consequence of terracing, soil thickness ranges from less than 50 cm in the inner part of the terraces to more than 2 or 3 m in their outer part (Latron et al., 2008). Another consequence of the terracing was the modification of the natural stream network, with the construction of artificial drainage ditches in the upper part of the catchment. Following land abandonment, spontaneous forestation by Pinus sylvestris has occurred (Poyatos et al., 2003) and forest now covers 34% of the catchment. The remainder of the catchment is widely covered by pasture and meadows. The main channel is 1 to 2 m wide and is not very deeply incised. No riparian zone is observed in the catchment.

Climate is humid Mediterranean, with a marked water deficit in summer. The mean annual rainfall (1988–2013) is 880 ± 200 mm, with a mean of 90 rainy days per year (Latron et al., 2014). Snowfall accounts for less than 5% in volume. The rainiest seasons are autumn and spring. Winter is the season with the least rainfall. In summer, convective storms may provide significant rainfall input. Mean annual temperature at 1,260 m a.s.l. is 9.1ºC and mean annual potential evapotranspiration is 823 ± 26 mm (Latron et al., 2010a).

The combined dynamic of rainfall and evapotranspiration favours the succession of wet and dry or very dry periods during the year (Latron and Gallart, 2007). Dry and very dry periods occur in winter and summer, respectively, whereas wet periods correspond to spring and late autumn. Over the period 1995–2013, mean annual runoff in the Can Vila catchment was 302 ± 191 mm, representing 34% of rainfall (Latron et al., in prep.). The stream shows marked seasonality and often dries up in summer for several weeks.

2.2.2 Hydrometric monitoring

Rainfall in the Can Vila catchment is recorded every 5 min by means of three 0.2 mm tipping-bucket rain gauges (Casella Cel), located 1 m above the ground (Fig. 2.1). A standard meteorological station is located in the upper part of the catchment.

At the Can Vila gauging station, streamflow is measured by means of a 90° V-notch weir with a water pressure sensor (6542C-C, Unidata) connected to a datalogger (DT50, Datataker). Mean water level values (measured every 10 seconds) are recorded every 5 min and converted to discharge values with an established stage-discharge rating curve calibrated with manual discharge measurements (Latron and Gallart, 2008).

Water table data are collected from 13 piezometers distributed all over the catchment. Except for Z_{CV08} for an abandoned well, all piezometers were hand-augered as far down into the soil as possible to insert 55 mm–diameter PVC tubes. As a result, the piezometers have different depths (ranging from -1,300 to -4,220 mm) (Table 2.1). The piezometers were sealed for the top 0.5 m to prevent entrance of surface waters, with open access below. Water table level is continuously recorded every 10 min in each piezometer (Fig. 2.1) by means of a water pressure sensor (10m MiniDiver, Schlumberger Water Services), with compensation made for barometric pressure variations. The pressure sensors were calibrated by taking manual measurements of water table depth directly from the piezometers, at the time data were collected. Water table depth level is described as millimetres (mm) from soil surface.

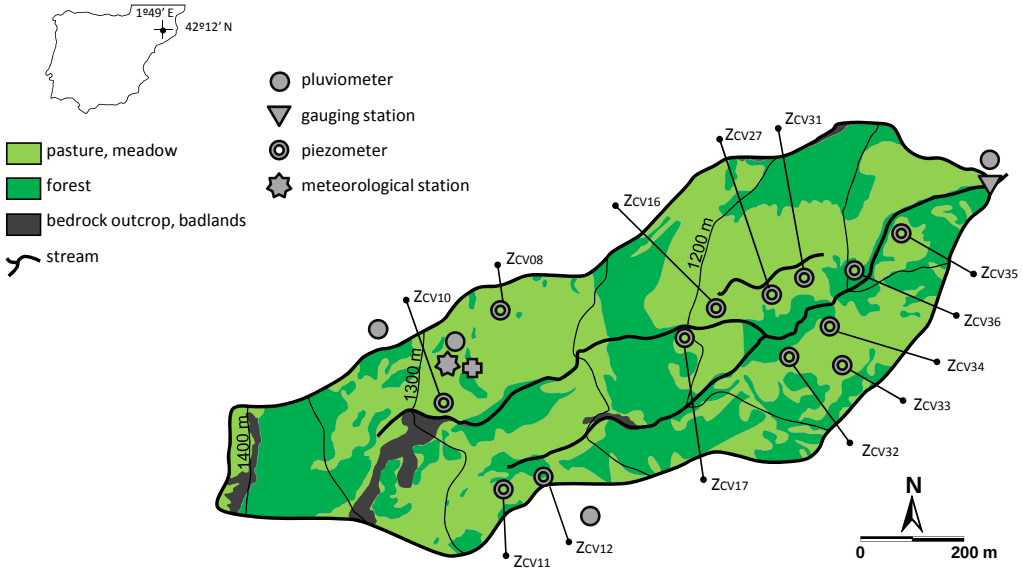

Fig. 2.1 Map of the Can Vila catchment, showing the monitoring design.

2.2.3 Characteristics of piezometer locations

The metrics for each piezometer were obtained from the 5 m resolution digital elevation model (DEM) of the catchment, provided by the Institut Cartogràfic de Catalunya. The piezometers' distance from the stream was calculated as the Euclidean distance to the nearest perennial stream channel. The Topographic Wetness Index (TWI) (Beven and Kirkby, 1979) was calculated by the open source software SAGA-GIS. All the piezometers were located in areas of similar soil properties and similar land–cover. Table 2.1 shows each piezometer's location.

Table 2.1 Characteristics of piezometer locations.

Location	Depth	Elevation a.s.l	Elevation above the stream	Distance from the stream	TWI
	(mm)	*(m)*	*(m)*	*(m)*	
Z_{CV08}	-4,220	1,267	21	135	8.2
Z_{CV10}	-1,917	1,279	14	36	6.2
Z_{CV11}	-1,936	1,283	9	63	8.1
Z_{CV12}	-1,524	1,272	8	61	8.2
Z_{CV16}	-2,137	1,190	1	49	7.9
Z_{CV17}	-2,389	1,199	0	16	8.8
Z_{CV27}	-1,300	1,178	9	26	10.2
Z_{CV31}	-2,215	1,163	11	35	8.1
Z_{CV32}	-2,306	1,184	11	62	7.0
Z_{CV33}	-2,422	1,174	19	128	7.1
Z_{CV34}	-2,383	1,165	10	50	8.5
Z_{CV35}	-2,062	1,138	8	36	6.1
Z_{CV36}	-1,613	1,141	7	31	7.4

a.s.l: above sea level

2.2.4 Analysis of rainfall-runoff events

The analysis of water table and discharge response to storm rainfall was based on rainfall-runoff events occurring between July 2009 and July 2013. To identify these events, storm-runoff depth and coefficient were derived for each selected significant rainfall-runoff event, using the classic "constant slope" hydrograph separation method of Hewlett and Hibbert (1967) with a modified slope value of 1.83 L s^{-1} km^{-2} day^{-1} (see Latron et al., 2008). During the study period 36 rainfall-runoff events were recorded, but only 19 were analysed in this study. These were the events with between 10 and 80 mm rainfall and with a resulting peak of specific discharge higher than 20.0 L s^{-1} km^{-2}. For each rainfall-runoff event, several variables were derived from the hyetograph and hydrograph. These were rainfall depth, maximum rainfall intensity in 30 min and 5 min (I_{max}), runoff depth, storm runoff coefficient (C_s) and pre-event specific discharge (Q_b).

To analyse the differing characteristics of the water table response, two phases were considered during each storm flow event.

First, the time to response ($t_{response}$) was defined as the time lag between the start of rainfall and the largest change between two successive water table level measurements, as in Rinderer et al. (2016). Water table responses with no rise (i.e. when the water table was already at the soil surface) were considered as $t_{response} = 0$. The water table at the start of the rainfall event was defined as the pre-event depth to water table (WT_i).

After the water table response, the water table rises to a maximum. The time to peak (t_{peak}) is the time between the start of the rainfall and the time at which the water table had risen to 95% of its maximum. As in Rinderer et al. (2016), the 95% value was used because it is more robust than the absolute water table peak. For example, on some occasions the water table may first rise quickly and then continue to rise at a much slower rate. Water table increase ($WT_{increase}$) is defined as the difference between water table at $t_{response}$ and at t_{peak}.

To contrast the water table response and the stream response, the time between peaks ($t_{peak-peak}$) is defined as the time lag between the time of peak discharge at the catchment outlet and the time at which the water table had risen to 95% of its maximum, as in Haught and van Meerveld (2011). Thus, a positive lag time means that discharge peaks earlier than the water table peak and *vice versa*.

All the variables were determined with a template in Excel. The median, 25% and 75% quartiles were calculated for all the variables. Piezometer readings greater than 0 (i.e. water table observed at the piezometer) were available in 95.5% of all 13 piezometers in the 19 events analysed in this study. The remaining 4.5% with 0 measurements (i.e. dry piezometer) were excluded from calculations.

The Shapiro test was applied. Then the non-parametric Spearman rank correlation coefficient (r_s) between the different characteristics was determined. The correlation was considered significant when $p < 0.01$ and $p < 0.05$. The software R (version 3.2.0) was used for the statistical analysis of the data.

2.3 Results

2.3.1 Locations and water table response characteristics

Fig. 2.2 shows the characteristics of each piezometer location (distance to the stream and TWI), as well as the median and quartiles of the water table depth at the start of the event (WT_i) and of the variables characterizing the water table response ($WT_{increase}$, $t_{response}$, t_{peak}, $t_{peak-peak}$). Locations are ranked according to the median value of WT_i. Results show that for seven locations WT_i was usually close to the surface. In other locations WT_i was deeper, with median values between -200 mm and -1,900 mm, and had greater variability (Fig. 2.2(a)).

Median $WT_{increase}$ ranged from 0 to 816 mm, with greater variability for major water table increases. Logically, the locations where WT_i was usually close to the surface had the smallest

water table increase. In general, there was an inverse relationship between WT_i and $WT_{increase}$, except for locations Z_{CV32} and Z_{CV33}, which, despite having the lowest median WT_i values, did not have the highest $WT_{increase}$ values (Fig. 2.2(b)).

For all 13 piezometers, median $t_{response}$ ranged from 0.0 to 6.6 h. The variability of $t_{response}$ was also high at each location, as shown by the quartiles range. For $WT_{increase}$, a general inverse relationship between WT_i and $t_{response}$ was visible, except for locations Z_{CV32} and Z_{CV33} (Fig. 2.2(c). The t_{peak} ranged between 0.0 and 18.8 h. Median t_{peak} increased overall as WT_i decreased and was more variable for locations where WT_i was not close to the surface (locations Z_{CV34} to Z_{CV33} in Fig. 2.2(d)). Piezometer Z_{CV32} showed the greatest variability in terms of its t_{peak}, with an interquartile range between 6.7 and 35.3 h.

The median $t_{peak-peak}$ value was positive at five locations (i.e. discharge peaks earlier than the water table peak), equal to zero at location Z_{CV11} and negative at seven locations (Fig. 2.2(e)). Except for location Z_{CV34}, negative $t_{peak-peak}$ values were always very low (i.e. close to 0) with small $t_{peak-peak}$ interquartile ranges.

2.3.2 Relationship between water table response and location characteristics

Table 2.2 shows the correlations between location characteristics (elevation above the stream, distance from the stream and TWI) and the median pre-event depth to the water table WT_i.

WT_i was correlated (r_s = -0.47, p > 0.05) with the piezometer distance from the stream (Table 2.2). In near-stream locations (i.e. fewer than 40 m from the stream) WT_i was close to the surface. While for locations further away than 40 m, WT_i was often much deeper and showed a higher degree of variability (i.e. larger quartiles) (Fig. 2.3(a)). However, at some locations (Z_{cv11}, Z_{cv12}), WT_i was close to the surface in spite of the greater distance from the stream (around 60 m).

In contrast, the elevation above the stream showed much lower correlation with WT_i (Table 2.2). Piezometers located at similar elevations above the stream (i.e. 0–1 m above the stream or around 10 m above the stream) showed very different WT_i levels (Fig. 2.3(c)).

The Topographic Wetness Index (TWI) also showed lower correlation with WTi (Table 2.2). For similar TWI values, the median WT_i varied widely. For example, WT_i from 0 to -1,500 mm corresponded to similar values TWI of around eight (Fig. 2.3(b)). These results suggested that the distance from the stream and the height of the piezometer above the stream were more important than the TWI in defining the pre-event depth to water table.

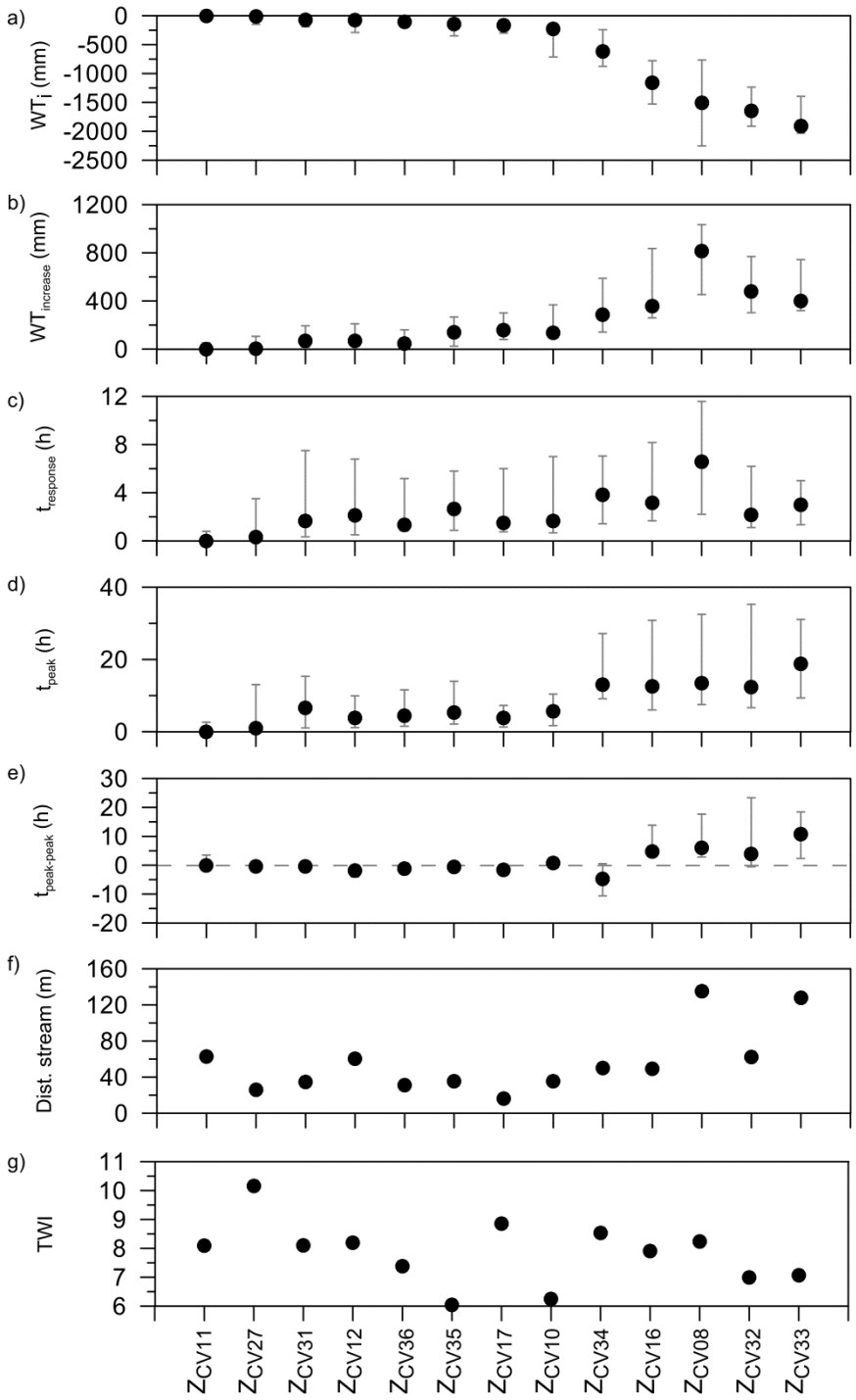

Fig. 2.2 Median and quartiles (25% and 75%) of (a) pre-event depth to water table, (b) water table increase, (c) response time, (d) time to peak, (e) time lag between water table peak and discharge peak at each piezometer location for the 19 observed rainfall-runoff events, (f) distance from the stream and (g) Topographic Wetness Index at each piezometer location. (Piezometers are ranked according to their WT_i value).

Table 2.2 Spearman rank correlation coefficient between location characteristics (elevation above the stream, distance from the stream and Topographic Wetness Index (TWI)) and the median pre-event depth to water table (WT_i).

	Elevation above the stream	Distance from the stream	TWI	WT_i
Elevation above the stream		0.57*	-0.20	-0.39
Distance from the stream			-0.22	-0.47
TWI				0.33
WT_i				

Significance:**p < 0.01; *p < 0.05

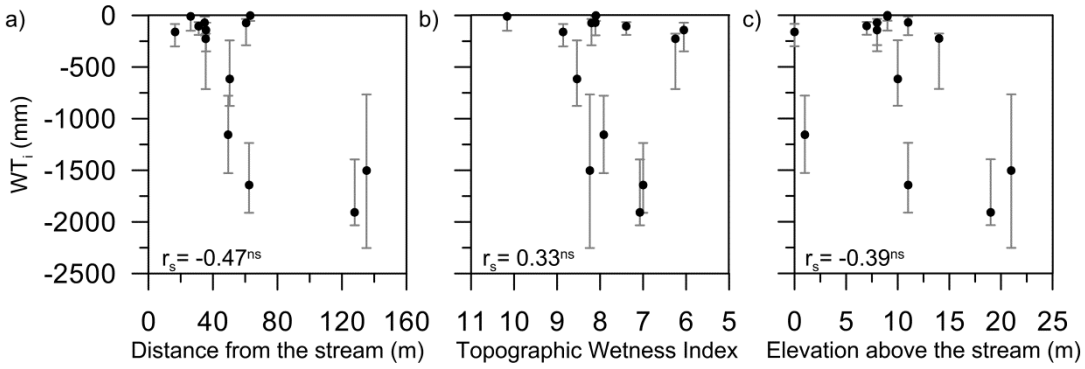

*Fig. 2.3 Relationship between the median pre-event depth to water table at each piezometer location and (a) the distance from the stream, (b) the Topographic Wetness Index and (c) the elevation above the stream. Black dots are the median values and bars correspond to quartiles (25% and 75%). Significance:**p < 0.01; *p < 0.05; ns p > 0.05.*

Table 2.3 shows the correlations between the median pre-event depth to water table (WT_i) and variables characterizing the water table response (median water table increase ($WT_{increase}$), median response time ($t_{response}$), median time to peak (t_{peak}) and median time lag between water table peak and discharge peak ($t_{peak-peak}$)) at each piezometer location. The median WTi significantly negatively correlated with the median $WT_{increase}$ (r_s = -0.94, p < 0.01) and with the median $t_{response}$ (r_s = -0.77, p < 0.01) and t_{peak} (r_s = -0.86, p < 0.01). A negative non-significant correlation existed with median $t_{peak-peak}$. This means that, the deeper the water table (lower WT_i), the higher the $WT_{increase}$ and the slower the water table response, increasing the response time and the time to peak.

The relationship between WT_i and $t_{response}$ in Fig. 2.4(a) shows that at locations with the water table close to the surface, the median $t_{response}$ was short (generally under two hours), whereas for other locations median $t_{response}$ was between two and six hours. The relationship between WT_i and t_{peak} was also clear (Fig. 2.4(b)) with t_{peak} values lower than 6 h at locations with the water table close to the surface and between 12 and 19 h for the other locations. Fig. 2.4(c) shows

that the median $t_{peak-peak}$ was relatively small except for locations with deeper WT_i, which were also more variable (greater interquartile ranges).

Table 2.3 Spearman rank correlation coefficient between depths to water table variables (i.e. median pre-event depth to water table (WT_i), median water table increase ($WT_{increase}$)) and timing variables (i.e. median time response ($t_{response}$), median time to peak (t_{peak}) and median time lag between water table peak and discharge peak ($t_{peak-peak}$)) at each piezometer location.

	WT_i	$WT_{increase}$	$t_{response}$	t_{peak}	$t_{peak-peak}$
WT_i		-0.94**	-0.77**	-0.86**	-0.52
$WT_{increase}$			0.85**	0.85**	0.47
$t_{response}$				0.87**	0.28
t_{peak}					0.49
$t_{peak-peak}$					

Significance: **p < 0.01; *p < 0.05

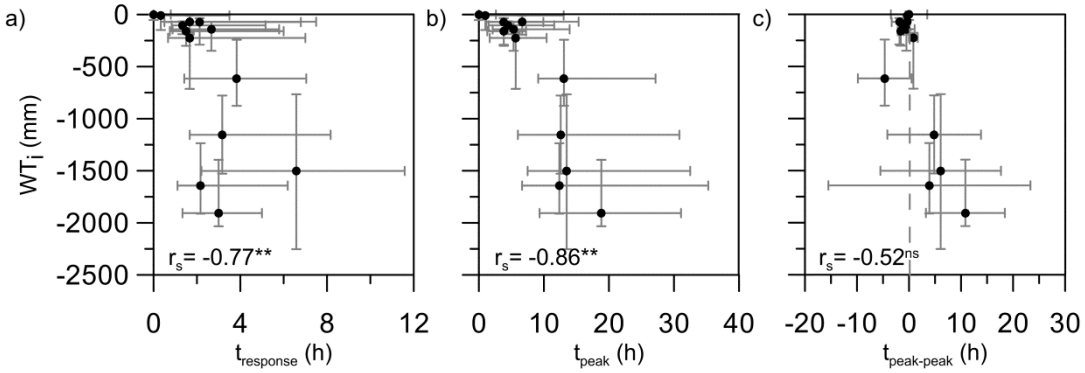

*Fig. 2.4 Relationship between the median pre-event depth to water table at each piezometer location and (a) response time, (b) time to peak and (c) time lag between water table peak and discharge peak. Black dots are the median values and bars correspond to quartiles (25% and 75%). Significance:**p < 0.01; *p < 0.05; ns p > 0.05.*

2.3.3 Water table response characteristics during rainfall-runoff events

The 19 rainfall-runoff events cover a wide range of magnitude, with rainfall depths from 11 to 80 mm and maximum rainfall intensities from 1 to 64 mm h^{-1}. They occurred under several hydrological conditions, as reflected by the wide range of pre-event discharges (Q_b) (0.1 and 41.8 L s^{-1} km^{-2}) and of median pre-event depth to water table (-849 to -69 mm). As a result, runoff responses of the 19 events were highly variable, with specific peak discharges ranging from 46.5 to 5,511.0 L s^{-1} km^{-2} and storm runoff coefficient (C_s) between 2.8% and 53.5%.

Fig. 2.5 gives an overview of the great variability of observed runoff responses, depending on the pre-event discharge as well as on rainfall depth and intensity. The lowest runoff responses corresponded to low rainfall depths or to low pre-event discharges. Largest runoff responses could be observed for pre-event discharges higher than 15 L s^{-1} km^{-2} in response to large or intense rainfall events.

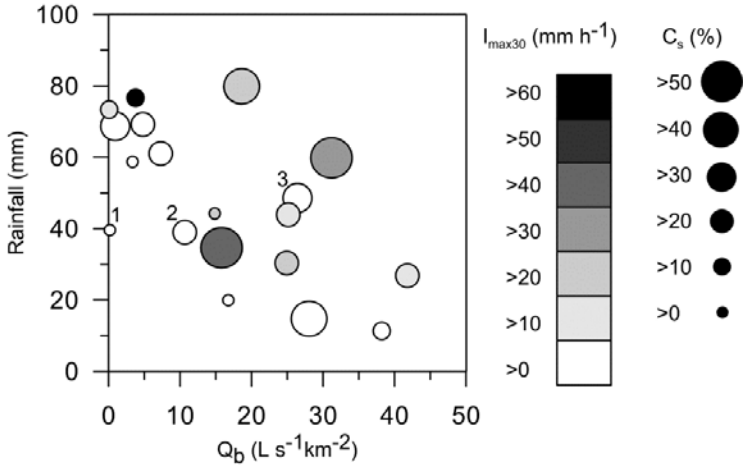

Fig. 2.5 Characteristics of the 19 rainfall-runoff events analysed. Pre-event discharge (Q_b) is shown on the x-axis; and rainfall on the y-axis. Dot size is proportional to the storm runoff coefficient (C_s) and the grey scale indicates rainfall intensity. Numbers refer to events analysed in Fig. 2.8.

Fig. 2.6 shows the ranked C_s of the 19 rainfall-runoff events analysed, and the WT_i and Q_b. In addition, Fig. 2.6 shows four variables ($WT_{increase}$, $t_{response}$, t_{peak} and $t_{peak-peak}$) characterizing the median (i.e. considering all piezometers) water table response during each rainfall-runoff event. There was significant correlation between Q_b and WT_i (r_s = 0.75, p < 0.01, Fig. 2.7(a) and Table 2.4). C_s correlated significantly with WT_i (r_s = 0.63, p < 0.01, Fig. 2.7(b) and Table 2.4) but not with Q_b. Finally, C_s correlated negatively with $WT_{increase}$ (r_s = -0.54, p < 0.05, Fig. 2.7 (c) and Table 2.4). These results suggest that the higher the water table was before a rainfall event, the greater the C_s was in response to a given rainfall. On the contrary, no correlation was found between C_s and the time variables ($t_{response}$, t_{peak} and $t_{peak-peak}$, see Fig. 2.6 and Table 2.4), showing (see Table 2.3) that these variables were much more closely related to the position of the water table before rainfall than to the magnitude of the runoff response.

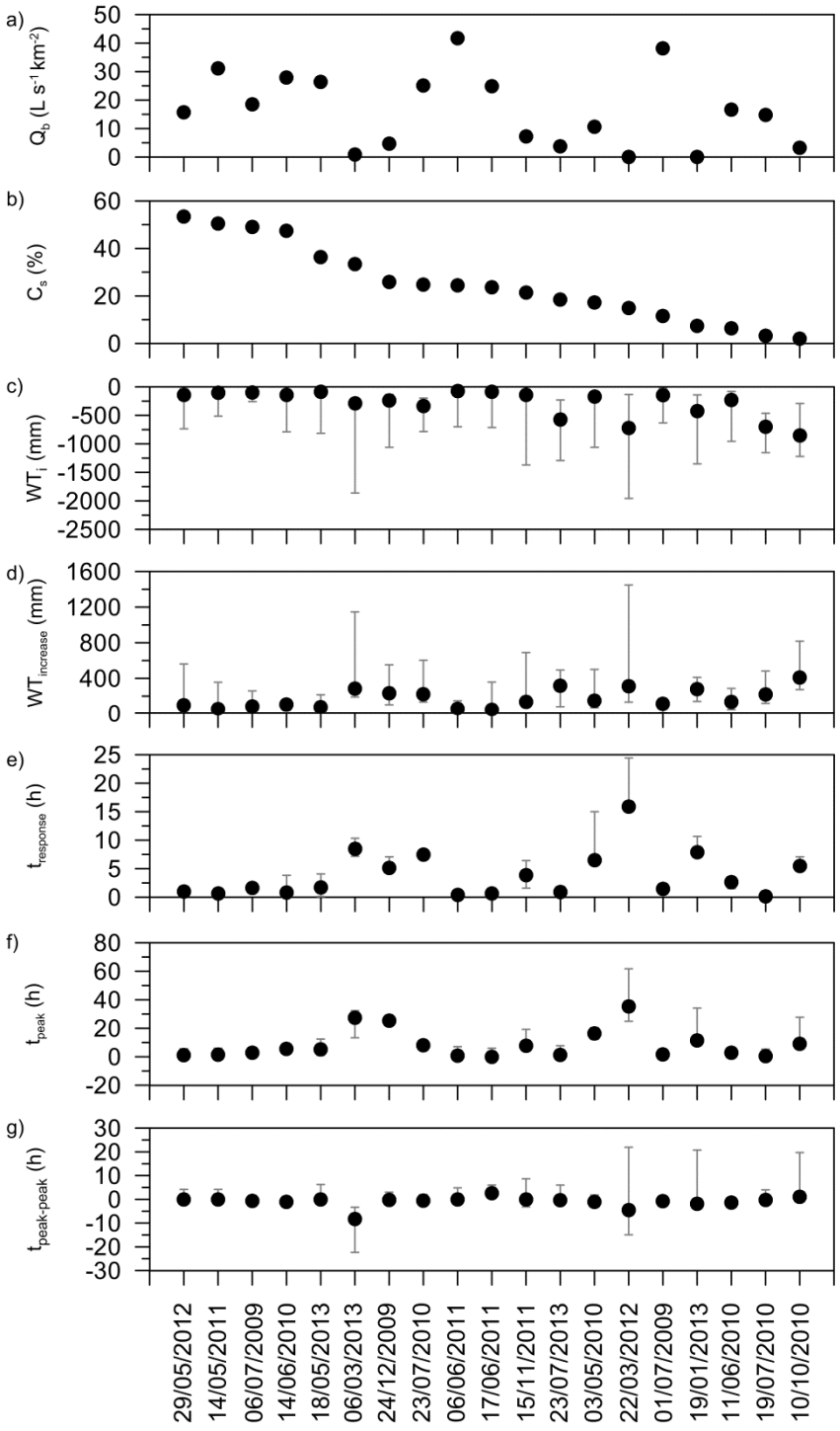

Fig. 2.6 (a) Pre-event discharge (Q_b) and (b) storm runoff coefficient (C_s) of the 19 rainfall-runoff events analysed. Median and quartiles (25% and 75%) of (c) pre-event depth to water table, (d) water table increase, (e) response time, (f) time to peak and (g) time lag between water table peak and discharge peak for each rainfall-runoff event at all piezometer locations. Rainfall-runoff events are ranked according to their storm runoff coefficient (C_s) value.

Table 2.4 Spearman rank correlation coefficient between the median pre-event depth to water table (WT_i), variables characterizing the water table response (median water table increase ($WT_{increase}$), median response time ($t_{response}$), median time to peak (t_{peak}) and median time lag between water table peak and discharge peak ($t_{peak-peak}$)) and rainfall-runoff event characteristics (pre-event discharge (Q_b) and storm runoff coefficient (C_s)).

	C_s	WT_i	$WT_{increase}$	$t_{response}$	t_{peak}	$t_{peak-peak}$
Q_b	0.40	0.75**	0.82**	- 0.66**	-0.60**	0.35
C_s		0.63**	-0.54*	-0.22	-0.95	0.19

Significance: **p<0.01; *p < 0.05

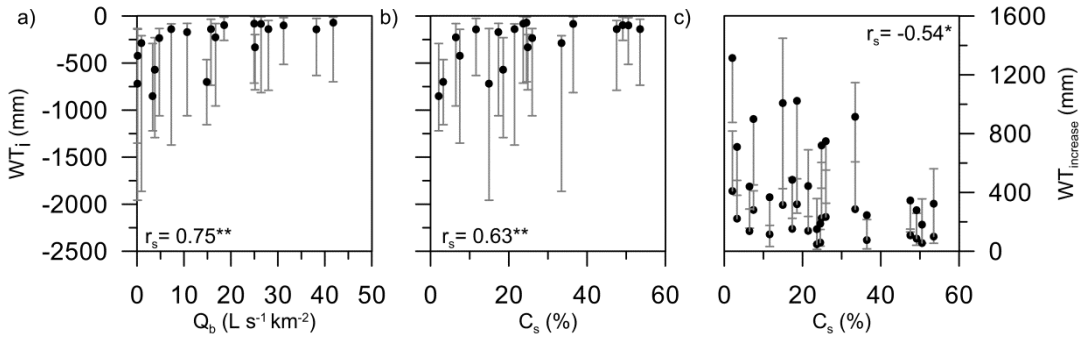

*Fig. 2.7 Relationship between the pre-event depth to water table and (a) pre-event discharge and (b) storm runoff coefficient. (c) Relationship between water table increase and storm runoff coefficient. Black dots are the median values and bars correspond to quartiles (25% and 75%). Significance:**p < 0.01; *p < 0.05; ns p > 0.05.*

2.3.4 Analysis of continuous water table dynamics during floods

To investigate further water table dynamics during floods, three floods that occurred under different antecedent wetness conditions were compared (Fig. 2.8). The three floods were characterized by similar rainfall amounts (39.1 to 48.8 mm) and precipitation intensities (3.5 to 8.0 mm h^{-1}), but by different antecedent wetness conditions, as shown by their different pre-event discharges (Q_b = 0.1, 10.7 and 26.4 L s^{-1} km^{-2}, respectively).

2.3.4.1 Water table dynamics during floods

The 19 January 2013 flood occurred during the dry winter season. Because of the dry antecedent conditions, the runoff response to the 39.6 mm rainfall was limited (Fig. 2.8(a)), as shown by the small C_s (7.5%). Median WT_i was -422 mm before the rainfall and saturation was not observed at any piezometer. Piezometers varied greatly for water table response: some reacted quickly to rainfall, some showed a delayed response and some had no response (Fig. 2.8(b)). Similar water table dynamics were observed for the six floods with low Q_b (floods one to six in Table 2.5 and Appendix B). Mean values of the median $t_{response}$, and t_{peak} for these floods were 7.3 and 18.4 h, respectively. However, there was some variability in the timing of the

water table response, as in the case of the 23 July 2013 event, where the high rainfall intensity (I_{max30} = 64 mm h^{-1}) yielded very small $t_{response}$ and t_{peak} values despite the low Q_b value.

The 3 March 2010 flood corresponded to intermediate antecedent conditions (Q_b = 10.7 L s^{-1} km^{-2}). The runoff response to the 39.1 mm rainfall was moderate (C_s = 17.4%) (Fig. 2.8(a)). Median WT_i was -169 mm and saturation was observed in one piezometer before the event. All piezometers reacted to the rainfall, but their responses were more or less delayed depending on the depth of the water table before the event (Fig. 2.8(b)). The observed water table dynamics during the six floods with intermediate antecedent conditions (floods 7 to 12 in Table 2.5 and Appendix B) were comparable. In this case, water table responses were quicker and mean values of the median $t_{response}$ and t_{peak} for these floods were 2.7 and 5.3 h, respectively. Again, high rainfall intensity (as for the 19 July 2010 event with I_{max5} = 84.0 mm h^{-1}) yielded smaller $t_{response}$ and t_{peak} values.

Finally, the 18 May 2013 flood occurred under wet conditions (Q_b = 26.4 L s^{-1} km^{-2}) and was characterized by a larger C_s (36.5%) (Fig. 2.8(a)). Median WT_i was -83 mm and saturation had been reached in three piezometers prior to the rainfall. All piezometers reacted quickly to the rainfall, but the dynamics of the response were different depending on the depth of the water table before the event (Fig. 2.8(b)). Quick water table reactions were observed almost systematically at all piezometers for floods in wet conditions (floods 13 to 19 in Table 2.5 and Appendix B); resulting mean values of the median $t_{response}$ and t_{peak} for these floods were 1.9 and 3.3 h, respectively. In this case, the variability observed in the timing of the water table response was also clearly related to the initial position of the water table, with higher $t_{response}$ and t_{peak} values for lower values of WT_i (i.e. deeper pre-event depth to water table).

2.3.4.2 Relation between the mean depth to the water table and its standard deviation

The mean depth to water table (20 minutes time step) was plotted against its corresponding standard deviation in order to characterize the variability of the water responses throughout the flood (Fig. 2.8(c)). At the start of the 19 January 2013 flood (dry antecedent conditions) the mean depth of the water table was -1,434 ± 754 mm. Both the mean depth to the water table and its standard deviation increased after the start of the rainfall. This increase lasted until the discharge peak, showing the great variability of the water table responses, with some piezometers reacting quickly to rainfall and others showing no response. After the discharge peak, the mean depth to the water table continued to increase slightly (due to the delayed response observed in some piezometers), but its standard deviation decreased, revealing a decrease in the spatial variability of the water table in the catchment, as it got wetter. Similar patterns of relationship between the mean depth to water table and its standard deviation were observed for all six floods with low Q_b. In some cases, however, the standard deviation of the depth to water table decreased shortly before the discharge peak was reached. Considering

all floods with low Q_b, the mean value of the depth to water table was -728 ± 798 mm, and the mean value of the depth to water table at the time of peak discharge was -677 ± 832 mm.

At the start of the 3 May 2010 flood (intermediate antecedent conditions) the mean depth of the water table was -866 ± 868 mm. After a very short period of increase in both the mean depth to the water table and its standard deviation following the start of the rainfall, the standard deviation of the water table decreased markedly. This decrease, combined with an increase in the mean depth to the water table continued long after the discharge peak, illustrating the reduction of the spatial variability of the water table in the catchment as all piezometers get wetter during the flood. Around one day after the discharge peak, the mean depth to the water table started to decrease slowly in most piezometers. This decrease in the mean depth to the water table was associated with a new rise in the standard deviation of the water table, which illustrates the re-increase of the spatial variability of the water table in the catchment during the recession period. Observed patterns between the mean depth to water table and its standard deviation were very similar for all six floods with intermediate Q_b, even if the mean value of the depth to water table during the flood varied between -912 and -308 mm. For all floods with intermediate Q_b, the mean value of the depth to water table was -554 ± 655 mm, and the mean value of the depth to water table at the time of peak discharge was -476 ± 693 mm.

Finally, at the start of the 18 May 2013 flood (wet antecedent conditions), the mean depth of the water table was -547 ± 666 mm. Both the mean depth to the water table and its standard deviation decreased shortly after the start of the rainfall. This decrease continued after the discharge peak, illustrating the reduction of the spatial variability of the water table in the catchment. After the discharge peak, the mean depth to the water table started to decrease. During the recession period, this decrease in the mean depth to the water table was associated with a rise in the standard deviation of the water table, which shows the increase in the spatial variability of the water table in the catchment. Similar patterns of relationship between the mean depth to water table and its standard deviation were observed for all seven floods with high Q_b and mean values of the depth to water table during the flood between -688 and -301 mm. Considering all floods with high Q_b, the mean value of the depth to water table was -456 ± 569 mm; and the mean value of the depth to water table at the time of peak discharge was -450 ± 617 mm.

Independently of the value of Q_b, the hysteresis of the relationship between the mean depth to the water table and its standard deviation was always anticlockwise, except for one flood (19 July 2010). Why this flood should show a clockwise relationship is not clear, but may be because of its extreme rainfall intensity (I_{max5} = 84 mm h^{-1}).

2.3.4.3 Discharge and mean depth to water table relationship

During the 19 March 2013 flood (dry antecedent conditions), an increase in the mean depth to water table of around 600 mm was observed before any rise in the discharge (Fig. 2.8(d)). In this case, the discharge increase was limited (42.8 L s^{-1} km^{-2}) and a small increase in the water table occurred during the recession period. The relationship between discharge and mean water table depth dynamics was similar for all six floods with low Q_b, with anticlockwise relationships and increases of mean depth to water table between 600 and 1,000 mm before any discharge increase (ranging from 42.8 to 1,914.8 L s^{-1} km^{-2}). Mean value of the median $t_{peak\text{-}peak}$ for these floods was -2.3 h (Table 2.5), being positive (i.e. peak discharge before median depth to water table peak) on only one occasion: for the 10 October 2010 flood that has the lowest value of median WT_i.

During the 3 May 2010 flood (intermediate antecedent conditions), the relationship between discharge and mean depth to water table was similar to the one observed for drier conditions. The only difference was that the increase in the mean depth to water table before a significant rise of the discharge was only around 200 mm (Fig. 2.8(d)). A similar relationship between discharge and mean water table depth dynamics was observed for all six floods with intermediate Q_b, with increases in mean depth to water table between 200 and 400 mm before any discharge increase. In all cases but one, observed relationships were anticlockwise and the mean value of the median $t_{peak\text{-}peak}$ for these floods was -0.5 h (Table 2.5), being equal to zero (i.e. peak discharge simultaneous to the median depth to water table peak) on two occasions.

Finally, the relationship between discharge and mean depth to water table during the 18 May 2013 flood (wet antecedent conditions) showed that there was an increase in the mean depth to water table of around 100 mm before the rise of the discharge (232.0 L s^{-1} km^{-2}) (Fig. 2.8(d)). A small increase in the water table occurred during the recession period, too. The relationship between discharge and mean water table depth dynamics was similar for all seven floods with high Q_b, with anticlockwise relationships and limited increases in mean depth to water table before any discharge increase. Mean value of the median $t_{peak\text{-}peak}$ for these floods was 0.1 h (Table 2.5), being equal to zero on three occasions.

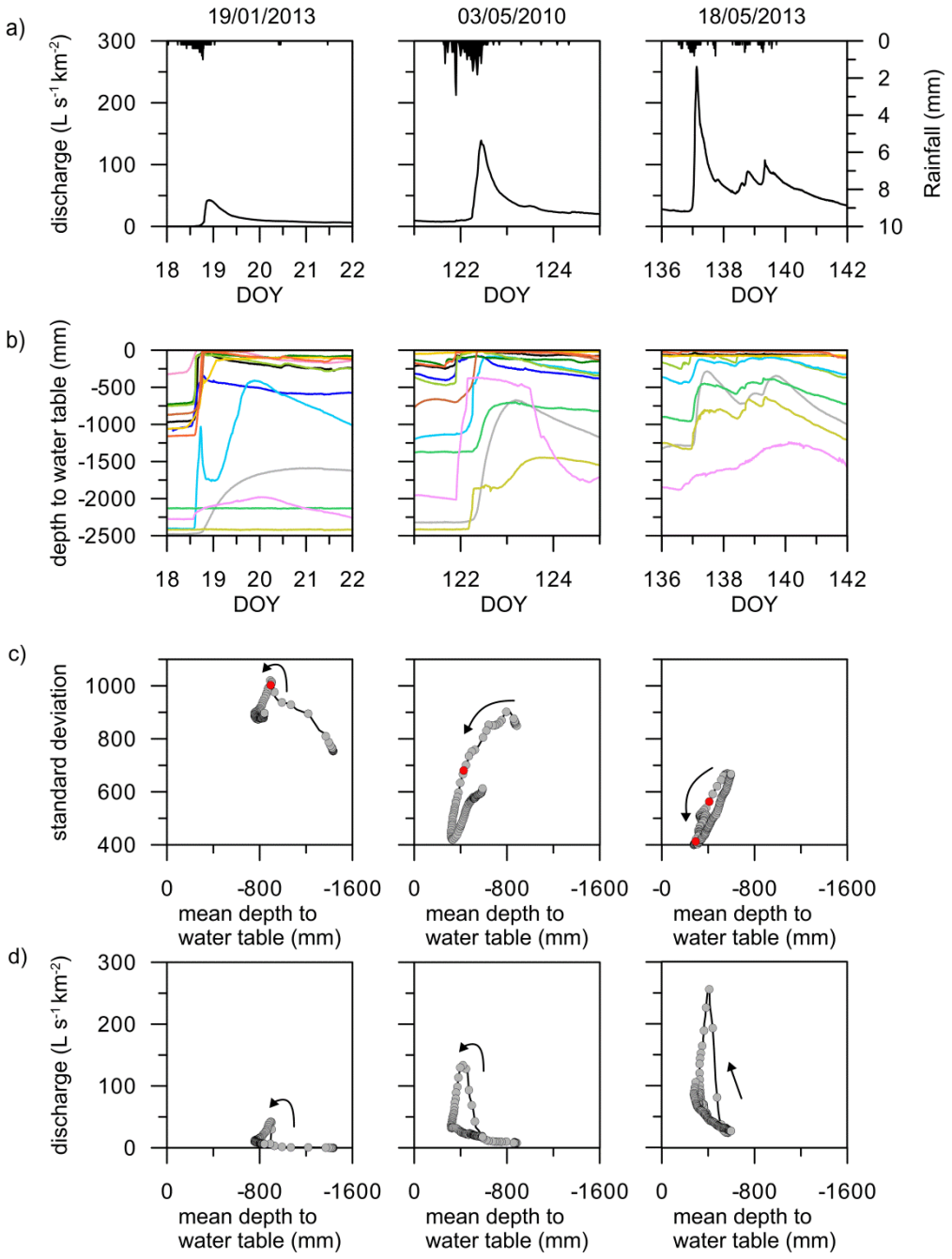

Fig. 2.8 (a) Rainfall and discharge and (b) depth to water table at the 13 piezometer locations, observed during three floods with different antecedent wetness conditions. (c) Relationship between the mean depth to water table and its standard deviation (red dots correspond to the time of peak discharge). (d) Relationship between the mean depth to water table and discharge (one hour time step).

Table 2.5 Characteristics of the rainfall-runoff events analysed in this study.

Event date	P	I_{max} 30	Q_b	Q_p	C_s	WT_i	$WT_{increase}$	$t_{response}$	t_{peak}	$t_{peak-peak}$	WT/Q
	(mm)	*(mm h^{-1})*	*(L $s^{-1}km^{-2}$)*	*(L $s^{-1}km^{-2}$)*	*(%)*	*(mm)*	*(mm)*	*(h)*	*(h)*	*(h)*	hysteresis
19/01/2013	39.6	8.0	0.1	42.9	7.5	-422	281	7.9	11.6	-1.8	A
22/03/2012	73.4	13.6	0.1	74.0	14.9	-718	315	15.9	35.4	-4.4	A
06/03/2013	68.8	6.4	0.9	279.4	33.5	-286	286	8.5	27.5	-8.2	A
10/10/2010	58.8	7.9	3.3	49.1	2.1	-849.5	411	5.5	9.2	1.2	A
23/07/2013	76.6	64.0	3.8	1,918.0	18.6	-570	320	0.9	1.4	-0.3	A
24/12/2009	69.2	6.3	4.8	524.7	26.0	-234	234	5.2	25.5	-0.2	A
Mean ± s.d.			*2.2 ± 2.0*		*17.1 ± 11.6*	*-513 ± 243*	*307 ± 59*	*7.3 ± 5*	*18.4 ± 13.0*	*-2.3 ± 3.5*	
15/11/2011	61.2	5.6	7.3	183.4	21.5	-139	139	3.9	7.9	0.0	A
03/05/2010	39.1	3.5	10.7	139.0	17.4	-169	152	6.5	16.5	-1.0	A
19/07/2010	44.2	21.8	14.9	101.4	3.3	-699	222	0.2	0.5	-0.2	A
29/05/2012	34.8	41.2	15.8	2,417.2	53.5	-139	101	1.0	1.2	0.0	A
11/06/2010	20.0	5.2	16.7	59.2	6.5	-225	138	2.7	3.0	-1.3	C
06/07/2009	79.9	27.9	18.5	5,511.1	49.1	-95	88	1.7	3.0	-0.6	A
Mean ± s.d.			*14.0 ± 4.2*		*25.2 ± 21.4*	*-244 ± 227*	*140 ± 47*	*2.7 ± 2.3*	*5.3 ± 6.0*	*-0.5 ± 0.6*	
17/06/2011	30.4	23.2	24.9	176.4	23.7	-81	47	0.7	0.0	2.7	A
23/07/2010	44.0	16.7	25.1	874.0	24.9	-332	225	7.5	8.2	-0.5	A
18/05/2013	48.8	6.8	26.4	258.4	36.4	-83	77	1.8	5.3	0.0	A
14/06/2010	14.9	1.0	28.0	292.7	47.5	-137	108	0.8	5.7	-1.0	A
14/05/2011	60.0	33.2	31.2	1,728.5	50.5	-99	57	0.7	1.5	0.0	A
01/07/2009	11.4	5.5	38.2	126.2	11.6	-142	115	1.5	1.7	-0.7	A
06/06/2011	27.0	16.4	41.8	325.0	24.5	-69	59	0.4	0.9	0.0	A
Mean ± s.d.			*30.8 ± 6.7*		*31.3 ± 14.1*	*-135 ± 91*	*98 ± 62*	*1.9 ± 2.5*	*3.3 ± 3.0*	*0.1 ± 1.2*	

P: rainfall; $I_{max}30$: maximum rainfall intensity (30'); Q_b: pre-event discharge; Q_p: peak flow discharge; C_s: storm runoff coefficient; WT_i: median pre-event depth to water table; $WT_{increase}$: median water table increase; $t_{response}$: median response time; t_{peak}: median time to peak; $t_{peak-peak}$: median time lag between water table peak and discharge peak; WT/Q hysteresis: loop direction of the hysteresis of the relationship between mean depth to water table and discharge (A: anticlockwise; C: clockwise); s.d.: standard deviation.

2.4 Discussion

At the Can Vila catchment, the piezometric response was highly variable in space and time during rainfall-runoff events. Even nearby locations sometimes showed distinct behaviour in terms of magnitude and timing. These results are consistent with those in other recent studies (Haught and van Meerveld, 2011; Bachmair et al., 2012; Penna et al., 2014).

2.4.1 Influence of location characteristics on depth to water table spatial variability

As noted, in recent papers (Penna et al., 2011; McMillan and Srinivasan, 2015), the study of the role of catchment characteristics is important if shallow water table spatial variability and dynamics are to be understood. In this study, however, none of the location characteristics (piezometer distance from the stream, TWI and elevation above the stream) correlated significantly with the pre-event depth to water table (WT_i). Despite this, the distance from the stream and the elevation above the stream (both significantly related (Table 2.2)) still have an influence on WT_i, with deeper water table levels observed at locations farther from and higher than the stream (Fig. 2.3). In contrast, as also observed by Detty and McGuire (2010) and McMillan and Srinivasan (2015), near-stream locations have the most persistent water table.

Despite being far from the stream channel (Fig. 2.1), locations Z_{CV11} and Z_{CV12} were usually saturated, with the water table usually less than -107 mm deep. An explanation for this particular behaviour is that these two locations, each in the central part of a terrace, are in fact placed close to the original course of the stream (i.e. the original stream position before the terrace construction). Currently, since the abandonment of agricultural practices in about 1960, the lack of maintenance of these artificial stream networks favours a gradual return of flow to its original path that promotes more frequent saturation of these two locations.

The Topographic Wetness Index controls the spatial distribution of water table at the catchment scale, as stated by many authors for wet environments (Jordan, 1994; Kendall et al., 1999; Rinderer et al., 2014; Rinderer, 2016). In the Arnás Mediterranean catchment, Lana-Renault et al. (2007) also found a strong linear correlation between TWI and the percentage of time that each piezometer was saturated. In this study no simple relationship was found between the TWI and the median pre-event depth to water table at each piezometer location (Fig. 2.3). This result is similar to those obtained by Detty and McGuire (2010) for landform groups of wells or individual well transects. A possible reason that makes it difficult to highlight a direct relationship between TWI and WT_i may be that the effect of topography is masked by other local characteristics of the piezometer locations, such as, in this study, the terraced topography that could influence local saturation patterns. These difficulties to generalizing findings about the effect of catchment characteristics on the distribution of wetness conditions have been discussed recently by Rinderer et al. (2016), who also expressed the difficulty of extrapolating results from one catchment to another.

2.4.2 Influence of location characteristics on water table response

Differences were observed in the groundwater response between piezometers located near and far from the stream, as also described in other hydrological studies (Seibert et al., 2003; Tromp-van Meerveld and McDonnell, 2006 b; Kuraś et al., 2008). In near-stream locations the WT_i was shallower and the water table reacted faster to rainfall, as shown by values of $t_{response}$ and t_{peak} (Fig. 2.4(a) and (b)). As Peters et al. (2003) argue, this rapid response may be partly attributed to the infiltration of streamflow generated on low permeable areas through the channel bottom, but may also result from groundwater contribution in downslope areas. In contrast, when WT_i was deeper in locations far from the stream, $t_{response}$ and t_{peak} were greater, partly because larger water table increases were observed (Fig. 2.2), as also shown by Peters et al. (2003). Furthermore, as also seen in other catchments (Daniels et al., 2008; Lana-Renault et al., 2014; Penna et al., 2014), at deeper WT_i the lag time between discharge peak and water table peak ($t_{peak-peak}$) was different at each piezometer, with longer and more variable lag time values (Fig. 2.4(c)). In corroboration of Haught and van Meerveld (2011), this result suggested that the locations far from the stream, characterized by deeper WT_i, reached peak later than discharge (positive lag time) and near-stream locations. The positive lag times in piezometers far from the stream imply that these locations were not main contributors to peak streamflow.

In a wet catchment in Switzerland, Rinderer et al. (2016) observed that topography exerts great control over groundwater response timing. In the Can Vila catchment, no such role for groundwater response timing was found, possibly because of the effect of the terraced topography on the saturation patterns within the catchment, as shown by Latron et al. (2008).

2.4.3 Water table response during rainfall-runoff events

The analysis of the water table response during rainfall-runoff suggested that pre-event depth to water table had an important role in runoff production. The runoff response was higher when pre-event depth to water table was close to the surface. These observations are consistent with previous studies in humid areas (Evans et al., 1999; Seibert et al., 2003; Daniels et al., 2008; Bachmair et al., 2012) and Mediterranean catchments (Lana-Renault et al., 2007; Latron et al., 2008).

The effect of the pre-event depth to water table on runoff production probably masked any influence of the water table timing variables. Indeed, no apparent relationships between runoff coefficient and timing variables were observed in the Can Vila catchment. This absence of relationships between the magnitude of the response and its temporal dynamic may be explained by both the effect of the temporal distribution of the rainfall (which may differ between events) on timing variables and the difficulty of defining clear timing variables for piezometers at saturation prior to the rainfall-runoff event.

Rainfall characteristics (amount and intensity) did not correlate with $WT_{increase}$ or with the temporal variables characterizing the water table response ($t_{response}$, t_{peak}, $t_{peak-peak}$). These observations are consistent with those reported in other hydrological studies (Tromp-van Meerveld and McDonnell, 2006b; Bachmair et al., 2012; Penna et al., 2014), showing that antecedent wetness conditions often weigh more in water table and runoff responses than the characteristics of the rainfall events.

2.4.4 Influence of antecedent wetness conditions

The analysis of the spatio-temporal variability in the water table response during rainfall-runoff events showed three different types of response in the Can Vila catchment, according to antecedent wetness conditions. This conclusion supports previous observations in small catchments (Lana-Renault et al., 2007; Penna et al., 2014), where the piezometric responses for floods that occurred during dry and wet conditions clearly differed.

2.4.4.1 Water table response in dry conditions

Under dry conditions, when pre-event discharge was low and the water table was deep, rainfall events generated only small runoff responses, as previously observed by Latron et al. (2008). A wide variability of water table responses was observed among piezometers, as in Bachmair et al. (2012), on the hillslope scale. Some piezometers did not show any response, whereas others responded quickly to rainfall, increasing the spatio-temporal variability. Similar results were observed in summer dry conditions in a Mediterranean catchment (Lana-Renault et al., 2007) and for intermediate conditions in an Alpine catchment (Penna et al., 2014). For summer conditions, McMillan and Srinivasan (2015) also reported a spatial disconnection between the water table and stream channel. In the Can Vila catchment, the spatial variability of the water table during dry conditions is mostly controlled by distance from the stream. Piezometers located far from the stream channel responded later than the stream discharge (i.e. anticlockwise loop) and also reached their maximum after the peak discharge (positive $t_{peak-peak}$ value). Apparently, as also observed by several authors (Kendall et al., 1999; Peters et al., 2003; Haught and van Meerveld, 2011), the water table at these locations did not contribute to streamflow or only contributed during the recession. On the contrary, piezometers closer to the stream showed negative $t_{peak-peak}$ values as well as clockwise hysteresis in the relationship between discharge and depth to water table. This shows that, during dry conditions, near-stream locations are probably the only relevant areas contributing to streamflow, whether by direct groundwater contribution or by promoting surface runoff to the stream once the water table reaches the ground surface.

2.4.4.2 Water table response in intermediate conditions

Intermediate conditions between dry and wet periods are common in Mediterranean areas (Gaillard et al., 1995; Grésillon and Taha, 1998; Latron et al., 2008). During intermediate antecedent conditions, storm runoff coefficients were moderate and the median pre-event depth to water table and discharge values were higher than under dry conditions. During intermediate conditions all piezometers responded to the rainfall, but with different timings, in line with the pre-event water table depth. In other catchments the spatial variability of the water table was reported to increase during intermediate conditions (Lana-Renault et al., 2007). In this study, however, the spatio-temporal variability of the water table throughout the rainfall-runoff event was lower than under dry conditions. In addition, the initial variability of the water table responses observed during intermediate conditions decreased rapidly during the flood, as most piezometers got wetter. This decrease in spatial variability during the flood is consistent with observations made by Penna et al. (2014), who reported that the spatial variability of depth to water table was higher during the rising limb than during the recession.

The relationship between discharge and depth to water table at each piezometer location was the same as under dry conditions, but $t_{peak\text{-}peak}$ values were lower (median values usually less than 1 h). Indeed, during intermediate conditions the water table response within the catchment followed broadly similar patterns as in dry conditions, with the piezometers located far from the stream channel responding later than the stream discharge and reaching their maximum after the peak discharge. However, water table contribution in all piezometers was faster than during dry conditions.

2.4.4.3 Water table response in wet conditions

In wet conditions, when pre-event discharge and water table were high, large runoff responses were observed in the catchment. With some piezometers already saturated at the start of the rainfall event and some relatively close to saturation, a quick reaction of the water table was observed almost systematically. Small values of the time variables ($t_{response,}$ t_{peak} and $t_{peak\text{-}peak}$) were observed, as well as low spatial variability of water table dynamics during the flood.

In wet conditions, the water table in piezometers located close to the stream reached its maximum at the same time as the stream discharge. As also observed in the "winter mode" by McMillan and Srinivasan (2015), water table responses all over the catchment were more connected to the stream channel under wet conditions. However, in piezometers located far from the stream, the relationship between discharge and depth to water table was still anticlockwise, showing that the water table responded later than the stream discharge. $t_{peak\text{-}peak}$ values in locations far from the stream remained positive, but were much smaller than for dry or intermediate conditions.

These results show that in the Can Vila catchment there are still some differences, during wet conditions, in the timing and dynamics of the water table response, depending on the locations. This heterogeneity of the piezometric response is similar to that described for other Mediterranean catchments (Lana-Renault et al., 2007), but is clearly higher than in other catchments where more homogeneous dynamics were observed during wet conditions (e.g. Penna et al., 2014).

2.5 Conclusions

This study analyses the spatio-temporal variability of shallow groundwater dynamics during rainfall-runoff events, including hydrological variables (rainfall, discharge, depth to water table, etc.) and the catchment's specific characteristics. The investigation took place at the Can Vila Mediterranean catchment, where depth to water table was measured at 13 piezometers during 19 rainfall-runoff events.

The data showed that depth to water table did not rise uniformly throughout the catchment. The spatial variability was controlled by piezometer location characteristics, especially the piezometer's distance from the stream, which has an effect on the distribution of wetness conditions within the catchment. This, in turn, affects the timing of the water table response.

The results also demonstrated that pre-event depth to water table and rainfall event characteristics affected runoff production. The investigation of depth to water table and discharge dynamics during rainfall-runoff events in different antecedent wetness conditions showed that in dry conditions the spatio-temporal variability of the depth to water table was high throughout the event, decreasing only when the catchment gets progressively wetter. In dry conditions, the storm runoff was generated essentially by the contribution of shallow groundwater located near the stream channel. During intermediate conditions, lower spatio-temporal variability of water table throughout the flood event was observed and all piezometers responded to rainfall but with different timing. However, in general, catchment water table dynamics were not so different from those observed in dry conditions, even if response times were shorter. During wet conditions, the water table pre-event was closer to the soil surface, which gave more homogenous groundwater responses. Rainfall-runoff events were characterized by larger runoff responses, with the water table in piezometers located near the stream channel reaching its maximum at the same time as the stream discharge.

These results contribute to improving our understanding of the hydrological functioning of the Vallcebre Mediterranean catchments. They detail further shallow water table dynamics and the role of antecedent wetness conditions on the runoff response to rainfall events. Despite monitoring improvements since earlier studies, further work is still required, especially to evaluate subsurface connectivity during the whole year by means of deeper piezometers.

CHAPTER 3

SEASONAL AND STORMFLOW DYNAMICS OF DISSOLVED ORGANIC CARBON IN A MEDITERRANEAN MOUNTAIN CATCHMENT (VALLCEBRE, EASTERN PYRENEES)

published in Hydrological Sciences Journal

Maria Roig-Planasdemunt[1], Pilar Llorens[1], Jérôme Latron[1]

[1] Institute of Environmental Assessment and Water Research (IDAEA), CSIC

3 SEASONAL AND STORMFLOW DYNAMICS OF DISSOLVED ORGANIC CARBON

3.1 Introduction

In hydrological studies, dissolved organic carbon (DOC) is increasingly considered an important stream water constituent of organic origin. It is scavenged by precipitation, enriched during throughfall and leached from organic matter, contained in soils or stored in the channel bed (Meyer and Tate, 1983; Baron et al., 1991). It is often affected by hydrological and biochemical processes operating within the catchment. For this reason, the study of DOC dynamics in different pools and at different time scales has been used in the last three decades to characterize water origin and flow components, with the objective of improving our understanding of catchment hydrological functioning (Mulholland and Hill, 1997; Kendall et al., 1999; McGlynn and McDonnell, 2003; Morel et al., 2009).

On the annual scale, DOC concentration in rainwater may show some seasonality (Pan et al., 2010; Verstraeten et al., 2014). However, rainfall or throughfall are not the main sources of DOC in soil solution (Verstraeten et al., 2014); and seasonality observed in soil water DOC concentration is indeed associated with the time sequence of different processes, both biochemical and hydrological ones, acting in soils. Higher concentrations are observed during the growing season, while lower concentrations follow DOC losses due to water fluxes during the wet period (Meyer and Tate, 1983; McDowell and Wood, 1984; Buckingham et al., 2008; Verstraeten et al., 2014). The decrease in DOC concentration with depth in the soil profile, as organic matter content decreases, implies low DOC concentration in groundwater (Boyer et al., 1997; Aubert et al., 2013). Besides, no clear seasonality is observed in deep soil water and groundwater DOC concentrations (Neal et al., 2005; Clark et al., 2008). Finally, even though DOC concentration in stream water has been studied mainly during storm events, several studies also showed some seasonality of stream water DOC concentration during the year (Evansa et al., 1996; Bernal et al., 2002; Neal et al., 2005; Dawson et al., 2011).

On the storm event scale, the vast majority of studies, in catchments under different climates, reported an increase in stream water DOC concentration with increasing discharge during rainstorm or snowmelt events. This general behaviour leads to a positive correlation between stream water DOC concentration and discharge and implies that the main export of DOC occurs during storm events (Meyer and Tate, 1983; Soulsby, 1995; Hinton et al., 1997; Butturini and Sabater, 2000; Carey, 2003; Neal et al., 2005; Stutter et al., 2012).

The increase in DOC concentration with increasing discharge is generally explained by DOC being flushed from the shallow soil horizons by rising water tables or by infiltrating rainfall (Meyer and Tate, 1983; McDowell and Likens, 1988; Hinton et al., 1998). McGlynn and McDonnell (2003) pointed out that in upland catchments, prior soil moisture conditions and the

degree of connection between runoff contributing areas and the stream may influence this increase in DOC concentration observed at the catchment outlet. The correlation between DOC concentration and discharge has therefore led some authors to use DOC as a tracer to identify the contribution of water from organic soil layers during storm events (Ladouche et al., 2001; Carey and Quinton, 2005; Morel et al., 2009). However, the flushing of organic matter stored in the streambed has also been identified as an alternative source of DOC in stream water (Mulholland and Hill, 1997; Meyer et al., 1998; Bernal et al., 2002), somehow questioning the use of DOC as a usefull tracer of water origin.

In the last 30 years, most studies of stream water DOC dynamics, both during storm events and throughout the year, have been carried out in humid (Hinton et al., 1997; Inamdar et al., 2004; Neal et al., 2005; Morel et al., 2009; Dawson et al., 2011), alpine (Baron et al., 1991; Boyer et al., 1997) and polar regions (Peterson et al., 1986; Ivarsson and Jansson, 1994; Hudon et al., 1996; Carey, 2003). However, as Llorens et al. (2011) comment, Mediterranean catchments have received less attention.

Regions with Mediterranean climate are characterized by strong intra- and inter-annual precipitation variability and a marked seasonality of the evaporative demand, which define the seasonality of this climate, characterized by a drier period during the year. As a consequence, Mediterranean catchments often share hydrological processes of both wet and dry environments (Gallart et al., 2002), which makes it harder to understand their hydrological and biogeochemical behaviour through the year (Latron et al., 2009, 2010a; Llorens et al., 2011).

Concentrations of DOC in, and export from Mediterranean pristine catchments fall into the low range of those measured worldwide (Alvarez-Cobelas et al., 2012). For example, Von Schiller et al. (2008) reported mean stream DOC concentrations of 1 ± 0.37 mg L^{-1} in five pristine catchments, located in northeastern Spain. However, different DOC dynamics have been observed in some Mediterranean catchments located very close to one another. The increase in stream water DOC concentration with increasing discharge described in the La Riera Major catchment (Butturini and Sabater, 2000) was less clear in the nearby Fuirosos catchment except for large events, suggesting for this catchment a change in the water pathways under wet conditions (Bernal et al., 2002). However, for both these catchments a clear increase in stream DOC concentration during the wetting-up period was reported, due to the leaching of organic matter accumulated on the streambed and the stream bank during the drought period (Butturini and Sabater, 2000; Bernal et al., 2002; Vázquez et al., 2007). This process, more specific of seasonal streams, probably contributes to increasing the diversity of DOC-discharge responses observed during storm events in Mediterranean catchments (Butturini et al., 2008).

This study, performed in the Can Vila research catchment (northeast Spain), focused on the analysis of DOC concentration dynamics in different water compartments (rainfall, soil water, groundwater and stream water) through the year and during storm events. The specific

objectives were (a) to characterize DOC dynamics in rainfall, soil water, groundwater and stream water during the year; (b) to analyse DOC dynamics during storm events to assess possible differences in the hydrological functioning of the catchment during the year; and (c) to discuss the validity of the use of DOC as a tracer to identify water sources during rainfall–runoff events in Mediterranean catchments.

3.2 Methods

3.2.1 Study site

This study was performed in the Can Vila research catchment, located in the Vallcebre research area (Latron et al., 2010a) at the headwaters of the Llobregat River, on the southern margin of the Pyrenees, northeast Spain (42°12′N, 1°49′E). The Vallcebre research area, managed by the Surface Hydrology and Erosion group (IDAEA-CSIC), was selected in early 1990 for the analysis of the hydrological consequences of land abandonment and the hydrological and sediment yield behaviour of badlands areas. A complete overview of the general hydrological findings can be found in Latron et al. (2009, 2010a, 2010b), Llorens et al. (2010a) and Gallart et al. (2010).

The Can Vila catchment (Fig. 3.1) has an area of 0.56 km^2. Elevations range from 1,458 to 1,115 m a.s.l. at the outlet, and slope gradients are moderate, with a mean value of 25.6% (Latron and Gallart, 2007). The soils that have developed over red clayey smectite-rich mudrocks are predominantly of silt-loam texture. Topsoils are rich in organic matter (on average 4.1% from 0 to 55 cm below the ground surface) and well structured, with high infiltration capacity, although hydraulic conductivity decreases rapidly with depth (Rubio et al., 2008). Before and during the 19th century most of the hill slopes of the catchment were deforested and terraced for agricultural purposes. They were abandoned during the second half of the 20th century. As a consequence of terracing, soil thickness ranges from less than 50 cm in the inner part of the terraces to more than 2 or 3 m in their outer part (Latron et al., 2008). Following land abandonment, spontaneous forestation by *Pinus sylvestris* has occurred (Poyatos et al., 2003) and forest now covers 34% of the catchment. The remainder of the catchment is widely covered by pasture and meadows. The main channel is a first order channel of 1 to 2 m wide and is not very deeply incised. The stream bed is a riffle-pool sequence, the materials being mostly formed by coarse alluvium partly cemented by lime coatings. Mobile sediments are mostly fine sands and silt. No riparian zone is observed in the catchment.

Climate is humid Mediterranean, with a marked water deficit in summer. The mean annual rainfall is 862 ± 206 mm, with a mean of 90 rainy days per year (Latron et al., 2009). Snowfalls account for less than 5% in volume. The rainiest seasons are autumn and spring. Winter is the season with the least precipitation. In summer, convective storms may provide significant

precipitation input. Mean annual temperature at 1,260 m a.s.l. is 9.1ºC and mean annual potential evapotranspiration is 823 ± 26 mm (Latron et al., 2010a).

The combined dynamic of rainfall and evapotranspiration favours the succession of wet and dry or very dry periods during the year (Latron and Gallart 2007, 2008). Dry and very dry periods occur in winter and summer, respectively, whereas wet periods correspond to spring and late autumn. Over the period 1995–2013, mean annual runoff in the Can Vila catchment was 302 ± 191 mm, representing 34% of rainfall (Latron et al., in prep.). Streamflow shows marked seasonality and often dries in summer for several weeks.

3.2.2 Hydrometric monitoring

Rainfall in the Can Vila catchment is recorded every 5 min by means of three 0.2 mm tipping-bucket raingauges (Casella Cel), located 1 m above the ground (Fig. 3.1). A standard meteorological station is located in the upper part of the catchment.

At the Can Vila gauging station, streamflow is measured by means of a 90º V-notch weir with a water pressure sensor (6542C-C, Unidata) connected to a datalogger (DT50, Datataker). Mean water level values (measured every 10 seconds) are recorded every 5 min and converted to discharge values with an established stage-discharge rating curve calibrated with manual discharge measurements (Latron and Gallart 2008).

Water table data used in this study were collected in two piezometers, Z_{CV08} (–422 cm deep) and Z_{CV35} (–206 cm deep) (Fig. 3.1). The water table level was recorded every 10 min by means of a water pressure sensor (10m MiniDiver, Schlumberger Water Services), adjusted with barometric pressure variations. Pressure sensors were calibrated by taking manual measurements of water table depth at the piezometers at the same time as data collection.

Soil water content data used in this study were obtained from a set of three automatic 30-cm-long time-domain reflectometry (TDR) probes (CS616, Campbell), inserted vertically from 0 to 90 cm depth (Fig. 3.1). The TDR probes were connected to a datalogger (DT500, Datataker) that recorded mean frequency values every 5 min. Frequencies were subsequently converted to soil water content values, using, for each probe, linear regression between frequency and soil water content obtained from weekly manual TDR measurements (Tektronix 1502-C cable tester) at the same depth intervals.

Soil temperature was measured (Termistor 107, Campbell) every 5 min at 20 cm depth close to the TDR profile.

3.2.3 DOC water sampling and laboratory analyses

Rainwater was sampled automatically, at 5 mm rainfall intervals, using an open collector (34 cm diameter) connected to an automatic water sampler (24 500-mL bottles, ISCO 2900). The rainfall sampling site is located at the outlet of the catchment (Fig.3.1). To eliminate the effect of the possible washing of the open collector at the beginning of rainfall, the first sample of rainfall events was discarded. The last rainfall sample was also excluded when less than 1 mm was collected.

Stream water was sampled at the gauging station with two automatic water samplers (24 1000-mL bottles, ISCO 2700). Both samplers were triggered by the datalogger (DT50, Datataker). One sampler took samples at variable time intervals (depending on water level changes), once a predetermined water level threshold, defining flood conditions, was reached. The other sampler took a daily sample at 00:00 h. Water samples were collected just after a rainfall–runoff event. In the absence of flood, only a weekly sample from the automatic sampler was kept.

In addition to rainfall–runoff automatic sampling, spatially distributed water samples were taken every two weeks, in order to characterize the seasonality of DOC sources. Soil water was sampled at two locations in the catchment (L_{CV01} and L_{CV02}, see Fig. 1), with a battery of suction cup lysimeters installed between 50 and 90 cm depth. The soil water sample at each location was a mix of the water collected at different depths. Groundwater was sampled at locations Z_{CV08} (422 cm deep) and Z_{CV35} (208 cm), at maximum piezometers depth, using a manual peristaltic pump. Finally, stream water was sampled manually (grab sample) at the gauging station.

During the study period, 958 samples were collected and analysed. This total corresponds to 187 rainwater, 92 soil water, 102 groundwater and 577 stream water samples. Of the stream water samples, 228 corresponded to flood conditions.

All samples were collected in 120 ml opaque muffled glass bottles and filtered in the laboratory through a 0.45-µm membrane filter (Millipore). Subsamples were then acidified with HCl (2 N) and stored at 4°C in cleaned and muffled glass bottles. DOC analyses were performed within one week.

The DOC concentration value was the average of three measurements for each sample, using a Total Organic Carbon Analyzer (TOC-VCSH/CSN, Shimadzu). The detection limit measured was 0.06 mg L^{-1}, following the method of Rubinson and Rubinson (2000).

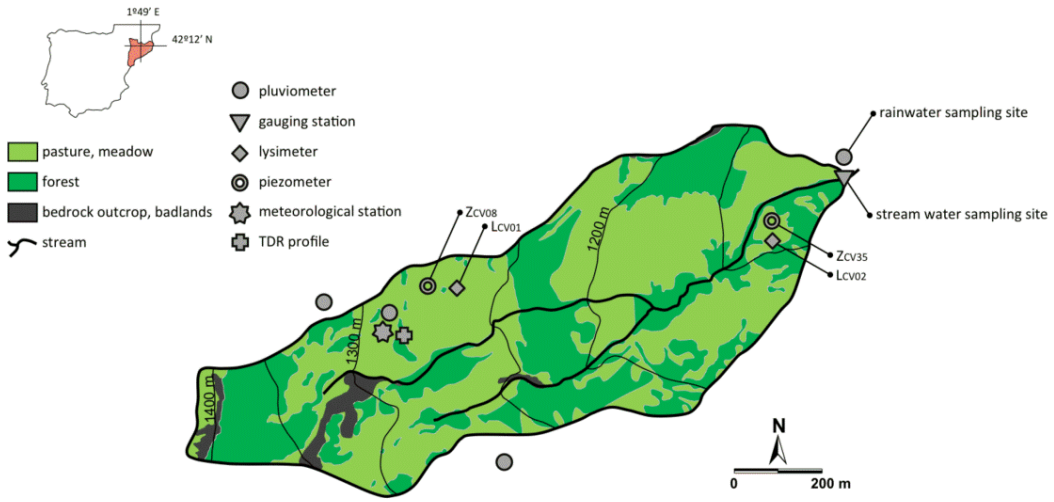

Fig. 3.1 Map of the Can Vila catchment, showing locations of the main instruments and of the sampling sites.

3.2.4 Data analyses

The study reported here, investigating both seasonal and event scale dynamics, is based on hydrometric and DOC data covering a 27-month period from May 2011 to July 2013. During this period, 11 significant rainfall–runoff events (i.e. with a peak discharge higher than 20.0 L s^{-1} km^{-2}) were recorded and sampled. At the event scale, storm runoff depth was derived for each selected significant rainfall–runoff event, using the classic "constant slope" hydrograph separation method of Hewlett and Hibbert (1967) with a modified slope value of 1.83 L s^{-1} km^{-2} d^{-1} (see Latron et al., 2008). For each rainfall–runoff event, several variables were finally derived from the hyetograph and hydrograph. These were rainfall depth, storm runoff coefficient, pre-event (at the start of the event) and peak flow specific discharges. At the event scale, the slope of the linear relationship between stream water DOC concentrations and specific discharges (at the time the samples were taken) was also determined. Soil water content, water table depth and stream water DOC concentration at the start and at the peak of the event were identified.

As DOC concentrations and dynamics throughout the year are likely to be influenced by temperature, biological activity and the hydrological conditions of the catchment, the data of the whole study period were grouped into four different periods, as in Bernal et al., (2005): a dormant period (December–March), a vegetative period (April–July), a dry period (August) and a wetting-up period (September–November). The correlation between variables was assessed by the Pearson correlation coefficient; the correlation was considered statistically significant if $p < 0.05$.

3.3 Results

3.3.1 DOC dynamics throughout the year

3.3.1.1 DOC dynamics in rainfall, soil water, groundwater and stream water

During the 27-month study period (May 2011 to July 2013), 41 rainfall events were sampled at 5-mm rainfall intervals. Events sampled ranged from 5.6 to 74.8 mm (median value: 24.2 mm), most of which occurred during the vegetative period (23 events). Eleven (11) rainfall events were sampled during the wetting-up period and seven during the dormant period. All events taken together gave a mean (± standard error) DOC concentration in rainwater of 1.1 ± 0.06 mg L^{-1}. The DOC concentration in rainwater followed a seasonal dynamic each year (Fig. 3.2), with higher DOC concentrations during the vegetative period (1.3 ± 0.08 mg L^{-1}). During the dormant period, the average DOC concentration was 0.5 mg L^{-1} lower than the mean value of the vegetative period (Table 3.1). The variability of DOC in rainwater during rainfall events was similar in all periods, with an average standard error of the mean close to 0.1 mg L^{-1}. Taking into account all rainfall events, no relationship between the mean DOC concentration in rainwater and rainfall depth or intensity (in 30 min) was found. The same result was obtained after grouping the rainfall events in periods.

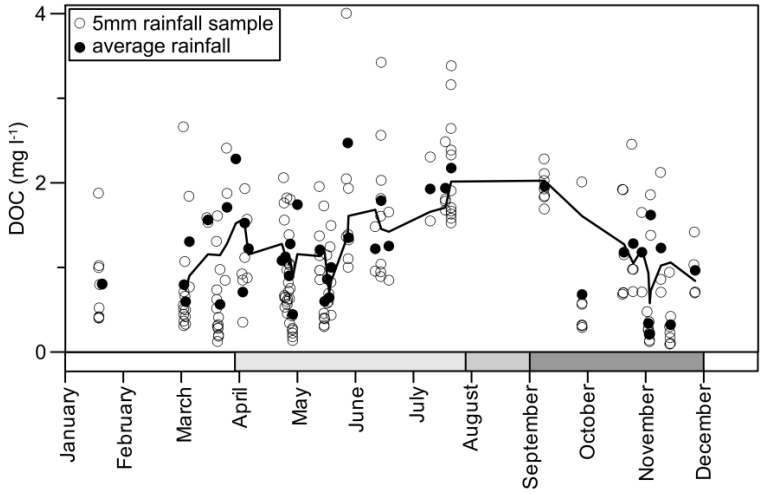

Fig. 3.2 Temporal dynamic of DOC concentration in rainwater during the study period (May 2011 to July 2013). White dots correspond to the concentrations of 5mm rainfall increment samples. Black dots correspond to the mean concentration of a rainfall event. The solid line is a running average. The colour scale on the x axis represents the dormant period, vegetative period, dry period and wetting-up period (see text).

From May 2011 to July 2013, mean DOC concentration in soil water was 6.5 ± 0.31 mg L^{-1} at L_{CV01} and 16.7 ± 1.42 mg L^{-1} at L_{CV02}. Despite the difference in the absolute values between the two sites, significant linear regression (r^2 = 0.53, p < 0.01) and a similar temporal evolution of soil water DOC concentration at both locations were observed. The seasonal dynamics of soil water DOC concentrations at L_{CV01} are shown in Fig. 3.3(b). The dynamics followed a sinusoidal trend (r^2 = 0.39, p < 0.01), with higher DOC concentrations during the vegetative, dry and wetting-up periods and lower concentrations during the dormant period (Table 3.1). This dynamic was similar to the soil temperature dynamic and inverse to the dynamic observed in soil water content. Thus, higher DOC concentrations occurred under dry soil conditions, when soil temperature was high (Fig. 3.3(a)). At $L_{CV01,}$ soil water DOC concentration correlated positively with soil temperature (r^2 = 0.36, p < 0.01) and correlated negatively, though slightly, with soil water content (r^2 = 0.16, p < 0.01). These relationships were not so clearly observable at L_{CV02}, partly because of the fewer samples collected.

Mean DOC concentration in groundwater was 2.9 ± 0.19 mg L^{-1} at Z_{CV08} and 5.6 ± 0.4 mg L^{-1} at Z_{CV35}. The DOC concentration absolute values and dynamics were different between the two sites. No clear seasonal dynamic of DOC concentration was observed (Table 3.1) and some of the lowest values of DOC concentrations were observed in all periods. At Z_{CV08} (but not at Z_{CV35}), groundwater DOC concentrations were strongly related to the dynamics of the water table and both variables correlated positively (r^2 = 0.37, p < 0.01), with an increase in DOC concentrations when the water table level rises (Fig. 3.3(c)). DOC concentrations down to 1.0 mg L^{-1} were measured when the water table was at its lowest (-3,500 mm), whereas they reached 6 or 7 mg L^{-1} when the water table was close to the surface.

The mean DOC concentration in stream water during the study period was 2.7 ± 0.05 mg L^{-1} at the catchment outlet. Considering only low flow conditions (specific discharge lower than 20 L s^{-1} km^{-2}), the mean DOC concentration in stream water was 2.1 ± 0.03 mgl^{-1}; whereas for flood conditions (discharge higher than 20 L s^{-1} km^{-2}), it was 3.5 ± 0.09 mg L^{-1}. The DOC concentration in stream water increased markedly during storms, up to values of 6 to 10 mg L^{-1} for larger flood peaks. Consequently, there was no apparent seasonality in stream water DOC concentration (Table 3.1). Changes in DOC concentrations appeared to be more influenced by stream discharge dynamics than by biological activity (Fig. 3(d)). For low flow conditions, DOC concentrations showed few variations and there was no seasonality in DOC concentration here, either. While there was a positive significant correlation between DOC concentration and discharge during flood conditions (r^2 = 0.47, p < 0.01, Fig. 3.4), for low flows a weak positive correlation was observed (r^2 = 0.08, p < 0.01).

Table 3.1 Mean DOC concentration (mg L^{-1}, ± standard error) measured in rainwater, soil water, groundwater and stream water over the whole study period and during the dormant, vegetative, dry and wetting-up periods (n is the number of samples analysed).

	Rainwater	Soil water		Groundwater		Stream water		
		L_{cv01}	L_{cv02}	Z_{cv08}	Z_{cv35}	Baseflow	Stormflow	Total
Total	1.1 ± 0.1	6.5 ± 0.3	16.7 ± 1.4	2.9 ± 0.2	5.6 ± 0.4	2.1 ± 0.0	3.5 ± 0.1	2.7 ± 0.0
	n = 187	*n* = 60	*n* = 32	*n* = 70	*n* = 32	*n* = 349	*n* = 228	*n* = 577
Dormant	0.8 ± 0.1	4.9 ± 0.3	9.4 ± 1.5	2.5 ± 0.4	5 ± 0.5	1.9 ± 0.1	4.4 ± 0.2	2.7 ± 0.1
	n = 42	*n* = 19	*n* = 10	*n* = 19	*n* = 13	*n* = 79	*n* = 39	*n* = 118
Vegetative	1.3±0.1	7.2 ± 0.5	20.5 ± 1.7	3.7 ± 0.3	5.9 ± 0.6	2.1 ± 0.1	3.4 ± 0.1	2.8 ± 0.1
	n = 96	*n*= 28	*n* = 17	*n* = 30	*n* = 17	*n* = 126	*n* = 149	*n* = 275
Dry	–	6.5±0.0	–	1.9 ± 0.3	–	1.4 ± 0.0	–	1.4 ± 0.0
	n = 0	*n* = 1	*n* = 0	*n* = 3	*n* = 0	*n* = 13	*n* = 0	*n* = 13
Wetting-up	1 ± 0.1	7.6 ± 0.8	18.8 ± 2.9	2.4 ± 0.3	6.8 ± 0.5	*2.3 ± 0.0*	3.1 ± 0.1	2.5 ± 0.1
	n = 49	*n* = 12	*n* = 5	*n* = 18	*n* = 2	*n* = 131	*n* = 40	*n* = 171

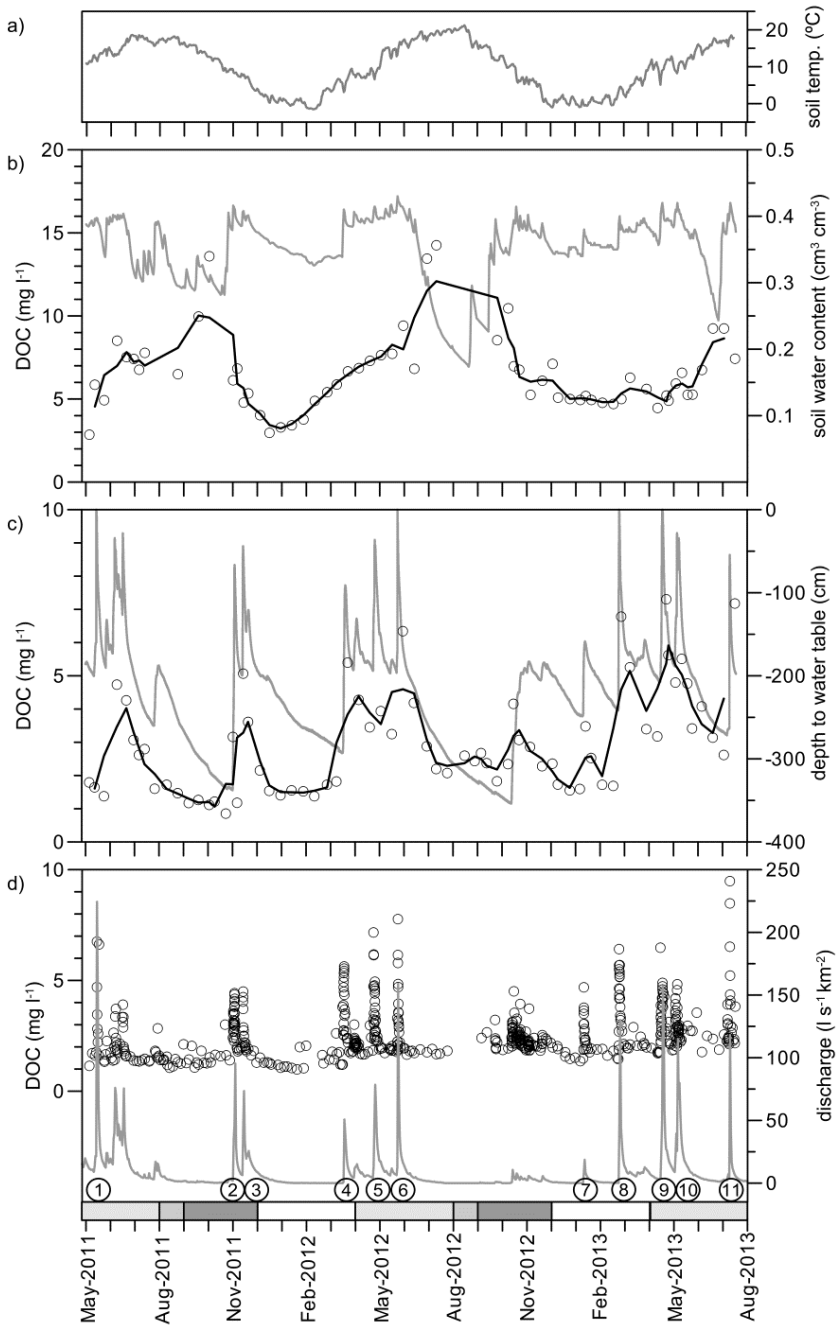

Fig. 3.3 Temporal dynamic (May 2011 to July 2013) of (a) soil temperature, (b) soil water content and DOC concentration in soil water (L_{CV01}), (c) depth to water table and DOC concentration in groundwater (Z_{CV08}) and (d) daily mean discharge at the outlet and DOC concentration in stream water. White dots correspond to samples DOC concentrations and black solid lines to running averages (three values). Numbers refer to floods sampled (see Table 3.2). The colour scale on the x axis represents the dormant period, vegetative period, dry period and wetting-up period (see text).

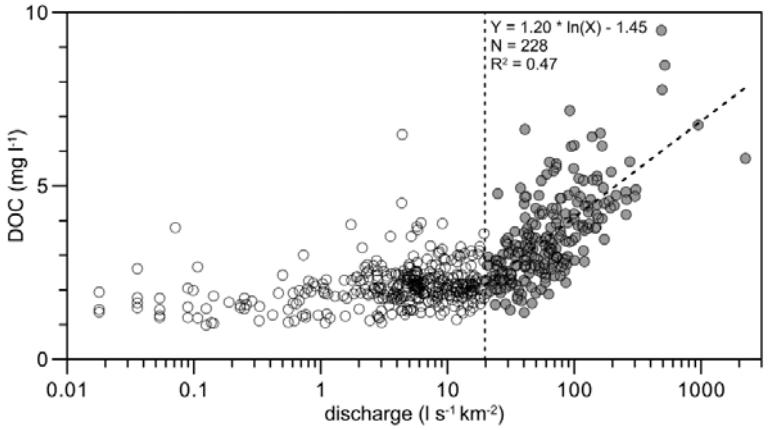

Fig. 3.4 Relationship between discharge measured at the outlet of the catchment and the DOC concentration in stream water. Two different dynamics are observable below and above a threshold of 20 L s^{-1} km^{-2}, roughly defining flood conditions.

3.3.1.2 Relationship between DOC concentrations in soil water, groundwater and stream water

As indicated in 3.3.1.1, there was a statistically significant linear relationship between soil water DOC concentrations measured fortnightly at the two sampling sites. However, no significant linear relationship existed between DOC concentrations measured at the piezometers, Z_{CV08} and Z_{CV35}.

On comparing the different water compartments at all sampling sites (using samples taken fortnightly), no significant linear relationships between soil water DOC concentrations and groundwater or stream water concentrations were found. On the contrary, a positive and statistically significant linear relationship between DOC concentration in groundwater and in stream water was found. This relationship was somewhat stronger for piezometer Z_{CV08} (r^2 = 0.42, $p < 0.01$, Fig. 3.5(a)) than for Z_{cv35} (r^2 = 0.13, $p < 0.01$). The relationship between the depth to the water table (Z_{CV08}) and the specific discharge (outlet of the catchment) at the time the samples were taken followed a semi-logarithmic trend (Fig. 3.5(b)).

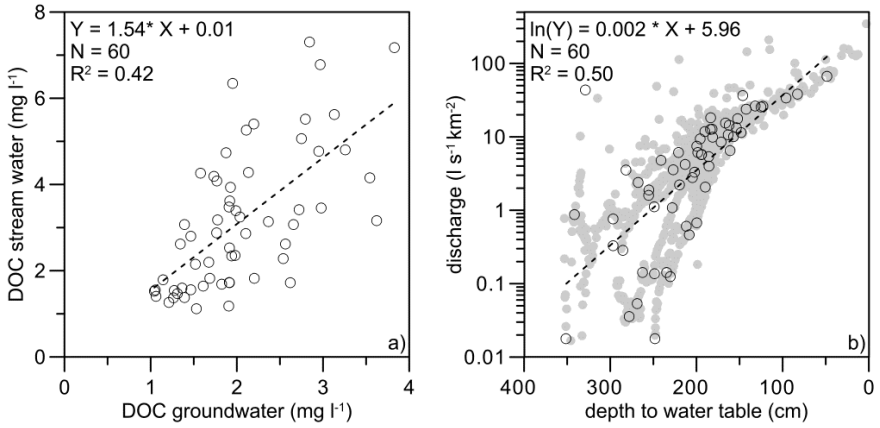

Fig. 3.5 (a) Relationship between DOC concentration in groundwater (Z_{CV08}) and stream water. (b) Relationship between mean daily values of depth to water table (Z_{CV08}) and discharge measured at the outlet of the catchment. White dots correspond to days when groundwater and stream were sampled for DOC.

3.3.2 DOC dynamics in the stream during rainfall–runoff events

Over the study period, all 11 rainfall–runoff events with peak discharge higher than 20 L s^{-1} km^{-2} were sampled (Fig. 3.3(d) and Appendix C). The sampled events (Table 3.2) cover a wide range of magnitude, with peak discharges ranging from 46.5 to more than 2400 L s^{-1} km^{-2} and runoff coefficients between 7.5 and 53.5%. Sampled events also covered a range of prior wetness conditions; with some occurring in dry conditions (19 January 2013) and some occurring in wet or very wet conditions (29 May 2012). Three floods occurred in the dormant period, six in the vegetative period and two in the wetting-up period.

Taking all floods together, a significant positive correlation existed between the increase in DOC concentration during the flood and the increase in discharge ($r^2 = 0.49$, $p < 0.05$). However, when taking the three larger events separately (with peak flow values four times higher than the rest of the floods), this correlation was no longer apparent ($r^2 = 0.03$, $p > 0.05$). Data from the 11 floods also revealed that the magnitude of the flood correlated significantly with prior wetness conditions. Indeed, a significant positive relationship existed between the storm runoff coefficient and the soil water content ($r^2 = 0.47$, $p < 0.05$) or the depth to the water table at the beginning of the flood (Z_{CV08} $r^2 = 0.48$, $p < 0.05$; Z_{CV35} $r^2 = 0.43$, $p < 0.05$). However, the change in stream water DOC concentrations was not clearly related to prior wetness conditions, and no significant linear relationship was found between the increase in DOC concentration during the flood and the soil water content ($r^2 = 0.13$ $p > 0.1$) or the depth to the water table at the beginning of the flood (Z_{CV08} $r^2 = 0.02$, $p > 0.1$; Z_{CV35} $r^2 = 0.01$ $p > 0.1$).

Table 3.2 Characteristics of the rainfall–runoff events sampled during the study period.

Event date	Period	P	Q_b	Q_p	C_s	WT pre-event	WT max	SWC pre-event	SWC max	DOC pre-event	DOC max	Slope DOC/Q	Slope DOC/Q	Slope DOC/Q
		(mm)	*(L s^{-1} km^{-2})*	*(L s^{-1} km^{-2})*	*(%)*	*(cm)*	*(cm)*	*(cm^3 cm^{-3})*	*(cm^3 cm^{-3})*	*(mg L^{-1})*	*(mg L^{-1})*	*1st peak*	*2nd peak*	*3rd peak*
14/05/2011	V	64.8	17.5	1,728.5	41.8	-160	0	0.39	0.40	1.7	6.8	0.005		
05/11/2011[a]	W	88.0	3.5	256.3	16.6	-337	-67	0.38	0.43	2.4	4.4	0.019	0.010	
15/11/2011	W	61.2	7.3	183.4	21.5	-199	-44	0.39	0.41	2.0	4.5	0.018		
22/03/2012	Do	73.4	0.1	74.0	14.9	-293	-91	0.34	0.41	1.2	5.6	0.051		
30/04/2012	V	75.2	4.5	174.8	27.3	-193	-36	0.39	0.41	1.8	7.2	0.050	0.020	
29/05/2012	V	34.8	15.8	2,417.2	53.5	-196	0	0.44	0.43	1.9	7.7	0.001		
19/01/2013	Do	39.6	0.1	46.5	7.5	-248	-159	0.34	0.38	1.5	4.7	0.058		
06/03/2013[a]	Do	68.8	0.9	279.4	33.5	-242	0	0.35	0.41	1.5	6.4	0.037	0.014	
29/04/2013	V	109.4	4.1	321.7	33.3	-206	0	0.36	0.39	1.8	4.9	0.040	0.010	
18/05/2013[a]	V	85.8	9.3	258.4	33.1	-1,863	-283	0.38	0.43	2.1	4.8	0.030	0.012	0.009
23/07/2013	V	76.6	3.8	1,918.0	18.6	-2,636	-546	0.39	0.42	2.1	9.5	0.012		

Period: V: vegetative, W: wetting-up, Do: dormant; P: rainfall; Q_b: discharge at the start of the flood; Q_p: peak flow discharge; C_s: storm runoff coefficient; WTpre-event: depth to water table (in piezometer Z_{CV08}) at the start of the flood; WTmax: highest level of the water table (in piezometer Z_{CV08}) during the flood; SWCpre-event: soil water content at the start of the flood; SWCmax: maximum soil water content during the flood; DOCpre-event: stream water DOC concentration at the start of the flood; DOCmax: maximum stream water DOC concentration during the flood; SlopeDOC/Q: slope of the linear relationship between stream water DOC concentration and discharge during a flood for the 1st, 2nd and 3rd peak. [a] : floods of Fig. 3.8

Further, significant positive correlation was found between the increase in DOC concentration during the flood and the initial (before the flood) DOC concentration in soil water at L_{CV01} (r^2 = 0.43, p < 0.05). However, it was not possible to confirm this finding for L_{CV02} due to the lack of data. The increase in DOC concentration during the flood was also related to the initial DOC concentration in groundwater at Z_{CV35}, even if the correlation was not significant (r^2 = 0.39, p > 0.05). No correlation was found with initial DOC concentrations at Z_{CV08} (r^2 = 0.06, p > 0.05).

During all floods, stream water DOC concentration followed the discharge pattern, increasing steadily during the hydrograph's rising limb, reaching the maximum concentration around peak flow and decreasing gradually during the recession (Fig. 3.6(a)). As a consequence of this dynamic, a mostly linear positive relationship between stream water DOC concentration and discharge existed for all events. The DOC concentration-discharge relationship showed some hysteresis (Fig. 3.6(b)), with higher values of DOC concentrations more frequent during the rising limb of the hydrograph than during the falling limb (i.e. positive hysteresis). Negative hysteresis was seen only during the three larger events (in terms of peak flow), characterized by an extremely rapid discharge increase (up to 650 L s^{-1} km^{-2} in 5 min).

Floods with two main discharge peaks (five events) showed that the slope of the relationship decreased from the first to the second peak (Fig. 3.6(b)). This indicated that, for a given value of discharge, stream water DOC concentration was always lower during the second discharge peak than during the first one. However, hysteresis observed at both peaks remained similar.

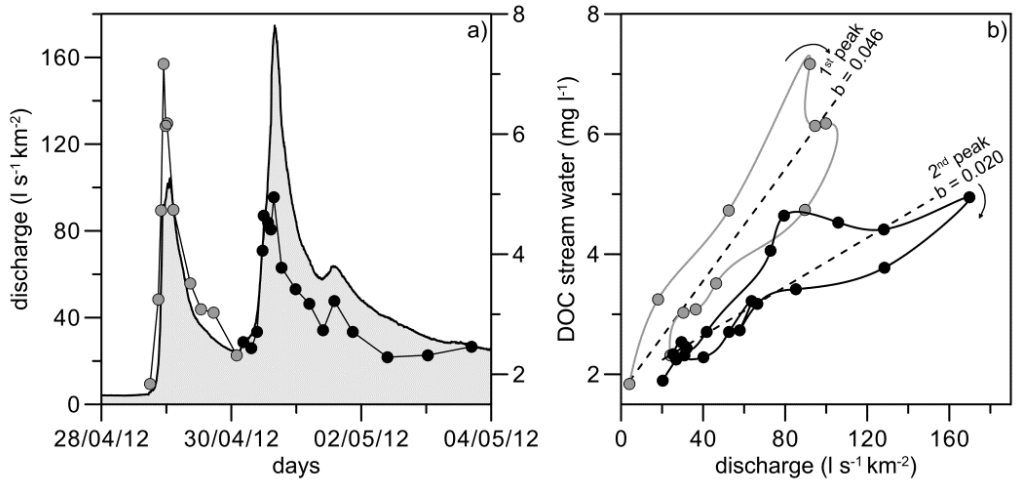

Fig. 3.6 (a) Discharge and DOC concentration in stream water during the two flood peaks of the 30 April 2012 event. (b) Relationship between discharge and DOC concentration in stream water throughout the event. (b) is the slope of the linear regression between discharge and DOC concentration.

The slopes of the DOC concentration–discharge relationship for all events (and all peaks) are shown in Table 3.2. Excluding the three larger events (with much lower slope values most probably related to the extremely rapid discharge increase), slope values ranged from 0.001 to 0.058 (first peak) and from 0.010 to 0.020 (second peak). The slopes of the DOC concentration–discharge relationship were similar during the dormant and vegetative periods (both for the first and second peaks) and lower for the first peak during the wetting-up period (Fig. 3.7).

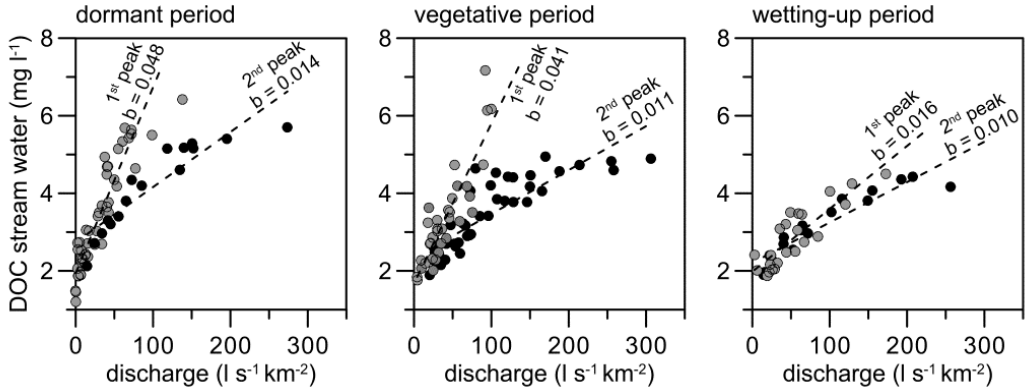

Fig. 3.7 Relationship between discharge and DOC concentration in stream water during dormant, vegetative and wetting-up periods. All data for the first and second peaks of floods observed during each of the periods were adjusted. (b is the slope of the linear regression between discharge and DOC concentration).

To investigate further the dynamics of DOC concentration during floods and to infer the possible causes of these dynamics, three floods that occurred in dormant, vegetative and wetting-up periods were compared (Fig. 3.8). The three floods were characterized by large rainfall amounts (68.8 to 88.0 mm) but by different prior wetness conditions, as shown by their different initial discharges (0.9 to 9.3 L s^{-1} km^{-2}).

The three floods presented a double peak with similar peak flow values (256 to 279 L $s^{-1}km^{-2}$) during the second peak. The dynamics of stream water DOC concentration during the three floods were comparable, following the discharge pattern and decreasing gradually during the recession (Fig. 3.8(a)). However, the DOC concentration-discharge relationship was different for the three floods during the first flood peak (Fig. 3.8(b)), with slopes of the relationship between 0.019 and 0.037. On the contrary, during the second peak (i.e. peak flow), the slopes of the DOC concentration–discharge relationship were much more similar (0.010 to 0.014). In all cases (first and second peaks) the DOC concentration–discharge relationship showed little positive hysteresis.

The dynamics of soil water content during the three floods showed a rapid response, regardless of the initial soil water content value. During the flood, soils were close to saturation in the vegetative and wetting-up periods, but not during the dormant period (Fig. 3.8(c)). The water table at Z_{CV35} showed a quick response during floods and reached temporary (wetting-up

period) or permanent (dormant and vegetative periods) saturation. The water table at Z_{CV08} showed a smooth delayed response during the three floods (i.e. limited response coinciding with the first flood peak, then reaching a maximum during the second flood peak), even if its magnitude was different for the three floods (Fig. 3.8(c)). In consequence, saturation at Z_{CV08} was only reached for the flood in the dormant period, whereas minimum water table depth was –283 and –666 mm for the floods in the vegetative and wetting-up periods, respectively.

The stream water DOC concentration–water table depth (Z_{CV08}) relationship showed for all floods (and all peak flows) positive hysteresis, indicating that the increase in DOC concentrations in the stream always preceded the rise of the water table at Z_{CV08} (Fig. 3.8(d)). No real differences were observed in this relationship between the different floods, even if the magnitude of the stream water DOC concentration increase differed between floods or in a single flood, between the first and the second peak flow. An opposite dynamic occurred in the stream water DOC concentration–soil water content relationship. For all floods (and all peak flows), negative hysteresis (i.e. soil water content increase always preceding the increase in DOC concentration in the stream) was observed (Fig. 3.8(e)). Again, this dynamic was common to all floods, regardless of the period considered and of the magnitude of the stream water DOC concentration increase.

Therefore, the results given in Fig. 3.8 imply a broadly similar dynamic of stream water DOC concentration during similar floods occurring in dormant, vegetative and wetting-up periods. Only the magnitude of the stream water DOC concentration increase during the first flood peak was found to be somewhat different. These results suggest that seasonality may not play a relevant role in stream water DOC concentration dynamics during rainfall–runoff events.

3.4 Discussion

3.4.1 Seasonal patterns of DOC

In the Can Vila catchment, as observed elsewhere (Meyer and Tate, 1983; Hinton et al., 1998; Michalzik et al., 2001; Neal et al., 2005; Morel et al., 2009), the concentration of DOC in rainfall was lower than in soil water, groundwater or stream water (Table 3.1). In this study, the mean annual DOC concentration in rainfall measured was 1.1 ± 0.06 mg L^{-1}, which was in the low range of mean DOC concentrations in precipitation observed in different European regions, where mean values were always lower than 2.5 mg L^{-1} (Morel et al., 2009; Verstraeten et al., 2014). Rainfall water DOC concentration showed, moreover, some seasonality, with higher values measured during the growing season (April-July) due to the increase in biological activity, as described by other authors (Pan et al., 2010; Verstraeten et al., 2014).

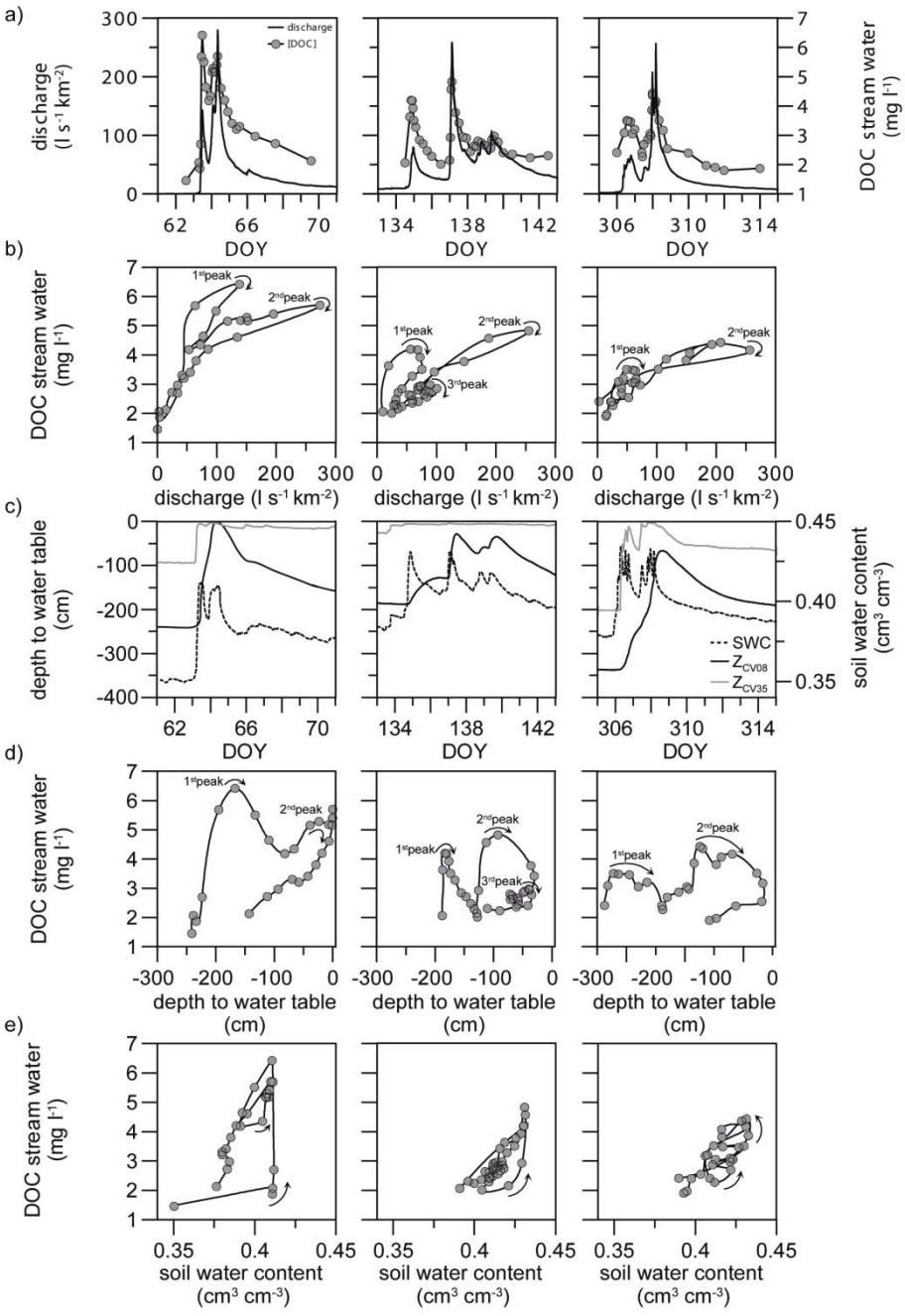

Fig. 3.8 a) Discharge and DOC concentration in stream water during three floods observed during dormant, vegetative and wetting-up periods. (b) Relationship between discharge and DOC concentration in stream water during the event. (c) Soil water content (SWC at 0–90 cm depth) and depth to the water table (piezometers Z_{CV08} and Z_{CV35}) during the event. (d) Relationship between the depth to the water table at ZCV08 and DOC concentration in stream water during the event. (e) Relationship between the soil water content (0–90 cm) and DOC concentration in stream water during the event. In (b), (d) and (e), arrows indicate the directions of the hysteresis for each flood peak.

The low DOC concentrations normally observed in rainfall have, therefore, a limited influence on soil water DOC concentrations (Verstraeten et al., 2014). In the study catchment, DOC concentrations were higher in soil water than in the other water compartments, in line with results generally reported (Meyer and Tate, 1983; Carey 2003; McGlynn and McDonnell, 2003; Inamdar et al., 2004; Morel et al., 2009). The mean concentrations observed at the two sampling locations (6.5 ± 0.31 mg L^{-1} at L_{CV01} and 16.7 ± 1.42 mg L^{-1} at L_{CV02}) are in the order of magnitude reported in several review studies in temperate areas (Buckingham et al., 2008; Wu et al., 2010; Camino-Serrano et al., 2014). These reviews do not include Mediterranean areas, but as the Can Vila catchment is a humid Mediterranean mountain area 1,100 m a.s.l., sharing characteristics of temperate environments during some periods of the year, it makes sense to compare Can Vila catchment DOC concentrations with those of temperate areas. Seasonal changes were observed in soil water DOC concentration. As in other studies (Meyer and Tate, 1983; McDowell and Wood, 1984; Buckingham et al., 2008; Verstraeten et al., 2014), the highest DOC concentrations were observed during the vegetative period till the end of wetting-up, i.e. the whole growing season (Fig. 3.3(b)). This DOC temporal variation reflects the succession of biochemical processes controlling DOC concentration in soils (Lambert et al., 2013), which are in turn affected by soil temperature (McDowell and Wood, 1984). Indeed, soil water DOC concentration and soil temperature had similar seasonal dynamics in the Can Vila catchment, with a positive statistically significant relationship between them (Fig. 3.3(a) and (b)). This effect of temperature on soil water DOC concentration has been described in several field and laboratory studies (Christ and David, 1996; Michalzik et al., 2001; Wu et al., 2010).

The mean groundwater DOC concentrations measured in Z_{CV35} (5.6 ± 0.4 mg L^{-1}) and Z_{CV08} (2.9 ± 0.19 mg L^{-1}) were slightly higher than concentrations observed in several Mediterranean and Temperate catchments (Butturini and Sabater, 2000; Neal et al., 2005; Vázquez et al., 2007; Aubert et al., 2013). The highest concentrations observed at Z_{CV35} may be explained by that, as it is a shallow piezometer (208 cm deep), its DOC concentrations are similar to those usually found in soil water. At Z_{CV08} DOC concentration showed some stratification with depth, with lower concentrations, closer to the values described in the literature (Neal et al., 2005; Vázquez et al., 2007; Aubert et al., 2013), when the water table level was deeper than 350 cm, as shown in Fig. 3.3(c), and explained by DOC retention within mineral soil horizons by sorption (Kalbitz et al., 2000). Additionally, the absence of seasonal variability in groundwater DOC concentration may be explained by the low effect of temperature and of biochemical activity at this depth, as observed in other catchments (Neal et al., 2005).

The mean stream water DOC concentration measured at Can Vila (2.7 ± 0.05 mg L^{-1}) was comparable to the values reported in Mediterranean and Temperate catchments (Butturini and Sabater, 2000; Bernal et al., 2002; Neal et al., 2005; Dawson et al., 2008). In the study catchment, DOC concentrations were higher during stormflow periods than during low flows, as observed in other streams (Meyer and Tate, 1983; Hinton et al., 1997; Bernal et al., 2005).

During storm events, DOC increased in the stream, probably due to the contribution of DOC–rich soil water, whereas during low flow periods DOC concentration in stream water was similar to the concentrations observed in groundwater (Table 3.1), suggesting that this was the main stream water source during low flows, especially during the dry period, as described by Schiff et al. (1997).

In the Can Vila catchment, as in other Mediterranean intermittent streams (Butturini and Sabater, 2000), it was not possible to identify the stream water DOC seasonality usually observed in catchments with low hydrological variability (Evansa et al., 1996; Neal et al., 2005; Dawson et al., 2011). This was probably related to the strong variability of the hydrological regime, characteristic of Mediterranean catchments, which masks possible seasonal variations of stream water DOC concentrations. The absence of seasonality in stream water DOC concentrations may also be explained by the positive relationship observed between DOC concentrations in stream water and in groundwater (Fig. 3.5), where no seasonality was observed, either.

3.4.2 DOC dynamics in stream water during rainfall–runoff events

During rainfall–runoff events, DOC concentration in Can Vila stream water rapidly increased with increasing discharge, leading to a positive relationship between stream water DOC concentration and discharge (Fig. 3.4). This relationship is consistent with patterns observed in both humid (Meyer and Tate, 1983; Hinton et al., 1997; Morel et al., 2009) and Mediterranean (Butturini and Sabater, 2000) catchments. The positive relationship between DOC concentration and discharge was less apparent during base flow conditions as observed in other catchments (Singh et al., 2014).

The little positive hysteresis observed in this relationship (except for the largest events) is also consistent with responses described in a set of Mediterranean catchments (Butturini et al., 2006).

For rainfall–runoff events with several peaks, the observed decrease of the slope of the DOC concentration-discharge relationship from the first peak to the following peaks (Fig. 3.6) and the rapid decrease in DOC concentration during the falling limb show that the DOC contribution was mainly flushed at the beginning of the event (during the first peak).

In the Can Vila catchment, the increase in stream water DOC concentration during floods suggests a relevant contribution of soil water (with higher DOC concentration), with storm water flowing through the upper organic soil layers, as suggested by several authors (Bishop et al., 2004; Laudon et al., 2011; McDowell and Likens, 1988; McGlynn and McDonnell, 2003). The rapid increase of DOC concentration in stream water in the Can Vila catchment always followed soil water content increase, but preceded the significant rise of the water table (Fig. 3.8(d) and (e)), reinforcing the idea of the relevant role of soil water. In fact, even if the absence of a

distinct riparian zone in the catchment, the combination of a higher hydraulic conductivity of the upper soils (Rubio et al., 2008) and a high DOC concentration in soil water (Table 3.1) can explain the rapid increase of DOC concentration in streamflow as described elsewhere (Bishop et al., 2004; Laudon et al., 2011).

Moreover, the synchronism found between DOC and the discharge peak could also indicates the possibility of stream water DOC sources near or in the stream bed during rainfall events, as suggested by several authors (Hinton et al., 1998; Butturini and Sabater, 2000; Bernal et al., 2002). The rapid DOC increase could correspond partly to the removal along the first flood peak of organic matter accumulated in the stream bed. In Mediterranean catchments, characterized by a succession of wet and dry periods during the year (Latron et al., 2009), several authors (Bernal et al., 2005; Vazquez et al., 2007; Von Schiller et al., 2015) indicated that the leaching of particulated organic matter accumulated in the streambed, specially following a dry period, can lead to a pulse of DOC in stream water. Indeed, the accumulation of particulated organic matter in these Mediterranean streambeds was estimated being 10 times greater after a dry spell, than during a wet year, with no flow interruption (Acuña et al., 2004).

In Can Vila catchment, the DOC dynamics in response to similar discharge events seem invariant through seasons (Fig. 3.8). Furthermore, DOC dynamics during floods were not related to prior wetness conditions, as already shown by Bernal et al. (2002) in another Mediterranean catchment. The non–changing behaviour of DOC dynamics during floods contrasts with the diversity of hydrological responses in the 11 floods included in this study. As shown in Table 3.2, peak discharges ranged from 47 to more than 2,417 L s^{-1} km^{-2} and runoff coefficients were between 7.5 and 53.5%. In addition, prior discharge, rainfall depth and rainfall intensity also differed greatly between sampled events. This changing and non–linear hydrological behaviour of the Can Vila catchment, described in Latron and Gallart (2007, 2008) and Latron et al. (2008), results mainly from the succession of dry and wet periods and the characteristic occurrence of wetting-up transitions between the two. The succession of these different periods increases the complexity of the rainfall–runoff relationship by triggering a different combination of hydrological processes, which depend on catchment wetness conditions.

The fact that rather similar dynamics of stream water DOC concentration were observed in all floods sampled in this study is apparently in contradiction with the observed to explain whether the systematic DOC concentration increase observed during floods results from various hydrological contributions (DOC–enriched surface runoff, soil water subsurface flow, etc.). This, in turn, would confirm that different combinations of dominant hydrological processes might lead to similar DOC dynamics during a flood; and that DOC sources and water flow paths cannot be easily inferred from catchment outflow concentrations alone, as shown by McGlynn and McDonnell (2003). For these reasons, more information is needed to use DOC as tracer to identify water sources during rainfall events in this mediterranean catchment. A better

understanding of DOC sources, and especially of the DOC transfer in the soil–stream continuum (Bishop et al., 2004), combined with the hydrological process–based knowledgement of the catchment, is necessary before using DOC as an environmental tracer for runoff processes identification.

3.5 Conclusions

This study provides detailed information on dissolved organic carbon (DOC) dynamics in a seasonal Mediterranean catchment. The data obtained on DOC concentrations in the different hydrological compartments, and at different temporal scales, give some insights into the factors that control DOC delivery to the stream.

The Can Vila catchment had some seasonality in rainwater and soil water DOC concentrations, which was related to biological activity. However, no clear seasonality was observed in stream water and groundwater, where DOC dynamics were closely related to discharge and water table variations.

During storm events, stream water DOC concentration followed the discharge pattern closely. However, in storm events with several discharge peaks a flushing of DOC during the first discharge peak and, in consequence, a reduction in DOC concentration at the following peaks were found. The increased stream water DOC concentration during floods suggests a relevant contribution of soil water, but also the existence of stream water DOC sources near or on the stream bed.

The similar stream water DOC dynamics during all the floods considered in this study clearly contrast with the diversity of their prior conditions (soil water content, rainfall characteristics…), as well as with the diversity of their magnitude (peak flow, storm-flow coefficient…). This contrast raises the question of the origin of the rapid DOC increase observed and confirms that water flow paths cannot be easily inferred from catchment outflow concentrations alone. The sampling of all water compartments during the flood (not only stream water) and the simultaneous use of other environmental tracers, especially isotopes, appear two interesting lines for future research, in order to advance in the identification of spatial and temporal sources of catchment runoff.

CHAPTER 4

MEAN TRANSIT TIME ESTIMATION USING STABLE ISOTOPES AND TRITIUM

part of this study is included in

Francesc Gallart[1], Maria Roig-Planasdemunt[1], Mike Stewart[2], Pilar Llorens[1], Uwe Morgenstern[3], Willibald stichler[4], Laurent Pfister[5] Jérôme Latron[1]. A glue framework to improve the analysis of catchment baseflows: a proof-of-concept study relying on tritium and tracer analytical errors.

submitted to Hydrological Processes

[1] Institute of Environmental Assessment and Water Research (IDAEA), CSIC
[2]Aquifer Dynamics and GNS Science
[3]GNS Science
[4]Helmholtz Zentrum Muenchen
[5]Luxembourg Institute of Science and Technology

4 MEAN TRANSIT TIME ESTIMATION USING STABLE ISOTOPES AND TRITIUM

4.1 Introduction

Mean transit time (MTT),or water age, is the time water spends travelling within the subsurface through a catchment to the stream network (see a review in McGuire and McDonnell, 2006). The MTT reflects the catchment's ability to retain and release water, which is a useful descriptor of its hydrological functioning. MTT have been estimated in a wide range of catchments worldwide using different tracers as Oxygen-18 (e.g. DeWalle et al., 1997), radioisotopes (e.g. Maloszewski and Zuber, 1982; Stewart and Fahey, 2010) or a combination of tracers (e.g. Dinçer et al., 1970; Uhlenbrook et al., 2002; Green et al., 2014; McCallum et al., 2014). Recently, the affordable acquisition of high-frequency tracer data (e.g. Birkel et al., 2012), long-term data (e.g. Tetzlaff et al., 2007) and high analysis precision (e.g. Morgenstern and Taylor, 2009) have helped to increase the number of MTT studies.

Oxygen-18 ($\delta^{18}O$) and Deuterium ($\delta^{2}H$) have been used typically, as natural tracers, to identify water sources during storm events (see a review in Klaus and McDonnell, 2013) and to estimate water MTT (see a review in McGuire and McDonnell, 2006). Water MTT have been estimated from the amplitude of the isotopes seasonal variations in precipitation and subsurface waters (e.g. DeWalle et al., 1997; Soulsby et al., 2000; McGuire et al., 2002; Rodgers et al., 2005; Viville et al., 2006; Mueller et al., 2013). These variations are mainly controlled by the fractionation that occurs during evaporation and condensation processes (Epstein and Mayeda, 1953). In some catchments stable isotopes seasonal variations have been clearly observed, suggesting shallow stream water sources subject to fractionation, especially in summer (Durand et al., 1993). However, the isotope seasonal amplitude in subsurface water (and stream water) is damped compared to the one of the precipitation input (e.g. O'Driscoll et al., 2005; Birkel et al., 2011; Kirchner, 2015). As a result, stable isotopes are more suitable for dating waters younger than 4-5 years. For older waters, the amplitude of the output signal becomes narrow providing unreliable water ages (McGuire and McDonnell, 2006; Stewart et al., 2007; Stewart et al., 2010; Kirchner et al., 2015).

Tritium isotope (^{3}H) is a radioisotope that allows the estimation of water MTT in a catchment since this isotope is deposited with rain. Cosmogenic sources produce small tritium concentration in the atmosphere. However tritium concentration was augmented by nuclear weapons testing in the 1950s and 60s, mainly in the North hemisphere (NH). Since then the NH atmospheric concentration has tended to return close to natural concentrations, except in some regions with important nuclear industry (Rozanski et al., 1991). Despite that tritium decays (12.32 years), tritium concentration due to nuclear weapons still remains in older groundwater

systems in the NH (Michel el al., 2015), causing ambiguity in current MTT estimations. In the Southern hemisphere (SH) tritium dating is more straightforward (e.g. McGlynn et al., 2003; Stewart and Fahey, 2010; Stewart et al., 2010) and the smaller tritium concentration in the atmosphere impulses the development of high precision tritium measurements (Morgenstern and Taylor, 2009). Tritium concentrations distribution in the atmosphere changes depending on the latitude, altitude and the influence of the maritime moisture (Rozanski et al., 1991). For instance, coastal locations have lower tritium content because it is diluted by the influence of maritime moisture. Tritium have been commonly used to calculate water ages up to 100 years, because its decay covers several half-lives (McGuire and McDonnell, 2006; Stewart et al., 2007, Stewart et al., 2010).

The MTT is usually calculated using a lumped-parameter model (LPM) that relates the tracer input and output concentrations. MTT estimations depend on an input tracer function and a flow model, which describes the tracer transport through hydrological systems (Maloszewski and Zuber, 1982). The models assume the flow pattern to be in steady state. Therefore, currently the studies calculate the mean transit time at baseflow conditions (McGuire and McDonnell, 2006). The input tracer function represents the tracer that enters the system. It depends on: tracer concentration, precipitation volume and proportion of precipitation that reached the hydrological system.

In the literature, the lumped-parameter model most commonly used is the exponential-piston flow model (EPM) which combines a portion of an exponential flow model (EM) and a piston flow model (PFM) (Maloszewski and Zuber, 1982). The piston flow model assumes that all flow paths have the same transit time and there is no dispersion, then the tracer concentration only changes by radioactive decay. The exponential flow model considers that there is an exponential distribution of transit times (Maloszewski and Zuber, 1982). Then EPM model describes a system with an exponential distribution of transit times, but delayed in time because a proportion of the model is a piston flow model (McGuire and McDonnell, 2006). Other models used are the dispersion model (e.g. Maloszewski and Zuber, 1982; Uhlenbrook et al., 2002) that considers the dispersion of tracers throughout the system and the probabilistic gamma model (e.g. Soulsby et al., 2010; Hrachowitz et al., 2010; Hrachowitz et al., 2011; Birkel et al., 2012).

The identification of the most appropriate model type for each catchment and the optimal model parameters can be difficult (e.g. Mueller et al., 2013) as the structure of the hydrological system is rarely observable. Additionally, other issues complicate the water MTT estimation and increase the uncertainty of the water age modeling. The most common issues are related to the usually short length of the input data records, the lack of tracer input concentration data, the uncertainty of the recharge function, the analytical measurement errors, or the sampling frequency (McGuire and McDonnell, 2006). There have been different attempts to solve the

issue of short input data records using water stable isotopes. Some studies extended artificially the stable isotopes input data (e.g. Uhlenbrook et al., 2002; McGuire et al., 2005; Viville et al., 2006) others used stable isotopes sine-wave regression models (e.g. McGuire et al., 2002; Rodgers et al., 2005). To face the lack of tracer input concentration data, studies use data from nearby stations which has long-term records. For instance, Herrmann et al. (1999) used tritium data from IAEA (International Atomic Energy Agency) network stations.

Even if authors are generally aware of the uncertainty associated with water age modeling, derived from the issues mentioned above (e.g. McGuire and McDonnell, 2006; Jódar et al., 2014), only few studies have explicitly considered the uncertainty, with the exception of the works of Soulsby et al. (2010) and Timbe et al. (2014) who used a Monte Carlo methodology to constraint model parameters. Mueller et al. (2013) also considered the uncertainty generated by the input tracer function (precipitation volume, recharge, stable isotopes signals). However, considering at the same time, the uncertainty associated to model parameters and to input rainfall and output samples (analytical errors) still remains a challenge in current water age modeling studies.

Finally, there is also interest about the influence of catchment characteristics (e.g. topography, geology, soil type, basin size…) on water age spatial distribution. Some authors found that water age could be affected by the topography and the storage capacity of the ground (soil and bedrock) (e.g. Rodgers et al., 2005; McGuire et al., 2005; Soulsby et al., 2006; Morgernstern et al., 2014). In contrast, McGlynn et al. (2003) and Mueller et al. (2013) did not observe any effect of basin size or vegetation cover on water age distribution.

This study, performed in the Vallcebre research catchments (NE Spain), focuses on water mean transit time estimation in different water compartments: stream, springs and wells. The specific objectives of this work are: (a) to estimate water MTT using stable isotopes; (b) to perform a complete uncertainty analysis of MTT estimation using tritium and different sample designs; (c) to compare present and former (Herrmann et al., 1999) water MTT estimation in the same catchment; (d) to understand spatial water MTT variability.

4.2 Methods

4.2.1 Study area

This study has been carried out in the Vallcebre research area at the headwaters of the Llobregat River, 90 km from the sea, on the southern margin of the Pyrenees, NE Spain (42°12’ N, 1°49’ E). The Vallcebre research area, managed by the Surface Hydrology and Erosion group (IDAEA-CSIC), was selected in early 1990 to analyse the hydrological processes of Mediterranean mountain areas, the consequences of land abandonment on the hydrological response, as well as the sediment dynamics and transport of eroded areas.

The Cal Rodó catchment (4.17 km^2), where this study was carried out, includes the Can Vila (0.56 km^2) and Ca l'Isard (1.32 km^2) sub-catchments (Fig. 4.1).

In the Cal Rodó catchment, mean altitude is 1,300 m above sea level and the slope gradients is between 10% and 40% (mean value 28%) and have mostly north-east orientation. The soils have developed over the bedrock formed by red lutites with some sandstone, gypsum and limestone. Under this layer a limestone bed, from the Palaeocene, outcrops in the southern part of the catchment. Most of the hill-slopes of the catchment were deforested and terraced for agricultural purposes in the past and abandoned during the second half of the 20th century. As a consequence of terracing, soil thickness ranges from less than 50 cm in the inner part of the terraces to more than 2 or 3 m in their outer part (Latron et al., 2008). Following land abandonment, spontaneous forestation by *Pinus sylvestris* has occurred (Poyatos et al., 2003) and pine forest patches represented, in 2003, about 60% of the Cal Rodó catchment (34% of the Can Vila catchment). The remainder of the catchment is widely covered by pastures and meadows. The main streams are 1 to 3 m wide and are not very deeply incised. No riparian zone is observed in the catchment.

Climate is humid Mediterranean, with a marked water deficit in summer. The mean annual rainfall is 862 ± 206 mm, with a mean of 90 rainy days per year (Latron et al., 2009). Winds are pronominally from south-west direction. Snowfalls account for less than 5% of total annual rainfall. The rainiest seasons are autumn and spring. Winter is the season with the least rainfall. In summer, convective storms may provide significant precipitation inputs. Mean annual temperature at 1,260 m a.s.l. is 9.1ºC and mean annual potential evapotranspiration is 823 ± 26 mm (Latron et al., 2010a).

The combined dynamic of rainfall and evapotranspiration favours the succession of wet (late autumn and spring) and dry periods (winter and summer) during the year (Latron and Gallart, 2007; 2008).

4.2.2 Location characteristics

The metrics for each sampled location were obtained from the 5 m resolution digital elevation model (DEM) of the catchment, provided by the Institut Cartogràfic de Catalunya. The Topographic Wetness Index (TWI) (Beven and Kirkby, 1979) and the slope were calculated using the open source software SAGA-GIS.

4.2.3 Hydrological data

Rainfall series for the period 1953-2013 was calculated correlating the following data: (a) Data from the Spanish Meteorological Agency (AEMET) station located at Berga (664 m a.s.l), 11.5 km away from the catchment for the period 1953-1982, (b) data from an AEMET

pluviometric station located at Vallcebre (1,121 m a.s.l.) for the period 1982-1989, and (c) data measured at the Vallcebre research catchments during the period 1988-2013.

In the same way, temperature series was calculated correlating: (a) Data from La Molina station (1,704 m a.s.l), located at 17.3 km from the study area, during the period 1953-2002 and (b) data measured at the Vallcebre research catchments during the period 1989-2013. The Potential Evapotranspiration (PET) was calculated using the Thornthwaite (1948) equation from the temperature series.

During the 1953-2013 periods, the mean annual rainfall of the synthetic series was 907 mm and the potential evapotranspiration was 712 mm.

Streamflow was measured at the Can Vila (CV) gauging station (Fig. 4.1), by means of a 90° V-notch weir with a water pressure sensor (6542C-C, Unidata) connected to a datalogger (DT50, Datataker). Mean water level values (measured every 10 seconds) were recorded every 5 minutes and converted to discharge values with an established stage-discharge rating curve calibrated with manual discharge measurements (Latron and Gallart, 2008).

4.2.4 Water sampling

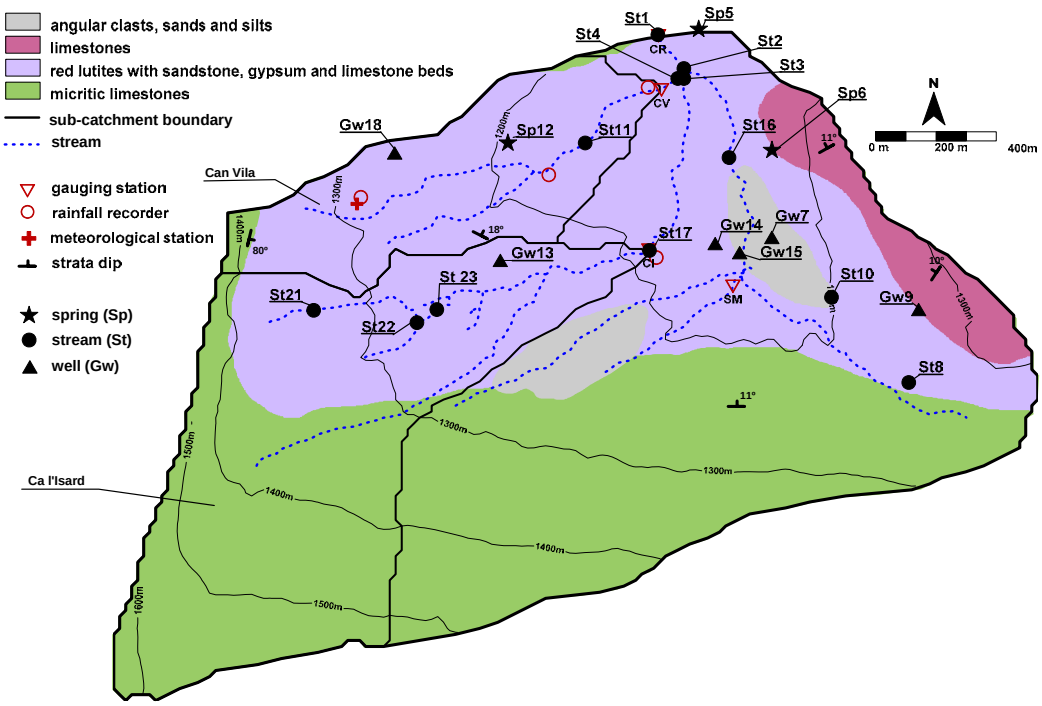

Fig. 4.1 Map of the Cal Rodó catchment and subcatchments (Can Vila and Ca l'Isard) showing the geological characteristics, the stream network, the monitoring design, and the sampling locations (springs, streams and wells).

4.2.4.1 Stable isotopes

Water for stable isotopes ($\delta^{18}O$ and $\delta^{2}H$) analysis was sampled from one spring (Sp12 on Fig. 4.1), one well (Gw18) and in rainfall and stream water at the outlet of the Can Vila sub-catchment from May 2011 to July 2013.

Rainwater was sampled automatically, at 5 mm rainfall intervals, using an open collector (340 mm diameter) connected to an automatic water sampler (24 500-mL bottles, ISCO 2,900). With all samples collected during the week, a weighted weekly sample was prepared in the laboratory.

Stream water was sampled daily at Can Vila gauging station using an automatic water sampler (24 1000-mL bottles, ISCO 2,700) triggered by the datalogger (DT50, Datataker). Stream water was also sampled manually (grab sample) at the gauging station, every two weeks. A weekly sample was analysed.

Water in spring Sp12 and well Gw18 was sampled every two weeks, manually (grab sample) and using a manual peristaltic pumps respectively.

Samples were collected in 3 ml glass directly from the sampled compartments (stream water, spring water and well water) or from the bottles of the automatic samplers (rainfall and stream waters). These vials were filled to avoid air bubbles and sealed with plastic paraffin film to avoid evaporation, and stored at 3-4ºC before analysis. Samples were filtered through a 0.45-µm membrane filter. $\delta^{2}H$ and $\delta^{18}O$ ratios were measured with, a Picarro L2120-i analyzer, by Serveis Científico-Tècnics of the Universitat de Lleida (Spain). Measurement precisions are 0.30-0.53 for $\delta^{2}H$ and 0.08-0.12 for $\delta^{18}O$. When samples contained organic compounds a post-processing correction was applied (Martínez-Gómez et al., 2015).

4.2.4.2 Tritium

Four water samples for Tritium (^{3}H) determination were collected on September 3th 2013 from: two streams (Cal Rodó (St1) and Can Vila (St4) gauging stations), a permanent spring (Sp12) and in a well (Gw18).

Previous samples for tritium determination were collected in 1990s from these four locations by Herrmann et al. (1999). These authors also collected samples for tritium analysis in other 17 locations in the Cal Rodó catchment (springs, wells and streams) (see Fig. 4.1, Appendix D. Table 2, for a list of all sampling dates and locations).

All the samples were collected during selected baseflow conditions to avoid dispersion of ages related to the influence of recent rainfall-runoff events (Stewart et al., 2012). All samples were collected in 1 L plastic bottles hermetically sealed against atmosphere interaction.

The samples collected in 2013 were analysed at the Water Dating Laboratory of GNS Science (New Zealand) with an ultra-low background Quantalus liquid scintillation counter

(Morgenstern and Taylor, 2009) and were previously electrolytically enriched in tritium by a factor of 90. The results were referred to the radioactive half-life of tritium of 12.32 years, and using the calibration of standard water SRM4926C (1.100462 ± 0.366% at 3 September 1998, Morgenstern and Taylor, 2009). Measurement error (1σ) on samples is about ± 0.09 tritium units (TU). For the Herrmann et al. (1999) samples the measurement error (1σ) ranged between 0.5 and 1.5 TU.

4.2.5 MTT estimation using oxygen-18 and deuterium

The MTT was estimated in one stream (St4), a spring (Sp12) and a well (Gw18) using oxygen-18 and deuterium. The water age estimation was performed as follows:

4.2.5.1 Input function

In order to use stable isotopes for MTT estimation, the rainfall input function should be known for a period of at least some years. However, in the Can Vila catchment rainfall samples for isotopes determinations were collected only during 27 months. Therefore we estimated an eight years long rainfall isotopic series by using four times the available 27 months series. In the synthetic eight years series, the observed rainfall stable isotopes seasonality and the mean isotope signal were maintained identical as in the original 27 months long series.

As the rainfall input in a catchment is affected by surface runoff and evaporation loss, leading to a lower recharge (R), the equation of Bergmann et al. (1986) was used to weight isotopic ratios using weekly measurements:

$$\delta_w = \frac{N\,\alpha_i P_i}{\sum \alpha_i P_i}\left(\delta_i - \delta_{gw}\right) + \delta_{gw} \qquad (1)$$

where δ_w and δ_i are the weighted and measured $\delta^{18}O$ or $\delta^{2}H$ values respectively. α_i and P_i are respectively the groundwater recharge parameter and the rainfall amount in the ith week. N is the number of measurements and δ_{gw} is the $\delta^{18}O$ or $\delta^{2}H$ mean groundwater value (taken as the mean of the measured isotope concentration at each sampled location) (Bergmann et al., 1986). As α_i P_i can be substituted by R_i (recharge) and (Σ α_i P_i)/N by R_{mean} (mean recharge) (see for details: Stewart et al., 2007), recharge (R_i) was calculated subtracting the weekly PET from the weekly rainfall.

4.2.5.2 Model

Water mean transit time (MTT) was calculated using the lumped-parameter approach. The flow pattern was assumed to be on stationary state (baseflow conditions) (Maloszewski and Zuber, 1982). The transport of the tracer through the catchment can be expressed mathematically by the convolution integral relating the output and input tracer

concentrations. From a known input tracer (rainfall) and the measured output tracer (streams, springs and wells), water MTT can be solved by:

$$C_{out}(t) = \int_0^{\infty} C_{in}(t-\tau)g(\tau)\exp(-\lambda\tau)\,d\tau \quad (2)$$

C_{in} and C_{out} are the input and output tracer contents, t is the calendar time, τ is the lag time between input and output tracer concentrations, $g(\tau)$ is the transit time distribution function. λ is the decay constant of the tracer. For stable isotopes $\lambda = 0$.

The lumped-parameter model used to calculate the mean transit time was the exponential-piston flow model (EPM) which combines the exponential and the piston-flow models (Maloszewski and Zuber, 1982). The response function was given by:

$$g(\tau) = 0 \quad \text{for } \tau < \tau_m(1\text{-}f) \quad (3)$$

$$g(\tau) = \frac{1}{f\,\tau_m}\exp\left(-\frac{\tau}{f\,\tau_m}+\frac{1}{f}-1\right) \quad \text{for } \tau \geq \tau_m(1\text{-}f) \quad (4)$$

where τ_m is the water MTT, and f the ratio of the exponential model versus the total (when f = 1 the model is totally exponential and when f = 0 is totally piston flow).

4.2.5.3 Model optimisation

Using $\delta^{18}O$ or $\delta^{2}H$ to estimate water MTT, the best fit between calculated and observed stable isotopes signal was obtained by optimisation (Excel solver) of the two model parameters: f and MTT. Least-squares were used to obtain the optimal fit to the measured data.

$$sd = \frac{\sqrt{\sum_i (S_i - C_i)^2}}{n} \quad (5)$$

where S_i and C_i is the simulated and measured data and n is the number of samples.

4.2.6 MTT estimation using tritium

4.2.6.1 Input function

As no tritium measurements of rainfall were available in the Cal Rodó catchment, other stations of the IAEA (International Atomic Energy Agency) network located "near" Vallcebre were considered. After some trials, the monthly measurements of Vienna (located at 203 m a.s.l.) were selected due to the long period of records compared to other stations. Therefore, in a first step, the data of the rainfall tritium concentration and the associated analytical error (i.e. standard error) in the Cal Rodó catchment were estimated by combining monthly records from Vienna IAEA station (International Atomic Energy Agency), from period 1961-2009, with those of 2010-2013 from Vienna ANIP (Austrian Network of Isotopes in Rainfall) station. For the period 1953-1960, when Vienna's data were not available, this information was obtained from Ottawa IAEA station, which had a good correlation with 1961-2013 Vienna's data. Data are presented as Tritium Units (TU). In a second step, Vienna's rainfall tritium concentration and

the analytical error measurements were scaled by a factor obtained by a multiple regressions between rainfall tritium measurements versus latitude and altitude at twelve IAEA stations (Barcelona, Genova, Girona, Grenoble, Guttannen, Madrid, Marseille, Penhas Douradas, Santander, Thonon-les-bains, Vienna and Zaragoza). The resulting regression was significant ($p < 0.01$) and a factor of 0.82 ± 0.17 (Gallart et al., in review) was obtained to simulate monthly rainfall tritium concentrations for the Cal Rodó catchment.

The annual mean tritium concentrations in recharge (C_{in}) were determined from monthly tritium rainfall concentration as described in Stewart et al. (2007) using the equation:

$$C_{in} = \sum_{i=1}^{12} C_i R_i / \sum_{i=1}^{12} R_i \quad (6)$$

Where C_i and R_i are the adjusted Vienna tritium concentrations in rainfall and the recharge amounts for the ith month, respectively. For each month with a negative recharge (i.e. no infiltration), the tritium concentration of the rainfall data was corrected. Equation 6 was applied to both rainfall tritium concentration and to the analytical error measurements.

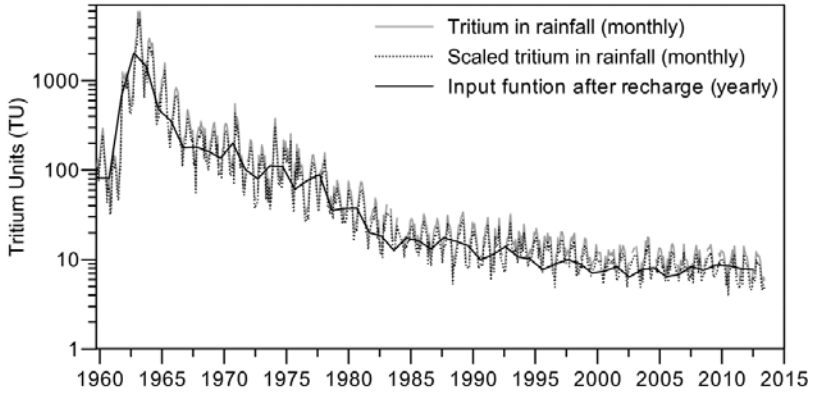

Fig. 4.2 Temporal sequences of monthly rainfall tritium concentration, monthly rainfall tritium concentration after applying the scaled factor of 0.82 and the yearly input function after applying the scaled factor and the recharge equation.

4.2.6.2 Modelling

MTT was estimated at 21 catchment locations (streams, springs and wells) were tritium was sampled (Fig. 4.1). MTT estimation was assessed by using the convolution integral (equation 2, where $\lambda = \ln 2/T_{1/2}$. $T_{1/2}$ was the half-life of tritium) into a framework of uncertainty analysis described in Gallart et al. (in review). This framework named TEPMGLUE (Tritium Exponential Piston Model GLUE), is based on the Generalized Likelihood Uncertainty Estimation (GLUE) methodology, proposed by Beven and Binley (1992, 2014).

The TEPMGLUE uses Monte Carlo parameters exploration and provides a set of acceptable simulated models (behavioural), instead of an optimal result. Additionally, the TEPMGLUE was adapted to cope with some uncertainty issues of MTT estimation process (see McGuire and McDonnell, 2006). These uncertainties are related to the analytical error associated with the

rainfall tritium determinations, the analytical error associated with the water tritium samples determinations (streams, springs and wells) and the error associated with the model parameters (*f* and MTT).

The uncertainty analysis was performed as follows (see details in Gallart et al., in review):

First, considering the tritium value (and the associated error) of the rainfall data and of the water samples, a set of replicated annual tritium input (rainfall) sequences and water tritium samples were obtained from Monte Carlo iterations, using the respective normal distribution generators. All the generated replicate series were used as TEPMGLUE input data.

Then using replicated tritium input, a pair of MTT and *f* parameter values was searched. The search was in a range of 0.05-1.00 for *f* and 1-35 years for MTT. The EPM model was run and the simulated tritium concentrations obtained were evaluated against the water tritium samples replicates. The evaluation of the fit was made using an efficiency measure.

The efficiency was measured with the Nash-Sutcliffe (1970) criterion. The inconvenience of this efficiency measure is that it cannot be applied when using one single tritium sample for validation, and that it gives flawed negative values when the variance of observations is small. Therefore, the efficiency measure used in a case of using one single sample was:

$$E = 1 - \left[\frac{MSE_S}{\max(var_0, w \cdot \overline{var}_a)}\right] \quad (7)$$

Where MSE_s is the mean squared error of the simulated model tritium concentration respect to the replicated values, var_0 is the variance of the tritium samples, *w* is the conventional factor and $\overline{var}_a$ is the mean analytical variance of the tritium samples. The *w* factor value was set to 2.33^2. This value means that, in the case of uncertainty being caused only by the precision of the tritium determinations in water samples, about 98% of trial values would be within the acceptability range (see in Gallart et al., in review.)

If the simulated model was rejected ($E \leq 0$), a new parameter pair (*f* and MTT) was generated and the procedure was repeated with the same data replicates. Only when an acceptable pair of parameters was found ($E > 0$) or when 10,000 sub-iterations were unsuccessful, a new set of replicated observations were sought in a next full iteration. In total, up to 50,000 full iterations were performed in each exercise.

After using TEPMGLUE, thousands of behavioural simulation models with a correspondent MTT, *f* and efficiency value were obtained. The likelihood measure for every pair of MTT and *f* values was calculated as its rescaled efficiency E (between zero and one), by dividing it by the total sum of efficiencies.

Thereafter, results were ordered by MTTs values and the likelihoods were cumulated, to obtain the likelihood weighted cumulative density function (lwcdf) (Fig. 4.3). Q-Q plots were performed to test if the distribution functions obtained were normally distributed or not.

When lwcdf showed bimodal shapes, two normal distributions were mixed to simulate this bimodal distribution (Gallart et al., in review). Using an optimisation procedure (Excel solver) the optimal proportions and the normal distribution parameters of each normal (weighted mean and standard deviation) were obtained minimizing differences.

Along with the likelihood weighted cumulative density functions, the weighted mean, weighted standard deviation (σ) and the confidence interval (0.05 and 0.95) of the distribution were calculated. The percentage of discarded model simulations was also quantified.

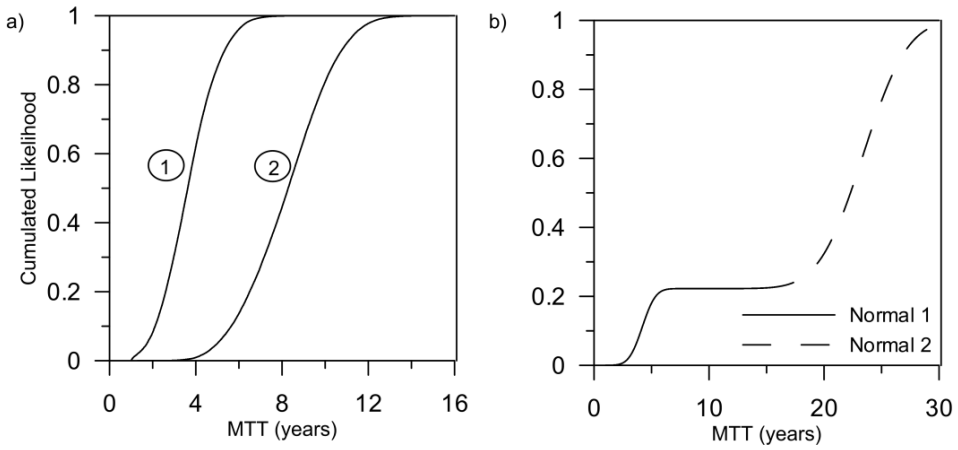

Fig. 4.3(a) Likelihood weighted cumulative density function for two normal distributions and (b) a bimodal distributions.

The statistical significance of the differences between pairs of lwcdf was investigated by performing a randomisation test (Gallart et al., in review). The differences were considered significant when $P < 0.05$, and marginally significant when $0.05 < P < 0.1$.

4.3 Results

4.3.1 Temporal variation of δ^2H and $\delta^{18}O$

In the Can Vila catchment the weekly mean and standard deviation of $\delta^{18}O$ and δ^2H signals in rainfall were -7.0 ± 3.3 ‰ and -42.8 ± 26.7 ‰, respectively (see Table 1, Appendix D). There was a significant linear correlation between air temperature and $\delta^{18}O$ ($r^2 = 0.63$, $p < 0.05$) or δ^2H signals ($r^2 = 0.55$, $p < 0.05$) showing that $\delta^{18}O$ and δ2H annual variations (Fig. 4.4(a)) reflected the effect of condensation and evaporation processes during the year. In summer, when air temperature was higher, $\delta^{18}O$ signal in rainfall was less depleted (-4.4 ± 1.8 ‰) than in winter (-9.7 ± 3.5 ‰). In contrast to rainfall, no clear seasonal variations were observed in the stream, spring and groundwater (well) (Fig. 4.4 and Table 1, Appendix D). Along the study period, mean $\delta^{18}O$ signal in stream water was -7.2 ‰, similar to that observed in spring water and in the well (-7.5 ‰ and -7.0 ‰ respectively), in all cases with slight variations (from ± 0.2 ‰ to 0.5‰).

The Can Vila Local Meteoric Water Line (LMWL) (equation 8), calculated from the weekly rainfall samples, is:

$$\delta^2H = 7.96\ \delta^{18}O + 13.37\ ‰ \qquad (r^2 = 0.96;\ n = 65) \qquad (8)$$

Stream water, spring water and groundwater isotope ratios were located on the LMWL, suggesting that they all were affected by similar isotopic fractionation. The stable isotopes signal in stream water ranged from -7.7 ‰ to -5.9 ‰ ($\delta^{18}O$) and from -47.3 ‰ to -37.1 ‰ (δ^2H). In spring water ranges were from -8.2 ‰ to -6.8 ‰ ($\delta\delta^{18}O$) and -50.9 ‰ to -41.2 ‰ (δ^2H) and in groundwater from -7.9 ‰ to -5.4 ‰ ($\delta^{18}O$) and -53.2 ‰ to -27.5 ‰ (δ^2H) (Fig. 4.5).

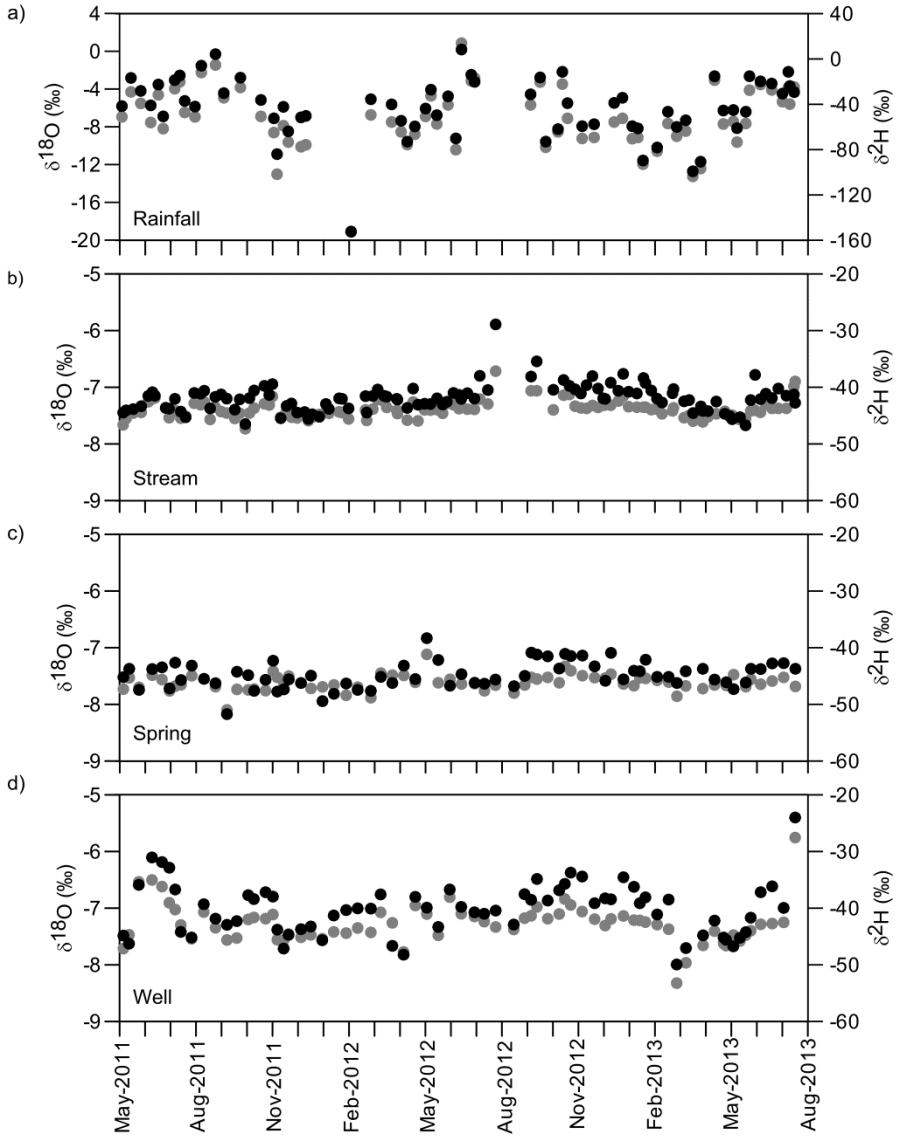

Fig. 4.4 Temporal dynamics of $\delta^{18}O$ and δ^2H signal in (a) rainfall, stream (b)water (St4), (c) spring water (Sp12) and (d) groundwater (Gw18) during the study period (May 2011 to July 2013) at baseflow conditions. Black dots correspond to $\delta^{18}O$ while grey dots correspond to δ^2H. Note the change of Y scale between rainfall graph and the other graphs.

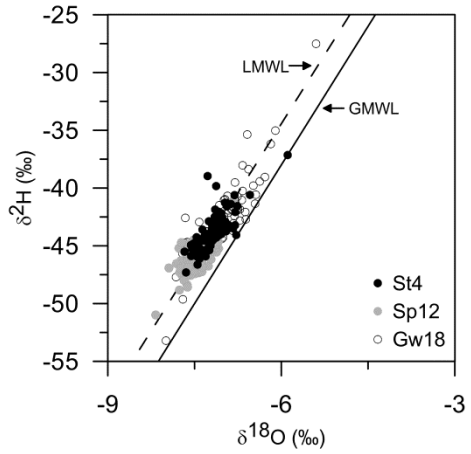

Fig. 4.5 Relationship between $\delta^{18}O$ and $\delta^{2}H$ signal in stream water (St4), spring water (Sp12) and groundwater (Gw18) throughout the study period (see Fig. 4.1 for sampling locations). The solid line plots the Local Meteoric Water Line (LMWL) obtained from rainfall samples (weekly data) whereas the dashed one the Global Meteoric Water Line (GMWL).

4.3.2 Estimation of mean residence time using stable isotopes

Results of the estimation of Mean Transit Time (MTT), in stream water, spring water and groundwater, using $\delta^{18}O$ and the Exponential Piston Model (EPM) with the f parameter ranging between 0.6 and 1, indicated that any of the calculated output tracer content (C_{out}) fitted optimality on the measured $\delta^{18}O$ values. When MTT was longer than two years, despite the different f values applied, smaller and constant standard deviations (< 0.4 ‰) were observed, making difficult to find an optimal fit. Fig. 4.6 shows the goodness-of fit when using the two extreme f values (0.6 and 1). Results indicate that sampled waters were definitely older than two years, but that their "exact" age remains totally uncertain.

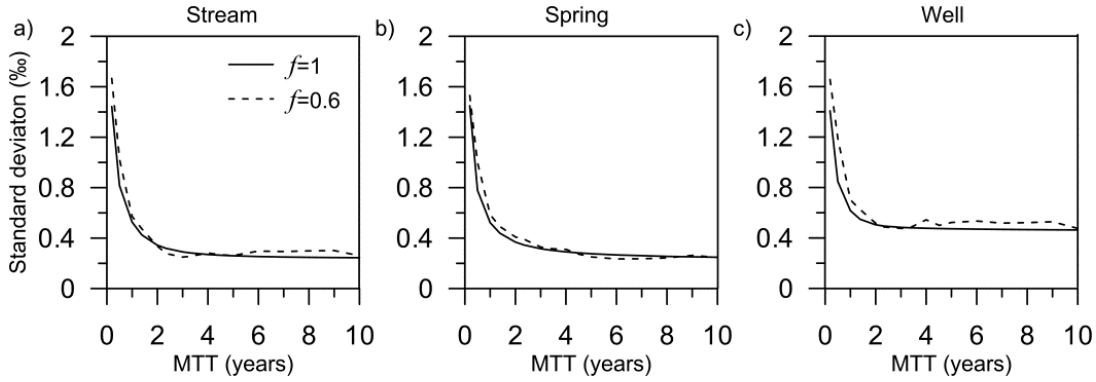

Fig. 4.6 $\delta^{18}O$ goodness-of fit (standard deviation) obtained with the Exponential Piston Model for different f and MTT for (a) stream water, (b) spring water and (c) groundwater.

4.3.3 Estimation of mean transit time using tritium

4.3.3.1 Mean transit time estimation considering different combinations of samples

At four catchment locations (St1, St4, Sp12 and Gw18) tritium was sampled in the 1990s (1996-1998) and 2013. The MTT at these locations was estimated using the TEPMGLUE methodology (Gallart et al., in review). At each location, MTT estimations were performed successively using the following samples/combination of samples: (i) all the samples (1990s and 2013 samples), (ii) only the 1990s samples and (iii) only the 2013 sample.

i) Estimation of MTT considering all the samples.

Using all tritium samples, results showed that the weighted mean of MTT ranged between 4.6 years in groundwater (Gw18) and 7.7 years in the stream water (St4), with similar weighted standard deviation of about three years and large confidence intervals in all locations (Table 4.1 and Fig. 4.7(b)). In addition, the percentage of discarded simulations in all cases was relatively low (<1%), which shows the good efficiency of the TEPMGLUE methodology.

Table 4.1 Results of MTT estimation using the EPM model and considering all the tritium samples. CI = confidence interval. σ = Standard deviation.

Location	N° of samples	Weighted mean of MTT *(years)*	Weighted σ *(years)*	0.05 CI *(years)*	0.95 CI *(years)*	Discarded simulations *(%)*
St1	6	7.0	3.0	2.5	12.5	0.1
St4	6	7.7	3.3	2.6	13.9	0.1
Sp12	6	7.4	3.2	2.5	13.5	0.0
Gw18	6	4.6	3.1	0.9	11.7	0.0

The likelihood weighted cumulative density functions lwcdf observed at each location is shown in Fig. 4.7(a).

Fig. 4.8 shows the normal Q-Q plots of observed and expected distributions of MTT at the four locations. All the likelihood weighted cumulative density functions lwcdf (white dots), with the exception of the extreme values, fit close to the expected normal distribution (line), showing that the lwcdf were not far from being approximately normal distributed. In groundwater (Gw18) the lwcdf was more distant from a normal distribution.

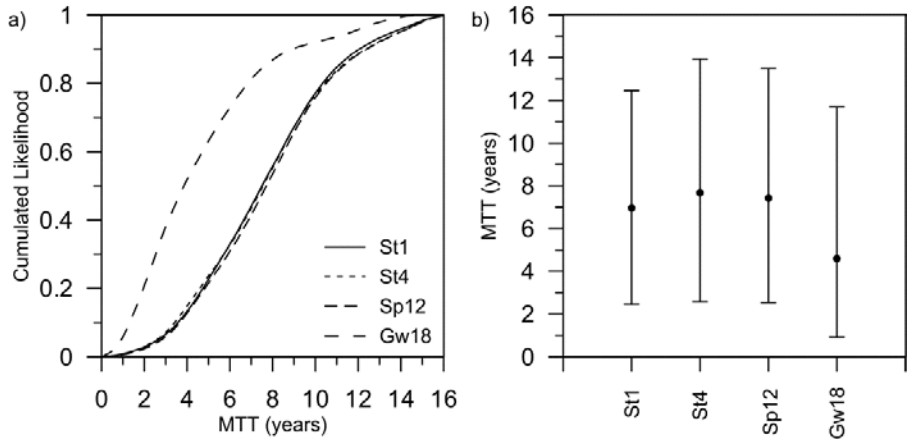

Fig. 4.7 (a) Likelihood weighted cumulative density function (lwcdf) for the four studied locations, considering all the tritium samples (1990s and 2013). (b) Weighted mean and [0.05-0.95] confidence intervals of estimated MTT for the same locations.

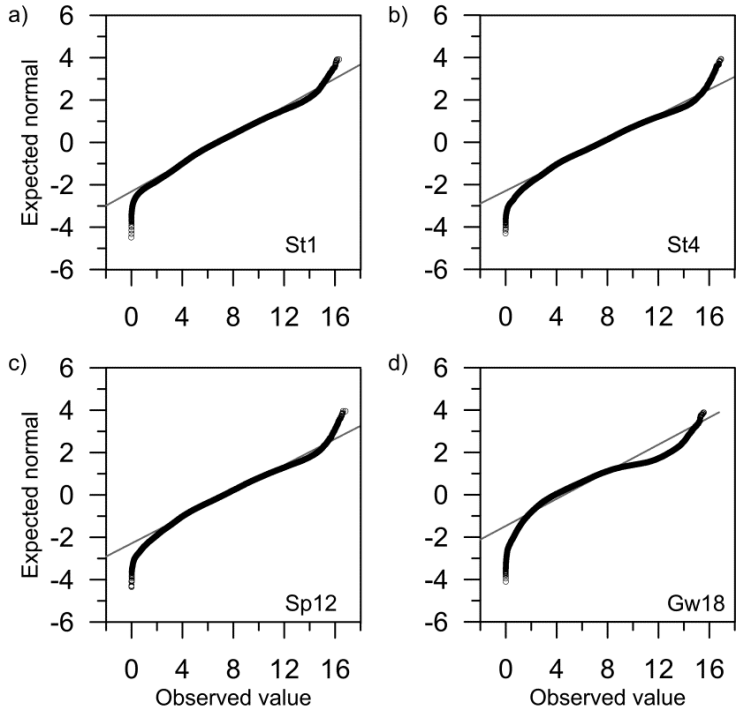

Fig. 4.8 Normal Q-Q plots comparing the observed MTT distribution and the expected normal distribution in St1 (a), St4 (b), Sp 12 (c) and Gw18 (d).

ii) Estimation of MTT considering only the 1990s samples.

Fig.4.9 shows the lwcdf distributions when using only the 1990s samples (1996-1998). The Q-Q plot analysis demonstrated that they were not far from normality. Again, differences in MTT were not significant (p > 0.1) between stream water (St1 and St4) and spring water (Sp12). No significant differences were also observed with groundwater (Gw18). When the lwcdf obtained

using all samples (section i) was compared to the lwcdf obtained using only the 1990s samples (this section), no statistically significant differences were observed ($p > 0.1$). For instance, in stream (St1) the weighted mean water age was 6.8 years when using all tritium samples, and 7.0 years using only the 1990s samples (Table 4.1 and Table 4.3). These comparisons indicated that adding the 2013 samples, despite their high analytical precision, did not provide relevant information for MTT estimation.

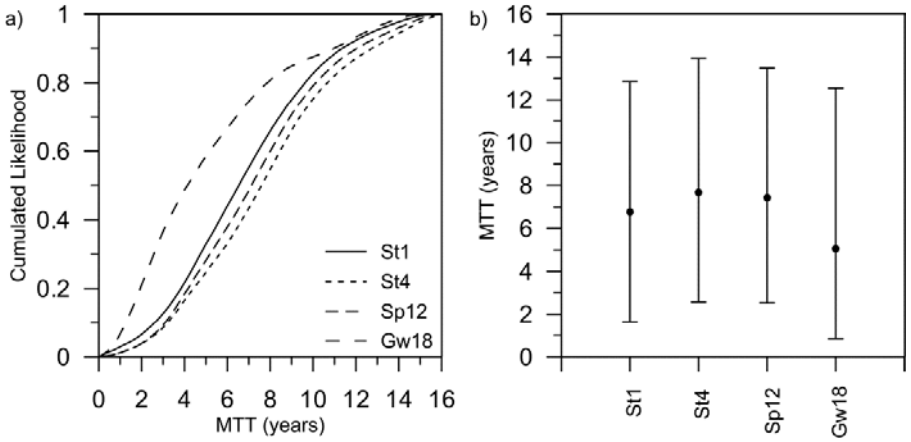

Fig. 4.9 (a) Likelihood weighted cumulative density function, (lwcdf) for the four studied locations, obtained considering only the 1990s samples (five samples). (b) Weighted mean and [0.05-0.95] confidence intervals of the estimated MTT for the same studied locations.

iii) Estimation of MTT considering only the 2013 samples.

When estimating water age using only the 2013 samples, all the observed lwcdf presented bimodal distributions, instead of the normal distributions observed with the other combinations of samples (Fig. 4.10(a)). These bimodal shapes indicated that there were two different solutions of MTT estimation; that could be decomposed into two normal distributions. In groundwater (Gw18) the two possible weighted mean of MTTs differed by 21.4 years, while at the other locations the difference was approximately of 11 years (Table 4.2). At each location, the confidence interval (5%) of the younger solution (i.e. first normal distribution) was smaller than the confidence interval of the older solution (i.e. second normal distribution) (Fig. 4.10(b)).

When both normal distributions (first and second) were compared (randomisation test), it was observed that at locations St1, St4 and Sp12 both normal distributions did not differed significantly in term of water MTT ($p = 0.20$, $p = 0.18$, $p = 0.19$, respectively for the sites). Contrarily, groundwater MTTs (Gw18) were marginally significantly different ($0.05 < p < 0.1$). Besides, at the four locations there were not statistically significant differences ($p > 0.1$) between the first normal distributions and the lwcdf obtained in the previous estimations (sections i and ii). For instance, at location Sp12 the difference between the first normal distribution and the lwcdf obtained using the five older samples (section ii) was not significant

(p = 0.48). In contrast, at location St4, Sp12 and Gw18 the second normal distributions and the lwcdf obtained in the previous sampling designs (sections i and ii) differed marginally.

Table 4.2 Results of MTT estimation using the EPM model and considering only the 2013 samples. CI = confidence interval. σ = Standard deviation.

Location	Solution	Weighted mean of MTT *(years)*	Weighted σ *(years)*	0.05 CI *(years)*	0.95 CI *(years)*	Discarded simulations *(%)*
St1	Younger	7.8	1.4	5.4	10.2	0.0
	Older	18.8	6.9	7.4	30.1	0.0
St4	Younger	8.2	1.8	5.2	11.2	0.0
	Older	19.8	6.1	9.7	29.2	0.0
Sp12	Younger	8.7	1.6	6.1	11.3	0.0
	Older	19.1	6.1	9.0	29.2	0.0
Gw18	Younger	4.9	0.8	3.5	6.2	0.0
	Older	26.2	4.2	19.3	33.1	0.0

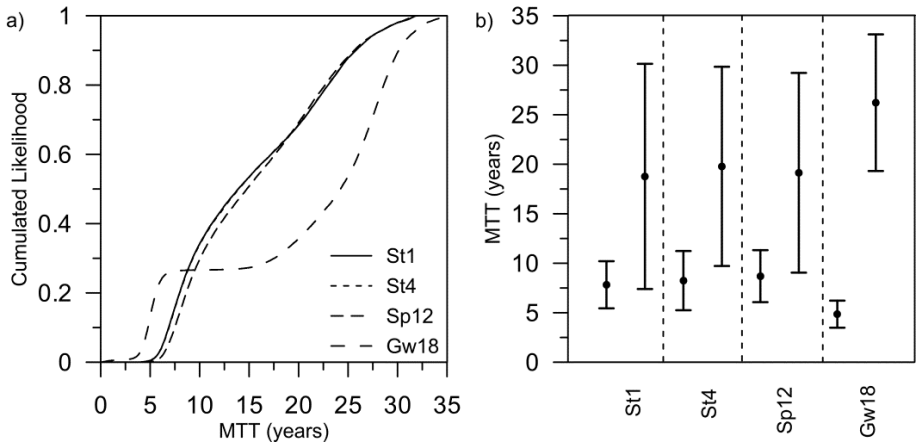

Fig. 4.10 (a) Likelihood weighted cumulative density function (lwcdf) for the four studied locations, obtained considering only the 2013 samples. (b) Weighted mean and [0.05-0.95] confidence intervals of the MTT two possible solutions (see text) for the same studied locations.

Fig. 4.11 shows the temporal series (1960-2015) of the tritium input function and tritium water samples, as well as the results of two behavioural models obtained from the former analysis (section iii) using the groundwater samples (Gw18) (Table 4.2). Whereas, the model simulation that yield the younger solution (MTT = 4.9 years and f = 0.66) fitted the six tritium samples, the other model simulation (MTT = 26.2 years and f = 0.63) only fitted the 2013 tritium sample. Similar results were observed using samples from the other catchment locations (Appendix D.).

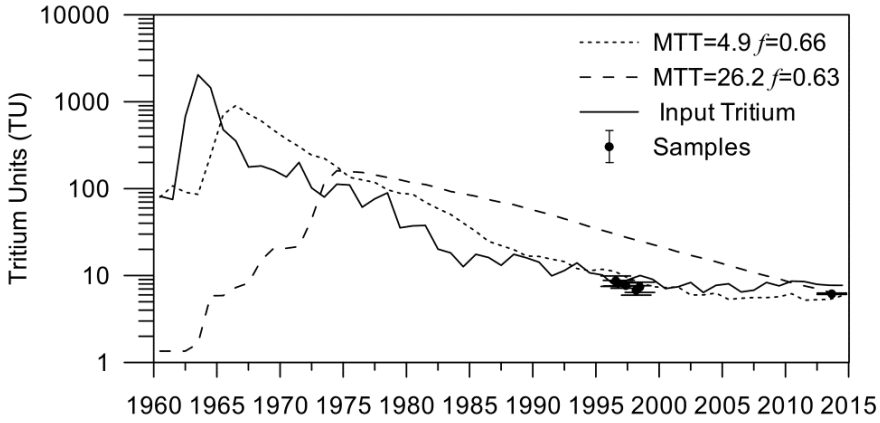

Fig. 4.11 MTT estimated in thethree springs, twelve streams and six wells of Cal Rodó catchment. The black dots are the weighted MTT and [0.05-0.95] confidence intervals estimated in the present study. The white dots and black squares are the MTT estimated by Herrmann et al., (1999) using the EM model and the dispersion model, respectively.

4.3.3.2 Comparison with the results obtained by Herrmann et al., (1999).

From 1996 to 1998, samples for tritium determination were collected in three springs, twelve streams and six wells (a total of 21 locations) of the Cal Rodó catchment. From these samples, MTTs were estimated, using the exponential and the dispersion models, by Herrmann et al. (1999) (Table 2, Appendix D.). Tritium determinations of Herrmann et al. (1999) have been used in the current study to obtain a new estimation of MTT applying TEPMGLUE.

Fig. 4.12 shows the MTT estimated using both approximations. Black squares and white circles correspond MTT estimations by Herrmann et al. (1999), whereas the present study results are shown as weighted MTT and 0.05 and 0.95 confidence intervals. The weighted means MTT obtained in the present study were always approximately three years younger than those obtained by Herrmann et al. (1999). However, there was a statistically significant linear relation between current and former MTT estimations, considering either the exponential model or the dispersion model (Fig. 4.13).

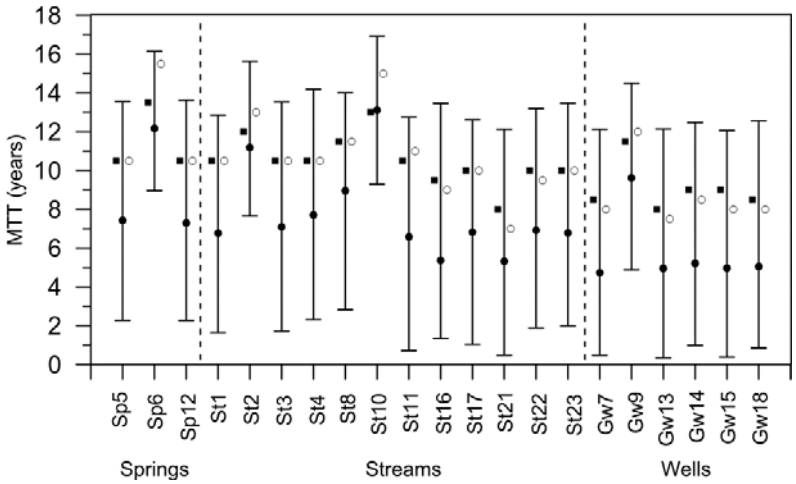

Fig. 4.12 MTT estimated in the three springs, twelve streams and six wells of Cal Rodó catchment. The black dots are the weighted MTT and [0.05-0.95] confidence intervals estimated in the present study. The white dots and black squares are MTTs estimated by Herrmann et al. (1999) using the EM model and the dispersion model, respectively.

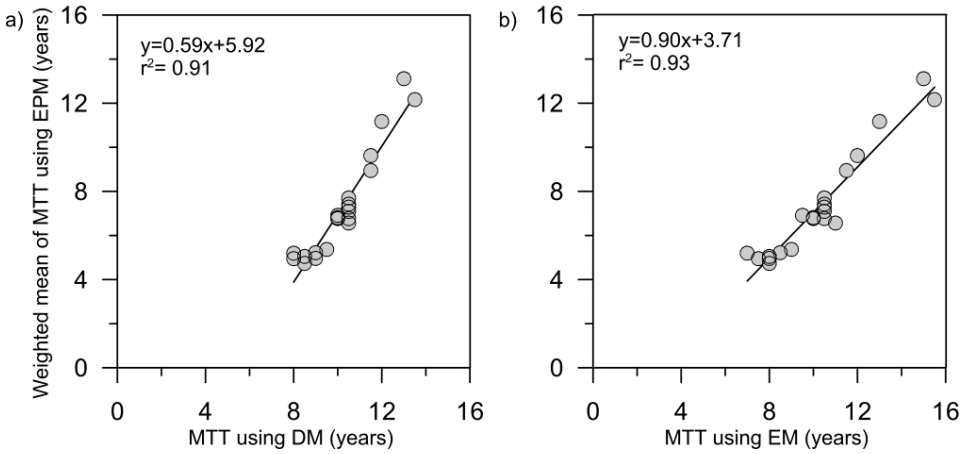

Fig. 4.13 Comparison between the weighted mean of MTTs estimated in this study, using the EPM, and those in Herrmann et al. (1999) using (a) the Dispersion model and (b) the Exponential model.

4.3.3.3 Spatial MTT variations in the Cal Rodó catchment.

The weighted mean of MTTs calculated at the 21 locations of Cal Rodó catchment, using only the 1990s samples and the TEPMGLUE methodology, ranged between 4.7 and 13.1 years (Table 4.3 and Fig. 4.14). On average, springs had the oldest waters (9.0 ± 3.0 years), followed by streams (7.7 ± 3.3 years) and wells (5.8 ± 3.5 years). The `lwcdf´ distribution of MTT at all locations were not far from being normally distributed. In addition, the percentage of discarded simulations in all cases was lower than 2.0%, which means that only 1,000 of 50,000 simulations were discarded.

Table 4.3 Results of MTT estimation using the EPM model and considering only the 1990s samples. CI = confidence interval. σ = Standard deviation.

Location	N° of samples	Weighted Mean of MTT *(years)*	Weighted σ *(years)*	0.05 CI *(years)*	0.95 CI *(years)*	Discarded simulations *(%)*
Sp5	5	7.4	3.3	2.3	13.5	0.1
Sp6	5	12.2	2.2	9.0	16.1	0.0
Sp12	5	7.3	3.4	2.3	13.6	0.0
St1	5	6.8	3.3	1.6	12.9	0.0
St2	5	11.2	2.5	7.7	15.6	0.5
St3	5	7.1	3.5	1.7	13.5	0.2
St4	5	7.7	3.5	2.3	14.2	0.2
St8	4	9.0	3.2	2.8	14.0	0.5
St10	3	13.1	2.5	9.3	16.9	0.0
St11	2	6.6	3.6	0.7	12.8	0.1
St16	2	5.4	3.7	1.3	13.5	0.6
St17	5	6.8	3.4	1.0	12.6	2.0
St21	2	5.3	3.6	0.5	12.1	1.6
St22	5	6.9	3.4	1.9	13.2	0.0
St23	5	6.8	3.4	2.0	13.5	0.1
Gw7	5	4.7	3.7	0.5	12.6	0.0
Gw9	5	9.6	2.8	4.9	14.5	0.0
Gw13	5	5.0	3.7	0.4	12.1	0.9
Gw14	5	5.2	3.5	1.0	12.5	0.0
Gw15	2	5.0	3.6	0.4	12.1	0.0
Gw18	5	5.1	3.6	0.8	12.5	0.0

The results of the randomisation test applied to the lwcdf of the stream locations (Table 4.4, Fig. 4.14), indicate that results corresponding to stream locations St2 and St10 were significantly different from the other locations, showing much higher MTT values (Fig. 4.12). Any of the other stream locations could be considered as representative of the stream water age within the catchment, because they were not significantly different between them. Considering springs, Table 4.5 indicated that spring Sp6 lwcdf was different from the two others ($p < 0.05$). Finally, there were not statistically significant differences in lwcdf between wells, excluding well Gw9 that was different of all the others (except of well Gw15) (Table 4.6).

Table 4.4 Probability of being different between pairs of `lwcdf´ of stream sampling locations using the randomisation test (see Fig. 4.1 for the localization of the sampling locations).

Location	St1	St2	St3	St4	St8	St10	St11	St16	St17	St21	St22	St23
St1		0.04**	0.44	0.35	0.20	0.03**	0.49	0.36	0.50	0.34	0.47	0.50
St2			0.05*	0.08*	0.16	0.20	0.10	0.08*	0.05*	0.08*	0.04**	0.04**
St3				0.40	0.24	0.04**	0.45	0.33	0.45	0.31	0.47	0.45
St4					0.31	0.05*	0.38	0.27	0.36	0.25	0.37	0.35
St8						0.09*	0.26	0.19	0.21	0.18	0.21	0.21
St10							0.08*	0.07*	0.04**	0.07*	0.04**	0.04**
St11								0.38	0.48	0.38	0.47	0.49
St16									0.35	0.50	0.34	0.36
St17										0.34	0.48	0.49
St21											0.33	0.34
St22												0.47
St23												

Significance : **p < 0.05, *0.05 < p <0.1

Table 4.5 Probability of being different between pairs of `lwcdf´ of the springs sampling locations using the randomisation test.

Location	Sp5	Sp6	Sp12
Sp5		0.03**	0.49
Sp6			0.03**
Sp12			

Significance : **p < 0.05, *0.05 < p <0.1

Table 4.6 Probability of being different between pairs of `lwcdf´ of the shallow groundwater sampling locations using the randomisation test.

Location	Gw7	Gw9	Gw13	Gw14	Gw15	Gw18
Gw7		0.05*	0.47	0.42	0.45	0.45
Gw9			0.06*	0.05*	0.11	0.05*
Gw13				0.46	0.48	0.48
Gw14					0.49	0.47
Gw15						0.49
Gw18						

Significance: $**p < 0.05$; $*0.05 < p < 0.1$

When analysing the possible effect of topographic characteristics on water MTT, no correlation was observed between the weighted mean of MTTs and the Topographic Wetness Index (TWI) nor with the slope at each location (Fig. 4.14). However, locations St2 and St10, with much higher MTTs values than other stream locations, corresponded to the lowest TWI among stream locations. In addition, location Gw9, with a higher MTT value than other well locations corresponded to the steepest slope among well locations.

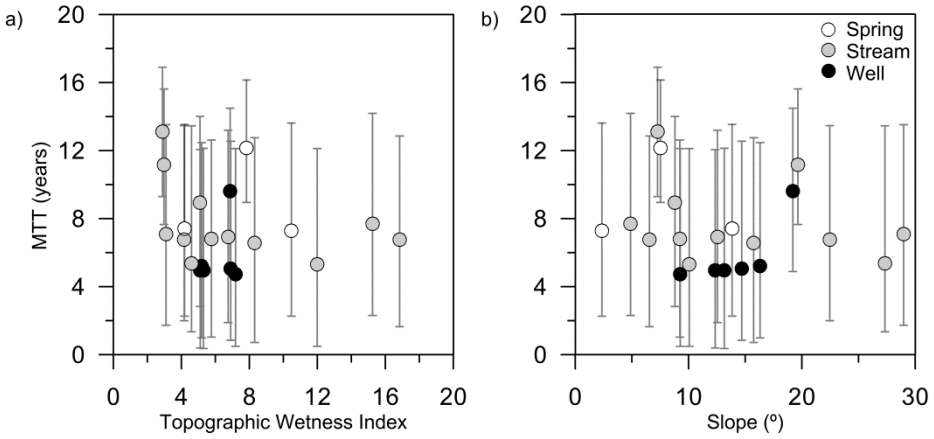

Fig. 4.14 (a) Relationship between MTTs and the Topographic Wetness Index of the 21 locations (springs, streams and wells). (b) Relationship between MTTs and the slope. Dots are the weighted mean MTT and bar the [0.05-0.95] confidence intervals.

Finally, Fig. 4.15 shows the spatial variability of water MTTs in Cal Rodó catchment. Overall, waters sampled in the western part of the Cal Rodó catchment (i.e. Can Vila and Ca l'Isard sub-catchments) were younger (brighter blue symbols in Fig. 4.15) than in the eastern part of the catchment. For instance, average MTT in groundwater and stream locations from both sub-catchments were 5.0 years and 6.4 years, respectively, whereas in the eastern part of the Cal Rodó catchment average MTT was 6.1 years in groundwater and 8.4 years in streams. The average MTT of Can Vila's spring was also 2.5 years younger than the springs of the eastern part.

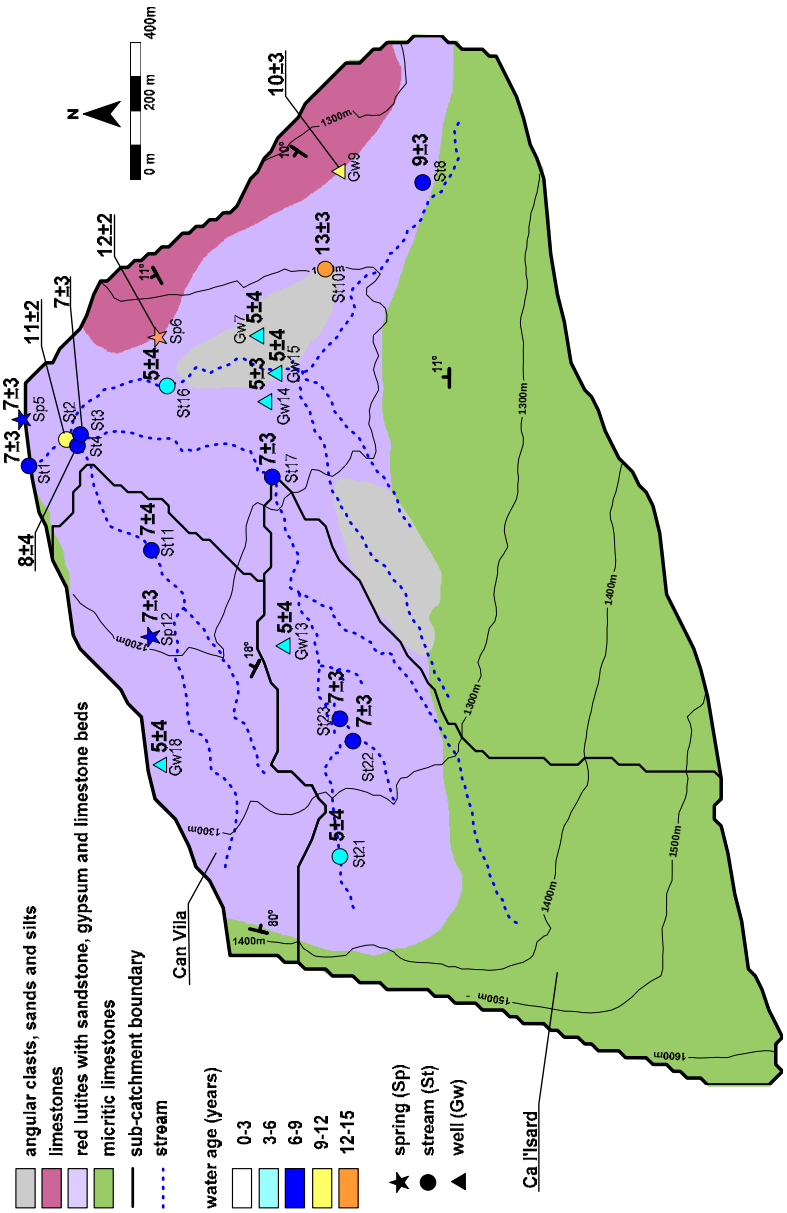

Fig. 4.15 Map of the Cal Rodó catchment and sub-catchments (Can Vila and Ca l'Isard) showing the weighted MTT ± weighted standard deviation of the the springs (star), streams (circle) and wells (triangle) estimated from samples taken in the nineties. The geological characteristics of the catchment are also shown.

4.4 Discussion

4.4.1 Temporal variation of stable isotopes

In the Can Vila catchment, as observed elsewhere (e.g. DeWalle et al, 1997; Soulsby et al., 2000), $\delta^{18}O$ and $\delta^{2}H$ signal in precipitation exhibited strong seasonal variations. As described in the literature these variations are controlled by temperature (Ingraham, 1998). Following the temperature dynamics the precipitation isotope signal tended to be more enriched during summer, as described in other Mediterranean catchments (e.g. Vallejos et al., 1997; Ayalon et al., 1998; Lambs et al., 2013). The LMWL calculated in the present study was close to the GMWL and to the LMWL calculated in Southwest of France (Lambs et al., 2013) and in Barcelona (Vandenschrich et al., 2002).

These variations of isotopic signal in precipitation are damped when water reaches the soil. Therefore the isotopic signal of water in the spring, the well and the stream at baseflow conditions did not exhibit clear seasonality, as observed in several studies (e.g. Neal et al., 1992; O'Driscoll et al., 2005; Birkel et al., 2011, 2012; Lambs et al., 2013). Beside, stream water, spring water and groundwater isotope ratios ranges were close (Fig. 4.5), suggesting a similar fractionation in each compartment as well as direct hydrological connection between them.

4.4.2 Estimation of mean residence time using stable isotopes

The uncertainty observed in the determination of the mean transit time (MTT) in the Can Vila catchment is due to several different issues as suggested elsewhere by McGuire and McDonnell, (2006).

One reason could be the complete loss of isotope signal variations in the sampled waters, which is often observed when using $\delta^{18}O$ and $\delta^{2}H$ for water age modelling (e.g. McGuire et al., 2005; Timbe et al., 2014; Kirchner, 2015). Another issue could be the short input data record length used in this study (27 months). The input data was extended, producing synthetic eight years series, like in other studies (e.g. Uhlenbrook et al., 2002; McGuire et al., 2005; Viville et al., 2006). Viville et al. (2006), despite having the same issues, modified the input function model and calculated that in the Strengbach catchment (northern France) the water age was of 3.2 years for springs. In the present study, a critical issue is related to the low variations in the isotopic signal of the spring, well and stream waters. Small signal variations allows determining minimum ages, but apparently in Can Vila water was more than two years old. Therefore, the results obtained hinder the suitability of using $\delta^{18}O$ and $\delta^{2}H$ for MTT estimation in the Can Vila catchment, as also observed in other studies (e.g. Stewart et al., 2007). In this context, the use of other tracers (i.e. tritium) is clearly needed to improve the MTT estimation.

4.4.3 Estimation of mean transit time using tritium

Tritium was used to calculate the Cal Rodó catchment MTTs. In this study, in addition to samples collected in 2013, the availability of samples collected in the 1990s by Herrmann et al. (1999) as well as the development of the TEPMGLUE (Tritium Exponential Piston Model GLUE) methodology by Gallart et al. (in review), allowed to analyse the effect of using different sets of samples on MTT estimation.

In contrast to Gallart et al. (in review), where model parameters were searched within a large range, some objectivity was added in this study when establishing a smaller range for model parameters (0.05-1.00 for f and 1-35 years for MTT). This smaller range was based on the parameters search, the reliability of the results obtained, Gallart et al. (in review) trials, and the knowledge of the catchment hydrological functioning. Despite that, approximately normal likelihood weighted cumulative density functions were obtained, at the four sampled locations, when using all tritium samples (section i) or only the 1990s (1996-1998) samples (section ii). Additionally, no significant differences were observed when comparing results of the MTT using all samples or only the 1990s samples. This indicates that tritium content in 1990s samples was enough to calculate MTT, despite the analytical standard error measurement error of ± about 0.8 TU. It also indicates that 2013 samples did not provide additional information, despite their high analytical precision. In fact, as in Gallart et al. (in review), when estimating MTT using only 2013 samples (section iii) two possible solutions (young and old solution) were obtained. When contrasting the younger solution with the previous sampling designs (section i and ii) similar results were obtained, indicating that the younger solution was the most reliable (Fig. 4.11) and that the older solution could be discarded thanks to the availability of the 1990s samples.

The relevance of the 1990s samples for MTT estimations in the Can Vila catchment is clear if compared to the results obtained recently in Luxemburg and Oregon. In this study, three possible water age solutions were also obtained when estimating MTT using a single measurement in 2015 (Stewart and Morgenstern, 2016), but the absence of older samples could not allow the choice of a more reliable solution. However, in a next future, when rainfall atmospheric tritium input will be stable and the quality of the analytical precisions in different laboratories improve, water age estimation in the Northern Hemisphere using recent samples may become possible, as done nowadays in the Southern Hemisphere (e.g. Morgenstern et al., 2010, 2015; Stewart and Fahey, 2010).

4.4.4 Choice of the input function and of the methodology

The 1990s tritium samples (1996-1988) were used by Herrmann et al. (1999) and in the present study to calculate MTT. Herrmann et al. (1999) used the tritium input function of Barcelona and exponential and dispersion models. In the present study, the tritium input

function of Vienna was used (it was scaled and a recharge equation was applied) and the TEPMGLUE methodology (Gallart et al., in review) was applied, providing a set of acceptable MTTs results. Despite the methodological differences, a significant linear relationship existed between the results obtained in the two studies, even if the weighted MTTs calculated in the present study were three years younger (Fig. 4.12) than those of Herrmann et al. (1999). The difference could be mainly attributed to the choice of the tritium input function that is a relevant issue in MTT studies (McGuire and McDonnell, 2006). This suggested that an alternative tritium function would provide a shift in the MTT but well correlated with the original ones.

4.4.5 Water ages distribution in the Cal Rodó catchment

The comparison of the calculated water ages obtained with tritium in the Cal Rodó catchment with other MTTs results in different headwater catchment worldwide (Stewart et al., 2010, Table 4.2), showed that MTT for springs, streams and wells were inside the ranges described in the literature.

The topography and the storage capacity of soils and bedrock have been found, by several authors, as factors influencing the water MTT spatial distribution (e.g. Rodgers et al., 2005; McGuire et al., 2005; Soulsby et al., 2006; Soulsby and Tetzlaff, 2008; Morgernstern et al., 2014). In this study no effect of topography (Topographic Wetness Index and slope) was observed, while it was possible to relate geologic features of Cal Rodó catchment with the different MTTs calculated. Apparently, the geologic features exert some control in Cal Rodó catchment, resulting in shorter MTT in wells, followed by the streams and the springs as observed formerly by Herrmann et al. (1999).

The MTT results suggested that younger water ages were calculated in wells that, in the Cal Rodó catchment, are generally fed by shallow free aquifers developing above an impervious red lutites layer. In the western part of the catchment, where there is a steep limestone outcrop and a less permeable layer (red lutites), water was found to be younger (Fig. 4.15). In this part of the catchment, the water sampled at the outlet of the Can Vila sub-catchment had a MTT very close to that of the main permanent spring (Sp12), presumably fed by a semiconfined aquifer. Whereas in the Ca l'Isard catchment the water sampled at the outlet had a similar MTT than upstream locations. Contrarily, in the eastern part of the Cal Rodó catchment, the structural arrangement (strip of limestones deposited in layers) probably retained water for a longer time period, as evidenced by MTT values in springs (Sp6), streams (St8 and St10) or wells (Gw9). Contributions from the western and eastern part of the Cal Rodó catchment mixed (locations St2, St3 and St4) close to the outlet (St1) where the MTT value was more similar to those from the western part of the catchment that is known to provide most of the flow during low flow conditions (Latron et al., 2008).

4.5 Conclusions

Water age was calculated from weekly variations in $\delta^{18}O$ and $\delta^{2}H$, and from tritium concentrations in streams, springs and wells of the Vallcebre Research Catchments.

Results obtained using $\delta^{18}O$ and $\delta^{2}H$ signal variations in surface and subsurface waters evidenced some limitations on water age estimation in these Mediterranean catchments. In the Can Vila catchment these limitations were mainly related to the small variations in the isotopic signal of the spring, well and stream water isotopic signal. Results obtained could only demonstrate that water was more than two years old at all sampled locations.

Results obtained using tritium and the TEPMGLUE methodology allowed consideration of various sources of uncertainty in water age determination and of the benefit of using samples of differing ages and analytical quality (1996-1998 and 2013 samples). Using the TEPMGLUE methodology considering only the samples taken in the 1990s, yielded similar results as when using all samples (1996-1998 and 2013 samples). Adding the 2013 samples did not, therefore, significantly modify the estimation of the MTT. However, when including only high-quality analytical samples taken in 2013, bimodal solutions for MTT were obtained with the TEPMGLUE approach, showing in each case two possible solutions (younge and older) for water age. The older solution could be discarded thanks to the availability of the 1990s samples.

The contrast between the results obtained in this study and those of Herrmann et al. (1999) mainly derived from different methodologies for determining the tritium input function (rainfall), showing its relevance on the MTT estimations. Despite this, results of both studies were highly correlated, and showed that in the Vallcebre catchments, wells water was younger, followed by streams and springs.

MTTs results obtained in the Cal Rodó catchment (using 1990s samples) showed that topography did not affect water MTT spatial distribution. The general geological settings of the catchment seemed to affect more clearly this distribution in relation with the ability of the catchment to retain or release water. In the eastern part of the catchment, older MTT were calculated, probably related to the presence of a strip of limestones deposited in layers, which could retain water for a longer period than in the western part of the catchment. The results also suggested the existence of shallow open aquifers feeding the catchments wells with MTT around five years. Streams and springs MTT in the catchment were older than in wells, with ages around seven and nine years respectively.

CHAPTER 5

GENERAL CONCLUSIONS

5 GENERAL CONCLUSIONS

Since detailed discussions of the results obtained at the Vallcebre Mediterranean catchments and the conclusions drawn from these are included in each chapter, only a general synthesis of the results, leading to the following outcomes, is given here:

Chapter Two:

- During rainfall-runoff events the depth to water table did not rise uniformly throughout the catchment, due to the effect of local characteristics of the piezometer locations. This, in turn, affects the distribution of wetness conditions and, therefore, the shallow groundwater response.
- Runoff production was affected by the pre-event depth to water table and the rainfall event's characteristics.
- Three types of shallow groundwater responses were observed, depending on antecedent wetness conditions. The results showed more heterogeneous and variable depth to water table response under dry conditions, followed by intermediate and wet conditions.
- The calculation of the timing variable between water table and discharge responses and the analysis of the relationship between the two (i.e. the hysteretic loop) provided relevant information for understanding the role of shallow groundwater contribution during rainfall-runoff events.

Chapter Three:

- Some seasonality in rainwater and soil water dissolved organic carbon (DOC) concentrations was observed, which could be related to biological activity. However, there was no clear seasonality in stream water and groundwater, where DOC dynamics were closely related to discharge and water table variations.
- For rainfall-runoff events with several peaks, the slope of the discharge/DOC concentration relationship was higher at the first peak, suggesting that the DOC contribution was mainly flushed during the first peak.
- The increase of DOC concentration in stream water during the events suggested a relevant contribution of soil water, but also the existence of stream water DOC sources near or in the stream bed.
- Despite the diversity observed in antecedent wetness conditions and in storm event magnitude, stream water DOC dynamics were broadly similar throughout all floods. This

result casts doubt on the origin of the rapid DOC increase and questions the validity of DOC as a tracer to identify water sources during storm events.

Chapter Four:

- The small variations in $\delta^{18}O$ and $\delta^{2}H$ signals observed in surface and subsurface waters impose some limitations on water age calculation in the catchment studied. Using stable isotopes, results only indicated that, in the Can Vila catchment, water was more than two years old.
- The TEPMGLUE methodology, developed in parallel to this study for mean transit time (MTT) calculation using tritium (Gallart et al., in review), permitted evaluation of various sources of uncertainty in water age determination and of the benefit of using samples of differing ages and analytical quality.
- MTT calculation using tritium results was similar when considering only the water samples taken in the nineties and when using all samples (1996-1998 and 2013). Adding the 2013 samples did not, therefore, modify the MTT values obtained. However, when including only high-quality analytical samples taken in 2013, two possible solutions (young and older) were obtained for MTT calculation. In this study, the older solution could be discarded thanks to the availability of the 1990s samples.
- MTT calculation in 21 catchment locations within Cal Rodó (using the 1990s water samples) showed that springs (9.0 ± 3.0 years) had the oldest water, followed by streams (7.7 ± 3.3 years) and wells (5.8 ± 3.5 years).
- Topography did not affect MTT spatial distribution at the Cal Rodó catchment, whereas the geological settings seemed to reflect the ability of the catchment to retain or release water.
- The contrast between the results obtained in this study and those of Herrmann et al. (1999) showed the relevance of the rainfall tritium input function to MTT calculation.

To follow on from the results of this thesis, these future research lines in the Vallcebre Research Catchments could be of interest:

- To investigate the subsurface connectivity of the water table within the catchment during non-stormflow periods. However, this would require monitoring deeper piezometers at most of the existing locations, in order to follow the water table dynamics throughout the year (i.e. also during drier conditions).
- To provide insight into the catchment response by complementing current monitoring and sampling with automatic sampling of groundwater and soil water during storm conditions.

- To use stable isotopes to calculate the relative contribution of new and old water during rainfall-runoff events. The first results for this (Latron et al., personal communication) show that the contributions are variable, depending on catchment wetness characteristics and, especially, rainfall characteristics.
- To study the seasonal and event-scale variations of other solutes in order to evaluate their validity for use as tracers.
- To sample and analyse tritium content, in order to evaluate the perspectives for the future put forward by Gallart et al. (in review).

REFERENCES

Acuña, V., Giorgi, A., Muñoz, I., Uehlinger, U., Sabater, S., 2004. Flow extremes and benthic organic matter shape the metabolism of a headwater Mediterranean stream. Freshwater Biology, 49(7): 960-971.

Agency, E.E., 2012. Map from the DISMED project (Desertification Information System for the Mediterranean) showing the sensitivity to desertification and drought as defined by the sensitivity to desertification index (SDI) based on soil quality, climate and vegetation parameters. European Environment Agency.

Alvarez-Cobelas, M., Angeler, D.G., Sánchez-Carrillo, S., Almendros, G., 2012. A worldwide view of organic carbon export from catchments. Biogeochemistry, 107(1-3): 275-293.

Anderson, M.G., Burt, T.P., 1977. Automatic monitoring of soil moisture conditions in a hillslope spur and hollow. Journal of Hydrology, 33(1–2): 27-36.

Anderton, S., Latron, J., Gallart, F., 2002a. Sensitivity analysis and multi-response, multi-criteria evaluation of a physically based distributed model. Hydrological Processes, 16(2): 333-353.

Anderton, S.P. et al., 2002b. Internal evaluation of a physically-based distributed model using data from a Mediterranean mountain catchment. Hydrology and Earth System Sciences, 6(1): 67-84.

Aubert, A.H. et al., 2013. Solute transport dynamics in small, shallow groundwater-dominated agricultural catchments: insights from a high-frequency, multisolute 10 yr-long monitoring study. Hydrology and Earth System Sciences, 17 (4): 1379-1391.

Avila, A., 1987. Balanç d'aigua i nutrients en una conca d'alzinar al Montseny, Universitat de Barcelona, Barcelona.

Ayalon, A., Bar-Matthews, M., Sass, E., 1998. Rainfall-recharge relationships within a karstic terrain in the Eastern Mediterranean semi-arid region, Israel: δ 18O and δD characteristics. Journal of Hydrology, 207(1–2): 18-31.

Bachmair, S., Weiler, M., 2012. Hillslope characteristics as controls of subsurface flow variability. Hydrology and Earth System Sciences, 16(10): 3699-3715.

Bachmair, S., Weiler, M., Troch, P.A., 2012. Intercomparing hillslope hydrological dynamics: Spatio-temporal variability and vegetation cover effects. Water Resources Research, 48(5): W05537.

Bárdossy, A., Lehmann, W., 1998. Spatial distribution of soil moisture in a small catchment. Part 1: geostatistical analysis. Journal of Hydrology, 206(1–2): 1-15.

Baron, J., McKnight, D., Denning, A.S., 1991. Sources of dissolved and particulate organic material in Loch Vale Watershed, Rocky Mountain National Park, Colorado, USA. Biogeochemistry, 15(2): 89-110.

Bergmann, H., Sackl, B., Maloszewski, P., Stichler, W., 1986. Hydrological investigations in a small catchment area using isotope data series, Proceedings of the fifth international symposium on underground water tracing. Institute of geology and mineral exploration, Athens, pp. 255-22.

Bernal, S., Butturini, A., Sabater, F., 2002. Variability of DOC and nitrate responses to storms in a small Mediterranean forested catchment. Hydrology and Earth System Sciences, 6(6): 1031-1041.

Bernal, S., Butturini, A., Sabater, F., 2005. Seasonal variations of dissolved nitrogen and DOC:DON ratios in an intermittent Mediterranean stream. Biogeochemistry,75(2): 351-372.

Beven, K.J., 1989. Interflow. In: Morel-Seytoux, H.J. (Ed.), Unsaturated Flow in Hydrologic Modeling-Theory and Practice. Kluwer Academic, The Netherlands, pp. 191-219.

Beven, K.J., 1991. Hydrograph separation?, 3rd National Hydrology Symposium, Southampton.

Beven, K.J., Kirkby, M.J., 1979. A physically based, variable contributing area model of basin hydrology. Hydrological Sciences Bulletin, 24(1): 43-69.

Beven, K., Binley, A., 1992. The future of distributed models: Model calibration and uncertainty prediction. Hydrological Processes, 6(3): 279-298.

Beven, K., Binley, A., 2014. GLUE: 20 years on. Hydrological Processes, 28(24): 5897-5918.

Birkel, C., Tetzlaff, D., Dunn, S.M., Soulsby, C., 2011. Using lumped conceptual rainfall–runoff models to simulate daily isotope variability with fractionation in a nested mesoscale catchment. Advances in Water Resources, 34(3): 383-394.

Birkel, C., Soulsby, C., Tetzlaff, D., Dunn, S., Spezia, L., 2012. High-frequency storm event isotope sampling reveals time-variant transit time distributions and influence of diurnal cycles. Hydrological Processes, 26(2): 308-316.

Bishop, K.H., Seibert, J., Köhler, S., Laudon, H., 2004. Resolving the Double Paradox of rapidly mobilized old water with higly warable response in runoff chemistry. Hydrological Processes, 18(1): 185-189.

Boyer, E.W., Hornberger, G.M., Bencala, K.E., McKnight, D.M., 1997. Response characteristics of DOC flushing in an alpine catchment. Hydrological Processes, 11(12): 1635-1647.

Buckingham, S., Tipping, E., Hamilton-Taylor, J., 2008. Concentrations and fluxes of dissolved organic carbon in UK topsoils. Science of The Total Environment, 407(1): 460-470.

Burch, G.J., Bath, R.K., Moore, I.D., O'Loughlin, E.M., 1987. Comparative hydrological behaviour of forested and cleared catchments in southeastern Australia. Journal of Hydrology, 90(1): 19-42.

Burns, D. et al., 2001. Quantifying contributions to storm runoff through end-member mixing analysis and hydrologic measurements at the Panola Mountain Research Watershed (Georgia, USA). Hydrological Processes, 15(10): 1903-1924.

Buttle, J.M., 1994. Isotope hydrograph separations and rapid delivery of pre-event water from drainage basins. Progress in Physical Geography, 18(1): 16-41.

Butturini, A., Sabater, F., 2000. Seasonal variability of dissolved organic carbon in a Mediterranean stream. Biogeochemistry, 51(3): 303-321.

Butturini, A., Gallart, F., Latron, J., Vazquez, E., Sabater, F., 2006. Cross-site comparison of variability of DOC and Nitrate c-q hysteresis during the autumn–winter period in three Mediterranean headwater streams: a synthetic approach. Biogeochemistry, 77(3): 327-349.

Butturini, A., Alvarez, M., Bernal, S., Vazquez, E., Sabater, F., 2008. Diversity and temporal sequences of forms of DOC and NO3-discharge responses in an intermittent stream: Predictable or random succession? Journal of Geophysical Research, 113: G03016.

Camino-Serrano, M. et al., 2014. Linking variability in soil solution dissolved organic carbon to climate, soil type, and vegetation type. Global Biogeochemical Cycles, 28: 497-509.

Carey, S.K., 2003. Dissolved organic carbon fluxes in a discontinuous permafrost subarctic alpine catchment. Permafrost and Periglacial Processes, 14(2): 161-171.

Carey, S.K., Quinton, W.L., 2005. Evaluating runoff generation during summer using hydrometric, stable isotope and hydrochemical methods in a discontinuous permafrost alpine catchment. Hydrological Processes, 19(1): 95-114.

Ceballos, A., Schnabel, S., 1998. Hydrological behaviour of a small catchment in the dehesa landuse system (Extremadura, SW Spain). Journal of Hydrology, 210(1–4): 146-160.

Christ, M.J., David, M.B., 1996. Temperature and moisture effects on the production of dissolved organic carbon in a Spodosol. Soil Biology and Biochemistry, 28(9): 1191-1199.

Cras, A., Marc, V., Travi, Y., 2007. Hydrological behaviour of sub-Mediterranean alpine headwater streams in a badlands environment. Journal of Hydrology, 339(3–4): 130-144.

Custodio, E., Llamas., M.R., 2001. Datación y trazado natural y accidental de las aguas subterráneas. In: Ediciones Omega, S.A. (Ed.), Hidrologia subterranea, Barcelona, pp. 1245-1287.

Daniels, S.M., Agnew, C.T., Allott, T.E.H., Evans, M.G., 2008. Water table variability and runoff generation in an eroded peatland, South Pennines, UK. Journal of Hydrology, 361(1–2): 214-226.

Dawson, J.J.C. et al., 2008. Influence of hydrology and seasonality on DOC exports from three contrasting upland catchments. Biogeochemistry, 90(1): 93-113.

Detty, J.M., McGuire, K.J., 2010. Topographic controls on shallow groundwater dynamics: implications of hydrologic connectivity between hillslopes and riparian zones in a till mantled catchment. Hydrological Processes, 24(16): 2222-2236.

DeWalle, D.R., Edwards, P.J., Swistock, B.R., Aravena, R., Drimmie, R.J., 1997. Seasonal isotope hydrology of three Appalachian forest catchments. Hydrological Processes, 11(15): 1895-1906.

Dinçer, T., Payne, B.R., Florkowski, T., Martinec, J., Tongiorgi, E., 1970. Snowmelt runoff from measurements of tritium and oxygen-18. Water Resources Research, 6(1): 110-124.

Durand, P., Neal, M., Neal, C., 1993. Variations in stable oxygen isotope and solute concentrations in small submediterranean montane streams. Journal of Hydrology, 144(1–4): 283-290.

Epstein, S., Mayeda, T., 1953. Variation of O18 content of waters from natural sources. Geochimica et Cosmochimica Acta, 4(5): 213-224.

Evans, M.G., Burt, T.P., Holden, J., Adamson, J.K., 1999. Runoff generation and water table fluctuations in blanket peat: evidence from UK data spanning the dry summer of 1995. Journal of Hydrology, 221(3–4): 141-160.

Evansa, C.D., Daviesa, T.D., Wigington Jr, P.J., Tranter, M., Kretser, W.A., 1996. Use of factor analysis to investigate processes controlling the chemical composition of four streams in the Adirondack Mountains, New York. Journal of Hydrology, 185(1–4): 297-316.

Freer, J. et al., 2002. The role of bedrock topography on subsurface storm flow. Water Resources Research, 38(12): 1269.

Gaillard, E., Lavabre, J., Isbérie, C., Normand, M., 1995. Etat hydrique d'une parcelle et écoulements dans un petit bassin versant du massif cristallin des Maures. Hydrogéologie, 4: 41-48.

Gallart, F., Llorens, P., Latron, J., 1994. Studying the role of old agricultural terraces on runoff generation in a small Mediterranean mountainous basin. Journal of Hydrology, 159(1): 291-303.

Gallart, F., Latron, J., Llorens, P., Rabadà, D., 1997. Hydrological functioning of mediterranean mountain basins in Vallcebre, Catalonia: Some challenges for hydrological modelling. Hydrological Processes, 11(9): 1263-1272.

Gallart, F., Latron, J., Regüés, D., 1998. Hydrological and Erosion Processes in the Research Catchments of Vallcebre (Pyrenees). In: Boardman, J., Favis-Mortlock, D. (Eds.), Modelling Soil Erosion by Water. NATO ASI Series. Springer Berlin Heidelberg, pp. 503-511.

Gallart, F., Llorens, P., Latron, J., Regüés, D., 2002. Hydrological processes and their seasonal controls in a small Mediterranean mountain catchment in the Pyrenees. Hydrology and Earth System Sciences, 6: 527-537.

Gallart, F., Latron, J., Llorens, P., 2005a. Catchment dynamics in a Mediterranean mountain environment. The Vallcebre research basins (southeastern Pyrenees) I: Hydrology. In: Garcia, C., Batalla, R.J. (Eds.), Developments in Earth Surface Processes. Elsevier, pp. 1-16.

Gallart, F., Balasch, J.C., Regüés, D., Soler, M., Castelltort, X., 2005b. Catchment dynamics in a Mediterranean mountain environment: the Vallcebre research basins (southeastern Pyrenees) II: Temporal and spatial dynamics of erosion and stream sediment transport. In: Celso, G., Ramon, J.B. (Eds.), Developments in Earth Surface Processes. Elsevier, pp. 17-29.

Gallart, F., Latron, J., Llorens, P., Beven, K., 2007. Using internal catchment information to reduce the uncertainty of discharge and baseflow predictions. Advances in Water Resources, 30(4): 808-823.

Gallart, F., Latron, J., Llorens, P., Beven, K.J., 2008. Upscaling discrete internal observations for obtaining catchment-averaged TOPMODEL parameters in a small Mediterranean mountain basin. Physics and Chemistry of the Earth, Parts A/B/C, 33(17–18): 1090-1094.

Gallart, F., Latron, J., Llorens, P., García-Pintado, J., 2010. Hydrology in a Mediterranean mountain environment – the Vallcebre research basins (northeastern Spain). IV. Implementing and testing hydrological models. IAHS Publ, 336: 286-291.

Gallart, F., Latron, J., Pérez-Gallego, N., Martínez-Carreras, N., 2014. Procesos de erosión y balance de sedimentos en las cuencas de Vallcebre: resultados obtenidos y cuestiones abiertas. In: Arnáez, J., González Sampériz, P., Lasanta, T., Valero Garcés, B. (Eds.), Geoecología, cambio ambiental y paisaje: Homenaje al Professor José María García Ruiz, Instituto Pirenaico de Ecología (CSIC) y Universidad de La Rioja, pp. 227-285.

Gallart, F., Roig-Planasdemunt, M., Stewart, M., Llorens, P., Morgenstern, U., Stichler, W.,Pfister, L., Latron, L., In review. A glue framework to improve the analysis of catchment baseflows: a proof-of-concept study relying on tritium and tracer analytical errors. Hydrological Processes.

Garcia-Estringana, P., Latron, J., Llorens, P., Gallart, F., 2012. Spatial and temporal dynamics of soil moisture in a Mediterranean mountain area (Vallcebre, NE Spain). Ecohydrology, 6(5): 741-753.

García-Ruiz, J.M., López-Moreno, J.I., Vicente-Serrano, S.M., Lasanta–Martínez, T., Beguería, S., 2011. Mediterranean water resources in a global change scenario. Earth-Science Reviews, 105(3–4): 121-139.

García-Ruiz, J.M. et al., 2008. Flood generation and sediment transport in experimental catchments affected by land use changes in the central Pyrenees. Journal of Hydrology, 356(1–2): 245-260.

Green, C.T., Zhang, Y., Jurgens, B.C., Starn, J.J., Landon, M.K., 2014. Accuracy of travel time distribution (TTD) models as affected by TTD complexity, observation errors, and model and tracer selection. Water Resources Research, 50(7): 6191-6213.

Grésillon, J.M., Taha, A., 1998. Les zones saturées contributives en climat méditerranéen: condition d'apparition et influence sur les crues. Hydrological Science Journal, 43(2): 567-282.

Haught, D.R.W., van Meerveld, H.J., 2011. Spatial variation in transient water table responses: differences between an upper and lower hillslope zone. Hydrological Processes, 25(25): 3866-3877.

Herrmann, A., Bahls, S., Stichler, W., Gallart, F., Latron, J., 1999. Isotope hydrological study of mean transit times and related hydrogeological conditions in Pyrenean experimental basins (Vallcebre Catalonia). In: C. Leibundgut, J.M.a.G.S. (Ed.), Integrated Methods in Catchment Hydrology - Tracer, Remote Sensing and New Hydrometric Techniques. IAHS, Birmingham, pp. 101-109.

Hewlett, J., Hibbert, A., 1967. Factors affecting the response of small watersheds to precipitation in humid areas. Forest Hydrology, Pergamon: 275-290.

Hinton, M.J., Schiff, S.L., English, M.C., 1997. The significance of storms for the concentration and export of dissolved organic carbon from two Precambrian Shield catchments. Biogeochemistry, 36(1): 67-88.

Hinton, M.J., Schiff, S.L., English, M.C., 1998. Sources and flowpaths of dissolved organic carbon during storms in two forested watersheds of the Precambrian Shield. Biogeochemistry, 41(2): 175-197.

Holloway, J.M., Dahlgren, R.A., 2001. Seasonal and event-scale variations in solute chemistry for four Sierra Nevada catchments. Journal of Hydrology, 250(1–4): 106-121.

Hooper, R.P., 2001. Applying the scientific method to small catchment studies: a review of the Panola Mountain experience. Hydrological Processes, 15(10): 2039-2050.

Hrachowitz, M., Soulsby, C., Tetzlaff, D., Malcolm, I.A., Schoups, G., 2010. Gamma distribution models for transit time estimation in catchments: Physical interpretation of parameters and implications for time-variant transit time assessment. Water Resources Research, 46(10): W10536.

Hrachowitz, M., Soulsby, C., Tetzlaff, D., Malcolm, I.A., 2011. Sensitivity of mean transit time estimates to model conditioning and data availability. Hydrological Processes, 25(6): 980-990.

Hudon, C., Morin, R., Bunch, J., Harland, R., 1996. Carbon and nutrient output from the Great Whale River (Hudson Bay) and a comparison with other rivers around Quebec. Canadian Journal of Fisheries and Aquatic Sciences, 53: 1513-1525.

Hursh, C.R., Brater, E.F., 1941. Separating storm-hydrograph from small drainage-areas into surface-and subsurface-flow. Transactions American Geophysical Union, 22: 863-871.

Inamdar, S.P., Christopher, S.F., Mitchell, M.J., 2004. Export mechanisms for dissolved organic carbon and nitrate during summer storm events in a glaciated forested catchment in New York, USA. Hydrological Processes, 18(14): 2651-2661.

Ingraham, N., 1998. Isotopic variations in Precipitation. In: Kendall, C., Mcdonell, J. (Eds.), Isotope tracers in catchment hydrology. Elsevier Science B.V., Amsterdam, pp. 87-118.

Institut Cartogràfic de Catalunya, 2012. Ortophoto (25cm/pixel). www.icc.es.

Ivarsson, H., Jansson, M., 1994. Temporal variations in the concentration and character of dissolved organic matter in a highly colored stream in the coastal zone of northern Sweden. Archiv fur Hydrobiologie, 132 (1): 45-55.

Jódar, J., Lambán, L.J., Medina, A., Custodio, E., 2014. Exact analytical solution of the convolution integral for classical hydrogeological lumped-parameter models and typical input tracer functions in natural gradient systems. Journal of Hydrology, 519, Part D(0): 3275-3289.

Joerin, C., Beven, K.J., Musy, A., Talamba, D., 2005. Study of hydrological processes by the combination of environmental tracing and hill slope measurements: application on the Haute-Mentue catchment. Hydrological Processes, 19(16): 3127-3145.

Jordan, J.P., 1994. Spatial and temporal variability of stormflow generation processes on a Swiss catchment. Journal of Hydrology, 153(1–4): 357-382.

Kalbitz, K., Solinger, S., Park, J.-H., Michalzik, B., Matzner, E., 2000. Control on the dynamics of dissolved organic matter in soils: A review. Soil Science, 165 (4): 277-304.

Kendall, C., McDonell, J., 1998. Isotope tracers in catchment hydrology. Elsevier.

Kendall, K.A., Shanley, J.B., J, M.J., 1999. A hydrometric and geochemical approach to test the transmissivity feedback hypothesis during snowmelt. Journal of Hydrology, 219(3–4): 188-205.

Kennedy, V.C., Kendall, C., Zellweger, G.W., Wyerman, T.A., Avanzino, R.J., 1986. Determination of the components of stormflow using water chemistry and environmental isotopes, Mattole River basin, California. Journal of Hydrology, 84(1–2): 107-140.

Kirchner, J., 2003. A double paradox in catchment hydrology and geochemistry. Hydrological Processes, 17: 871-874.

Kirchner, J., 2015. Aggregation in environmental systems: seasonal tracer cycles quantify young water fractions, but not mean transit times, in spatially heterogeneous catchments. Hydrology and Earth System Sciences, 12(3): 3059-3103.

Klaus, J., McDonnell, J.J., 2013. Hydrograph separation using stable isotopes: Review and evaluation. Journal of Hydrology, 505(0): 47-64.

Kuraś, P.K., Weiler, M., Alila, Y., 2008. The spatiotemporal variability of runoff generation and groundwater dynamics in a snow-dominated catchment. Journal of Hydrology, 352(1–2): 50-66.

Ladouche, B. et al., 2001. Hydrograph separation using isotopic, chemical and hydrological approaches (Strengbach catchment, France). Journal of Hydrology, 242(3–4): 255-274.

Lambert, T. et al., 2013. Hydrologically driven seasonal changes in the sources and production mechanisms of dissolved organic carbon in a small lowland catchment. Water Resources Research, 49(9): 5792-5803.

Lambs, L., Moussa, I., Brunet, F., 2013. Air Masses Origin and Isotopic Tracers: A Study Case of the Oceanic and Mediterranean Rainfall Southwest of France. Water, 5(2): 617-628.

Lana-Renault, N., Latron, J., Regüés, D., 2007. Streamflow response and water-table dynamics in a sub-Mediterranean research catchment (Central Pyrenees). Journal of Hydrology, 347(3–4): 497-507.

Lana-Renault, N., Regüés, D., Serrano, P., Latron, J., 2014. Spatial and temporal variability of groundwater dynamics in a sub-Mediterranean mountain catchment. Hydrological Processes, 28(8): 3288-3299.

Latron, J., 2003. Estudio del funcionamiento hidrológico de una cuenca mediterránea de montaña (Vallcebre, Pirineos Catalanes), Universitat de Barcelona, Barcelona.

Latron, J., Gallart, F., 2007. Seasonal dynamics of runoff-contributing areas in a small mediterranean research catchment (Vallcebre, Eastern Pyrenees). Journal of Hydrology, 335(1–2): 194-206.

Latron, J., Gallart, F., 2008. Runoff generation processes in a small Mediterranean research catchment (Vallcebre, Eastern Pyrenees). Journal of Hydrology, 358(3–4): 206-220.

Latron, J., Soler, M., Llorens, P., Gallart, F., 2008. Spatial and temporal variability of the hydrological response in a small Mediterranean research catchment (Vallcebre, Eastern Pyrenees). Hydrological Processes, 22(6): 775-787.

Latron, J., Llorens, P., Gallart, F., 2009. The Hydrology of Mediterranean Mountain Areas. Geography Compass, 3(6): 2045-2064.

Latron, J. et al., 2010a. Hydrology in a Mediterranean mountain environment - The Vallcebre research basins (North Eastern Spain). I. 20 years of investigations of hydrological dynamics. IAHS publ, 336: 38-43.

Latron, J., Soler, M., Llorens, P., Nord, G., Gallart, F., 2010b. Hydrology in a Mediterranean mountain environment-The Vallcebre research basins (North Eastern Spain). II. Rainfall runoff relationships and runoff processes. IAHS Publ, 336: 151-156.

Latron, J., Llorens, P., Garcia-Estringana, P., Roig-Planasdemunt, M., Gallart, F., 2014. Estudio y modelización de la dinámica hidrológica de un ambiente Mediterráneo de montaña. Síntesis de los resultados obtenidos a lo largo de 25 años de investigaciones en las cuencas de Vallcebre (Pirineo Oriental). In: Arnáez, J., González Sampériz, P., Lasanta, T., Valero Garcés, B. (Eds.), Geoecología, cambio ambiental y paisaje: Homenaje al Professor José María García Ruiz, Instituto Pirenaico de Ecología (CSIC) y Universidad de La Rioja, pp. 183-193.

Latron, J., Roig-Planasdemunt, M., Gallart, F., Llorens, P., in prep. Combining stable isotopes and hydrometric data to investigate the stormflow response of a Mediterranean mountain catchment (Vallcebre Research Catchments, Spain).

Laudon, H. et al., 2011. Patterns and dynamics of dissolved organic carbon (DOC) in boreal streams: the role of processes, connectivity, and scaling. Ecosystems, 14(6): 880-893.

Lavabre, J., Torres, D.S., Cernesson, F., 1993. Changes in the hydrological response of a small Mediterranean basin a year after a wildfire. Journal of Hydrology, 142(1): 273-299.

Leibundgut, C., Maloszewski, P., Külls, C., 2009. Tracers in Hydrology. John Wiley & Sons Ltd, 1-415 pp.

Linde, N. et al., 2007. Estimation of the water table throughout a catchment using self-potential and piezometric data in a Bayesian framework. Journal of Hydrology, 334(1–2): 88-98.

Lischeid, G., 2008. Combining Hydrometric and Hydrochemical Data Sets for Investigating Runoff Generation Processes: Tautologies, Inconsistencies and Possible Explanations. Journal Compilation: 255-280.

Llorens, P., 1997. Rainfall interception by a Pinus sylvestris forest patch overgrown in a Mediterranean mountainous abandoned area II. Assessment of the applicability of Gash's analytical model. Journal of Hydrology, 199(3–4): 346-359.

Llorens, P., Gallart, F., 1992. Small basin response in a Mediterranean mountainous abandoned farming area: Research design and preliminary results. CATENA, 19(3): 309-320.

Llorens, P., Latron, J., Gallart, F., 1992. Analysis of the role of agricultural abandoned terraces on the hydrology and sediment dynamics in a small mountainous basin (High Llobregat, Eastern Pyrenees). Pirineos(139): 27-46.

Llorens, P., Queralt, I., Plana, F., Gallart, F., 1997. Studying solute and particulate sediment transfer in a small Mediterranean mountainous catchment subject to land abandonment. Earth surface processes and landforms, 22(11): 1027-1035.

Llorens, P., Oliveras, I., Poyatos, R., 2003. Temporal variability of water fluxes in a Pinus sylvestris forest patch in Mediterranean mountain conditions (Vallcebre research catchments, Catalan Pyrenees). In: Servat, E., Najem, W., Leduc, C., Shakeel, A. (Eds.), Hydrology of Mediterranean and Semiarid Regions. IAHS, Wallingford, pp. 101-105.

Llorens, P. et al., 2010a. Hydrology in a Mediterranean mountain environment-the Vallcebre research basins (northeastern Spain). III. Vegetation and water fluxes. IAHS Publ, 336: 186-191.

Llorens, P. et al., 2010b. A multi-year study of rainfall and soil water controls on Scots pine transpiration under Mediterranean mountain conditions. Hydrological processes, 24(21): 3053-3064.

Llorens, P., Latron, J., Álvarez-Cobelas, M., Martínez-Vilalta, J., Moreno, G., 2011. Hydrology and Biogeochemistry of Mediterranean Forests. In: Levia, D.F., Carlyle-Moses, D., Tanaka, T. (Eds.), Forest Hydrology and Biogeochemistry. Ecological Studies. Springer Netherlands, pp. 301-319.

Llorens, P., Poyatos, R., Rubio, C., Latron, J., Gallart, F., 2013. Forest influence in the hydrological processes: examples in the Vallcebre research catchments (catalan Pre-Pyrenees). Cuadernos de Investigación Geográfica, 32: 27-44.

Llorens, P., Domingo, F., Garcia-Estringana, P., Muzylo, A., Gallart, F., 2014. Canopy wetness patterns in a Mediterranean deciduous stand. Journal of Hydrology, 512: 254-262.

Loÿe-Pilot, M.D., 1990. Isotopic and chemical hydrograph separation for a forested headwater mediterranean stream flood. A critical view. In: Hooghart, J.C., Posthumus, C.W.S., Warmerdam, P.M.M. (Eds.), Hydrological research basins and the environment. Netherlands Organization for Applied Scientific Research TNO, The Netherlands, pp. 189-198.

Małoszewski, P., Zuber, A., 1982. Determining the turnover time of groundwater systems with the aid of environmental tracers: 1. Models and their applicability. Journal of Hydrology, 57(3–4): 207-231.

Marc, V., Travi, Y., Lavabre, J., 1995. Etude du fonctionnement hydrologique de bassins versants méditerranéens par le traçage naturel chimique et isotopique. IAHS Publ, 229: 219-229.

Marc, V., Didon-Lescot, J.-F., Michael, C., 2001. Investigation of the hydrological processes using chemical and isotopic tracers in a small Mediterranean forested catchment during autumn recharge. Journal of Hydrology, 247(3–4): 215-229.

Martín-Gómez, P. et al., 2015. Isotope-ratio infrared spectroscopy: a reliable tool for the investigation of plant-water sources? New Phytologist, 207(3): 914-27.

Martínez-Carreras, N., Soler, M., Hernández, E., Gallart, F., 2007. Simulating badland erosion with KINEROS2 in a small Mediterranean mountain basin (Vallcebre, Eastern Pyrenees). CATENA, 71(1): 145-154.

Martínez-Carreras, N. et al., 2015. Hydrological connectivity inferred from diatom transport through the riparian-stream system. Hydrology and Earth System Sciences, 19(7): 3133-3151.

McCallum, J.L., Engdahl, N.B., Ginn, T.R., Cook, P.G., 2014. Nonparametric estimation of groundwater residence time distributions: What can environmental tracer data tell us about groundwater residence time? Water Resources Research, 50(3): 2022-2038.

McDowell, W., Wood, T., 1984. Podzolization: soil processes control dissolved organic carbon concentration in stream water. Soil Science, 137(1).

McDowell, W.H., Likens, G.E., 1988. Origin, Composition, and Flux of Dissolved Organic Carbon in the Hubbard Brook Valley. Ecological Monographs, 58(3): 177-195.

McGlynn, B., McDonnell, J., Stewart, M., Seibert, J., 2003. On the relationships between catchment scale and streamwater mean residence time. Hydrological Processes, 17(1): 175-181.

McGlynn, B.L., McDonnell, J.J., 2003. Role of discrete landscape units in controlling catchment dissolved organic carbon dynamics. Water Resources Research, 39(4): 1090.

McGuire, K.J., DeWalle, D.R., Gburek, W.J., 2002. Evaluation of mean residence time in subsurface waters using oxygen-18 fluctuations during drought conditions in the mid-Appalachians. Journal of Hydrology, 261(1–4): 132-149.

McGuire, K.J. et al., 2005. The role of topography on catchment-scale water residence time. Water Resources Research, 41(5): W05002.

McGuire, K.J., McDonnell, J.J., 2006. A review and evaluation of catchment transit time modeling. Journal of Hydrology, 330(3-4): 543-563.

McMillan, H.K., Srinivasan, M.S., 2015. Characteristics and controls of variability in soil moisture and groundwater in a headwater catchment. Hydrological and Earth System Sciences, 19(4): 1767-1786.

Meyer, J.L., Tate, C.M., 1983. The Effects of Watershed Disturbance on Dissolved Organic Carbon Dynamics of a Stream. Ecology, 64(1): 33-44.

Meyer, J.L., Wallace, J.B., Eggert, S.L., 1998. Leaf Litter as a Source of Dissolved Organic Carbon in Streams. Ecosystems, 1(3): 240-249.

Michalzik, B., Kalbitz, K., Park, J.H., Solinger, S., Matzner, E., 2001. Fluxes and concentrations of dissolved organic carbon and nitrogen – a synthesis for temperate forests. Biogeochemistry, 52 (2): 173-205.

Michel, R.L. et al., 2015. A simplified approach to analysing historical and recent tritium data in surface waters. Hydrological Processes, 29(4): 572-578.

Molina, A.J., Latron, J., Rubio, C.M., Gallart, F., Llorens, P., 2014. Spatio-temporal variability of soil water content on the local scale in a Mediterranean mountain area (Vallcebre, North Eastern Spain). How different spatio-temporal scales reflect mean soil water content. Journal of Hydrology, 516: 182-192.

Morel, B., Durand, P., Jaffrezic, A., Gruau, G., Molenat, J., 2009. Sources of dissolved organic carbon during stormflow in a headwater agricultural catchment. Hydrological Processes, 23(20): 2888-2901.

Morgenstern, U., Taylor, C., 2009. Ultra low-level tritium measurement using electrolytic enrichment and LSC. Isotopes in Environmental Health Studies, 45(2): 96-117.

Morgenstern, U., Stewart, M.K., Stenger, R., 2010. Dating of streamwater using tritium in a post nuclear bomb pulse world: continuous variation of mean transit time with streamflow. Hydrology and Earth System Sciences, 14(11): 2289-2301.

Morgenstern, U. et al., 2014. Groundwater lag times in the water discharges from the Whanganui, Rangitikei and Manawatu catchments, Institute of Geological and Nuclear Sciences Limited, Lower Hutt, New Zealand.

Morgenstern, U. et al., 2015. Using groundwater age and hydrochemistry to understand sources and dynamics of nutrient contamination through the catchment into Lake Rotorua, New Zealand. Hydrology and Earth System Sciences, 19(2): 803-822.

Mueller, M.H., Weingartner, R., Alewell, C., 2013. Importance of vegetation, topography and flow paths for water transit times of base flow in alpine headwater catchments. Hydrology and Earth System Sciences, 17(4): 1661-1679.

Mulholland, P.J., Hill, W.R., 1997. Seasonal patterns in streamwater nutrient and dissolved organic carbon concentrations: Separating catchment flow path and in-stream effects. Water Resources Research, 33(6): 1297-1306.

Musy, A., Higy, C., 2010. Hydrology: A Science of Nature. Science Publishers, 346 pp.

Muzylo, A., Llorens, P., Domingo, F., 2012a. Rainfall partitioning in a deciduous forest plot in leafed and leafless periods. Ecohydrology, 5(6): 759-767.

Muzylo, A., Valente, F., Domingo, F., Llorens, P., 2012b. Modelling rainfall partitioning with sparse Gash and Rutter models in a downy oak stand in leafed and leafless periods. Hydrological Processes, 26(21): 3161-3173.

Myrabø, S., 1997. Temporal and spatial scale of response area and groundwater variation in Till. Hydrological Processes, 11: 1861-1880.

Nash, J.E., Sutcliffe, J.V., 1970. River flow forecasting through conceptual models part I — A discussion of principles. Journal of Hydrology, 10(3): 282-290.

Neal, C. et al., 1992. Stable hydrogen and oxygen isotope studies of rainfall and streamwaters for two contrasting holm oak areas of Catalonia, northeastern Spain. Journal of Hydrology, 140(1–4): 163-178.

Neal, C., Robson, A.J., Neal, M., Reynolds, B., 2005. Dissolved organic carbon for upland acidic and acid sensitive catchments in mid-Wales. Journal of Hydrology, 304(1–4): 203-220.

O'Driscoll, M.A., DeWalle, D.R., McGuire, K.J., Gburek, W.J., 2005. Seasonal 18O variations and groundwater recharge for three landscape types in central Pennsylvania, USA. Journal of Hydrology, 303(1–4): 108-124.

Pan, Y. et al., 2010. Study on dissolved organic carbon in precipitation in Northern China. Atmospheric Environment, 44(19): 2350-2357.

Penna, D., Tromp-van Meerveld, H.J., Gobbi, A., Borga, M., Dalla Fontana, G., 2011. The influence of soil moisture on threshold runoff generation processes in an alpine headwater catchment. Hydrology and Earth System Sciences Discussions, 15: 689-702.

Penna, D., Mantese, N., Hopp, L., Dalla Fontana, G., Borga, M., 2014. Spatio-temporal variability of piezometric response on two steep alpine hillslopes. Hydrological Processes, 29(2): 198-211.

Petelet-Giraud, E., Negrel, P., 2007. Geochemical flood deconvolution in a Mediterranean catchment (Hérault, France) by Sr isotopes, major and trace elements. Journal of Hydrology, 337(1–2): 224-241.

Peters, N.E., Freer, J., Aulenbach, B.T., 2003. Hydrological Dynamics of the Panola Mountain Research Watershed, Georgia. Ground Water, 41(7): 973-988.

Peterson, B.J., Hobbie, J.E., Corliss, T.L., 1986. Carbon Flow in a Tundra Stream Ecosystem. Canadian Journal of Fisheries and Aquatic Sciences, 43(6): 1259-1270.

Pfister, L. et al., 2009. The rivers are alive: on the potential for diatoms as a tracer of water source and hydrological connectivity. Hydrological Processes, 23(19): 2841-2845.

Pfister, L., McDonnell, J.J., Hissler, C., Hoffmann, L., 2010. Ground-based thermal imagery as a simple, practical tool for mapping saturated area connectivity and dynamics. Hydrological Processes, 24(21): 3123-3132.

Poyatos, R., Latron, J., Llorens, P., 2003. Land use and land cover change after agricultural abandonment. Mountain Research and Development, 23(4): 362-368.

Poyatos, R., Llorens, P., Gallart, F., 2005. Transpiration of montane Pinus sylvestris L. and Quercus pubescens Willd. forest stands measured with sap flow sensors in NE Spain. Hydrology and Earth System Sciences, 9(5): 493-505.

Poyatos, R., Llorens, P., Piñol, J., Rubio, C., 2008. Response of Scots pine (Pinus sylvestris L.) and pubescent oak (Quercus pubescens Willd.) to soil and atmospheric water deficits under Mediterranean mountain climate. Annals of Forest Science, 65(3): 306/1-306/13.

Regüés, D., Pardini, G., Gallart, F., 1995. Regolith behaviour and physical weathering of clayey mudrock as dependent on seasonal weather conditions in a badland area at Vallcebre, Eastern Pyrenees. CATENA, 25(1–4): 199-212.

Regüés, D., Guàrdia, R., Gallart, F., 2000. Geomorphic agents versus vegetation spreading as causes of badland occurrence in a Mediterranean subhumid mountainous area. CATENA, 40(2): 173-187.

Regüés, D., Gallart, F., 2004. Seasonal patterns of runoff and erosion responses to simulated rainfall in a badland area in Mediterranean mountain conditions (Vallcebre, southeastern Pyrenees). Earth Surface Processes and Landforms, 29(6): 755-767.

Ribolzi, O. et al., 2000. Contribution of groundwater and overland flows to storm flow generation in a cultivated Mediterranean catchment. Quantification by natural chemical tracing. Journal of Hydrology, 233(1–4): 241-257.

Rinderer, M., van Meerveld, H.J., Seibert, J., 2014. Topographic controls on shallow groundwater levels in a steep, prealpine catchment: When are the TWI assumptions valid? Water Resources Research, 50(7): 6067-6080.

Rinderer, M., van Meerveld, I., Stähli, M., Seibert, J., 2016. Is groundwater response timing in a pre-alpine catchment controlled more by topography or by rainfall? Hydrological Processes, 30(7): 1036-1051.

Rodgers, P., Soulsby, C., Waldron, S., 2005. Stable isotope tracers as diagnostic tools in upscaling flow path understanding and residence time estimates in a mountainous mesoscale catchment. Hydrological Processes, 19(11): 2291-2307.

Rozanski, K., Gonfiantini, R., Araguas-Aragua, L., 1991. Tritium in the global atmosphere: distribution patterns and recent trends. Journal of Physics G: Nuclear and Particle Physics, 17(S): S523-S536.

Rubinson, K., A , Rubinson, J., F, 2000. Análisis Instrumental. Prentice Hall, Madrid, 872 pp.

Rubio, C.M., Llorens, P., Gallart, F., 2008. Uncertainty and efficiency of pedotransfer functions for estimating water retention characteristics of soils. European Journal of Soil Science, 59(2): 339-347.

Ruiz-Pérez, G. et al., 2016. Investigating the behavior of a small Mediterranean catchment using three different hydrological models as hypotheses. Hydrological Processes: n/a-n/a.

Ruprecht, J.K., Schofield, N.J., 1989. Analysis of streamflow generation following deforestation in southwest Western Australia. Journal of Hydrology, 105(1–2): 1-17.

Schiff, S.L. et al., 1997. Export of DOC from forested catchments on the Precambrian Shield of Central Ontario: Clues from 13C and 14C. Biogeochemistry, 36(1): 43-65.

Schnabel, S., Mateos Rodríguez, B., 2000. Hidrología superficial en ambientes adehesados, cuenca experimental Guadalperalón. Cuadernos de Investigación Geográfica, 26: 113-130.

Schuetz, T., Weiler, M., 2011. Quantification of localized groundwater inflow into streams using ground-based infrared thermography. Geophysical Research Letters, 38(3): L03401.

Seibert, J., Bishop, K., Rodhe, A., McDonnell, J.J., 2003. Groundwater dynamics along a hillslope: A test of the steady state hypothesis. Water Resources Research, 39(1): 1014.

Serrano Muela, M.P., 2012. Influencia de la cubierta vegetal y las propiedades del suelo en la respuesta hidrológica: generación de escorrentía en una cuenca forestal de la montaña media pirenaica, University of Zaragoza, 317 pp.

Singh, S., Inamdar, S., Mitchell, M., McHale, P., 2014. Seasonal pattern of dissolved organic matter (DOM) in watershed sources: influence of hydrologic flow paths and autumn leaf fall. Biogeochemistry, 118(1-3): 321-337.

Sklash, M.G., Farvolden, R.N., Fritz, P., 1976. A conceptual model of watershed response to rainfall, developed through the use of oxygen-18 as a natural tracer. Canadian Journal of Earth Sciences, 13(2): 271-283.

Soler, M., Latron, J., Gallart, F., 2008. Relationships between suspended sediment concentrations and discharge in two small research basins in a mountainous Mediterranean area (Vallcebre, Eastern Pyrenees). Geomorphology, 98(1–2): 143-152.

Soler, M., Regüés, D., Latron, J., Gallart, F., 2007. Frequency–magnitude relationships for precipitation, stream flow and sediment load events in a small Mediterranean basin (Vallcebre basin, Eastern Pyrenees). CATENA, 71(1): 164-171.

Soulsby, C., 1995. Contrasts in storm event hydrochemistry in an acidic afforested catchment in upland Wales. Journal of Hydrology, 170(1–4): 159-179.

Soulsby, C., Malcolm, R., Helliwell, R., Ferrier, R.C., Jenkins, A., 2000. Isotope hydrology of the Allt a' Mharcaidh catchment, Cairngorms, Scotland: implications for hydrological pathways and residence times. Hydrological Processes, 14(4): 747-762.

Soulsby, C., Tetzlaff, D., Rodgers, P., Dunn, S., Waldron, S., 2006. Runoff processes, stream water residence times and controlling landscape characteristics in a mesoscale catchment: An initial evaluation. Journal of Hydrology, 325(1–4): 197-221.

Soulsby, C., Tetzlaff, D., 2008. Towards simple approaches for mean residence time estimation in ungauged basins using tracers and soil distributions. Journal of Hydrology, 363(1–4): 60-74.

Soulsby, C., Tetzlaff, D., Hrachowitz, M., 2010. Are transit times useful process-based tools for flow prediction and classification in ungauged basins in montane regions? Hydrological Processes, 24(12): 1685-1696.

Stewart, M.K., Mehlhorn, J., Elliott, S., 2007. Hydrometric and natural tracer (oxygen-18, silica, tritium and sulphur hexafluoride) evidence for a dominant groundwater contribution to Pukemanga Stream, New Zealand. Hydrological Processes, 21(24): 3340-3356.

Stewart, M.K., Fahey, B.D., 2010. Runoff generating processes in adjacent tussock grassland and pine plantation catchments as indicated by mean transit time estimation using tritium. Hydrology and Earth System Sciences, 14(6): 1021-1032.

Stewart, M.K., Morgenstern, U., McDonnell, J.J., 2010. Truncation of stream residence time: how the use of stable isotopes has skewed our concept of streamwater age and origin. Hydrological Processes, 24(12): 1646-1659.

Stewart, M.K., Morgenstern, U., McDonnell, J.J., Pfister, L., 2012. The 'hidden streamflow' challenge in catchment hydrology: a call to action for stream water transit time analysis. Hydrological Processes, 26(13): 2061-2066.

Stewart, M.K., Morgenstern, U., 2016. Importance of tritium-based transit times in hydrological systems. Wiley Interdisciplinary Reviews: Water, 3(2): 145-154.

Stutter, M.I., Dunn, S.M., Lumsdon, D.G., 2004. Dissolved organic carbon dynamics in a UK podzolic moorland catchment: linking storm hydrochemistry, flow path analysis and sorption experiments. Biogeosciences, 9(6): 2159-2175.

Taha, A., Gresillon, J.M., Clothier, B.E., 1997. Modelling the link between hillslope water movement and stream flow: application to a small Mediterranean forest watershed. Journal of Hydrology, 203(1–4): 11-20.

Tetzlaff, D., Malcolm, I.A., Soulsby, C., 2007. Influence of forestry, environmental change and climatic variability on the hydrology, hydrochemistry and residence times of upland catchments. Journal of Hydrology, 346(3–4): 93-111.

Thornthwaite, C.W., 1948. An Approach toward a Rational Classification of Climate. Geographical Review, 38(1): 55-94.

Timbe, E. et al., 2014. Understanding uncertainties when inferring mean transit times of water trough tracer-based lumped-parameter models in Andean tropical montane cloud forest catchments. Hydrology and Earth System Sciences, 18(4): 1503-1523.

Travi, Y., Lavabre, J., Blavoux, B., Martin, C., 1994. Chemical and isotopic labelling (Cl−, 18O) of an autumnal flood for a small burnt Mediterranean basin. Hydrological Sciences Journal, 39(6): 605-619.

Tromp-van Meerveld, H.J., McDonnell, J.J., 2006b. Threshold relations in subsurface stormflow: 2. The fill and spill hypothesis. Water Resources Research, 42(2): W02411.

Uhlenbrook, S., Frey, M., Leibundgut, C., Maloszewski, P., 2002. Hydrograph separations in a mesoscale mountainous basin at event and seasonal timescales. Water Resources Research, 38(6): 1096.

Vallejos, A., Pulido-Bosch, A., Martin-Rosales, W., Calvache, M.L., 1997. Contribution of environmental isotopes the understanding of complex hydrologyc systems. A case study: Sierra de Gador, se Spain. Earth surface processes and landforms, 22: 1157-1168.

van Meerveld, H.J., Seibert, J., Peters, N.E., 2015. Hillslope–riparian-stream connectivity and flow directions at the Panola Mountain Research Watershed. Hydrological Processes, 29(16): 3556-3574.

Vandenschrick, G. et al., 2002. Using stable isotope analysis (δD–δ18O) to characterise the regional hydrology of the Sierra de Gador, south east Spain. Journal of Hydrology, 265(1–4): 43-55.

Vázquez, E., Romaní, A., Sabater, F., Butturini, A., 2007. Effects of the Dry–Wet Hydrological Shift on Dissolved Organic Carbon Dynamics and Fate Across Stream–Riparian Interface in a Mediterranean Catchment. Ecosystems, 10(2): 239-251.

Verstraeten, A., De Vos, B., Neirynck, J., Roskams, P., Hens, M., 2014. Impact of air-borne or canopy-derived dissolved organic carbon (DOC) on forest soil solution DOC in Flanders, Belgium. Atmospheric Environment, 83 (0): 155-165.

Viville, D., Ladouche, B., Bariac, T., 2006. Isotope hydrological study of mean transit time in the granitic Strengbach catchment (Vosges massif, France): application of the FlowPC model with modified input function. Hydrological Processes, 20(8): 1737-1751.

Viviroli, D., Dürr, H.H., Messerli, B., Meybeck, M., Weingartner, R., 2007. Mountains of the world, water towers for humanity: typology, mapping, and global significance. Water Resources Research, 43: W07447.

Von Schiller, D. et al., 2008. Influence of land use on stream ecosystem function in a Mediterranean catchment. Freshwater Biology, 53(12): 2600-2612.

Von Schiller, D. et al., 2015. Hydrological transitions drive dissolved organic matter quantity and composition in a temporary Mediterranean stream. Biogeochemistry, 123(3): 429-446.

Western, A.W., Blöschl, G., 1999. On the spatial scaling of soil moisture. Journal of Hydrology, 217(3–4): 203-224.

Woodward, J., 2009. The Physical Geography of the Mediterranean. Oxford University Press.

Wu, Y., Clarke, N., Mulder, J., 2010. Dissolved Organic Carbon Concentrations in Throughfall and Soil Waters at Level II Monitoring Plots in Norway: Short- and Long-Term Variations. Water, Air,and Soil Pollution, 205(1-4): 273-288.

LIST OF ACRONYMS

a.s.l	above sea level
C_s	storm runoff coefficient
DOC	dissolved organic carbon
GMWL	Global Meteoric Water Line
IAEA	International Atomic Energy Agency
ICC	Institut Cartogràfic de Catalunya
I_{max}	maximum rainfall intensity
LMWL	Local Meteoric Water Line
lwcdf	likelihood weighted cumulative density function
MTT	mean transit time
Q_b	pre-event specific discharge
r_s	Spearman rank correlation coefficient
TEPMGLUE	Tritium Exponential Piston Model GLUE
t_{peak}	time between the start of the rainfall and the time at which water table had risen to 95% of its maximum
$t_{peak-peak}$	time lag between the time of peak discharge at the catchment outlet and the time at which water table had risen to 95% of its maximum
$t_{response}$	time lag between the start of rainfall and the largest change between two successive water table level measurements
TWI	topographic wetness index
WT_i	pre-event depth to water table
$WT_{increase}$	difference between water table at $t_{response}$ and at t_{peak}

APPENDIX A. PHOTOGRAPHIC SUPPORTING INFORMATION

Fig. 1 (a) Can Vila gauging station. (b) Rainfall recorder and rainfall automatic sampler. (c) Soil water sampling with a suction lysimeter. (d) Spring Sp12. (e) Shallow groundwater sampling with a manual peristaltic pump (Z_{CV3S}). (f) Piezometer with water pressure sensor. Source: M.Roig-Planasdemunt.

Fig. 2 (a) Conductimeter, 250 ml polyethylene bottles, 120 ml glass bottle and 3 ml glass vials used to manual sampling. (b) The two automatic samplers of stream water of Can Vila gauging station. (c) Filtration and aliquot preparation in the IDAEA-CSIC laboratory. (d) Total Organic Carbon Analyzer (TOC-VCSH/CSN, Shimadzu) of IDAEA-CSIC. (e) The tritium electrolysis system of the Water Dating Laboratory of GNS Science (New Zealand). (f) $\delta^{2}H$ and $\delta^{18}O$ analyzer (Picarro L2120-i) of Serveis Científico-Tècnics of the Universitat de Lleida (Spain) (f). Source: (a), (b), (c), (d), (e) M.Roig-Planasdemunt; (f) M.Oromí.

APPENDIX B. COMPLEMENTARY INFORMATION OF CHAPTER 2

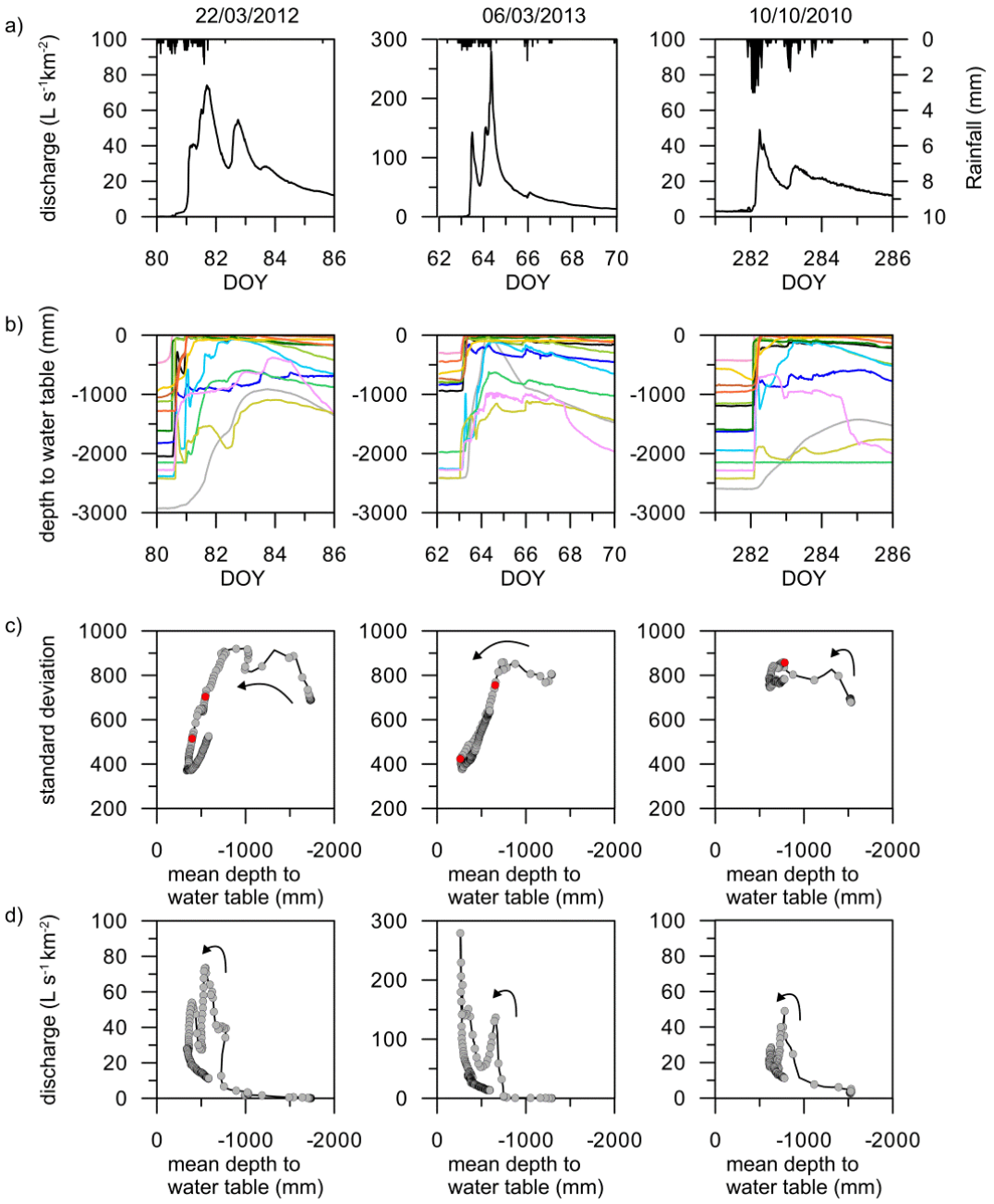

Fig.1 (a) Rainfall and discharge and (b) depth to water table in the 13 piezometer locations, observed during three floods with similar antecedent wetness conditions. (c) Relationship between the mean depth to water table and its standard deviation (red dot correspond to the time of peak discharge). (d) Relationship between the mean depth to water table and discharge (one hour time step).

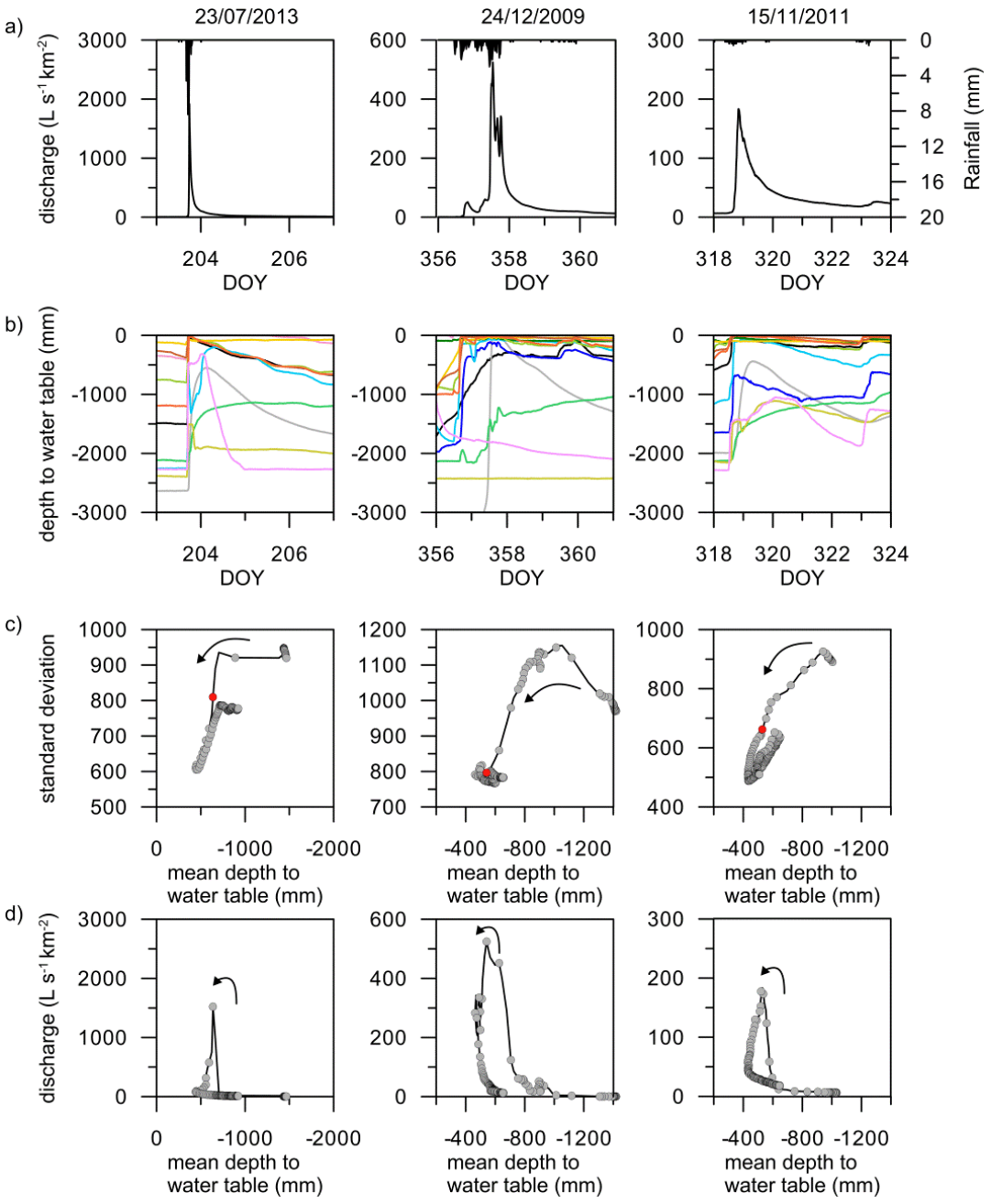

Fig. 2 (a) Rainfall and discharge and (b) depth to water table in the 13 piezometer locations, observed during three floods with similar antecedent wetness conditions. (c) Relationship between the mean depth to water table and its standard deviation (red dot correspond to the time of peak discharge). (d) Relationship between the mean depth to water table and discharge (one hour time step).

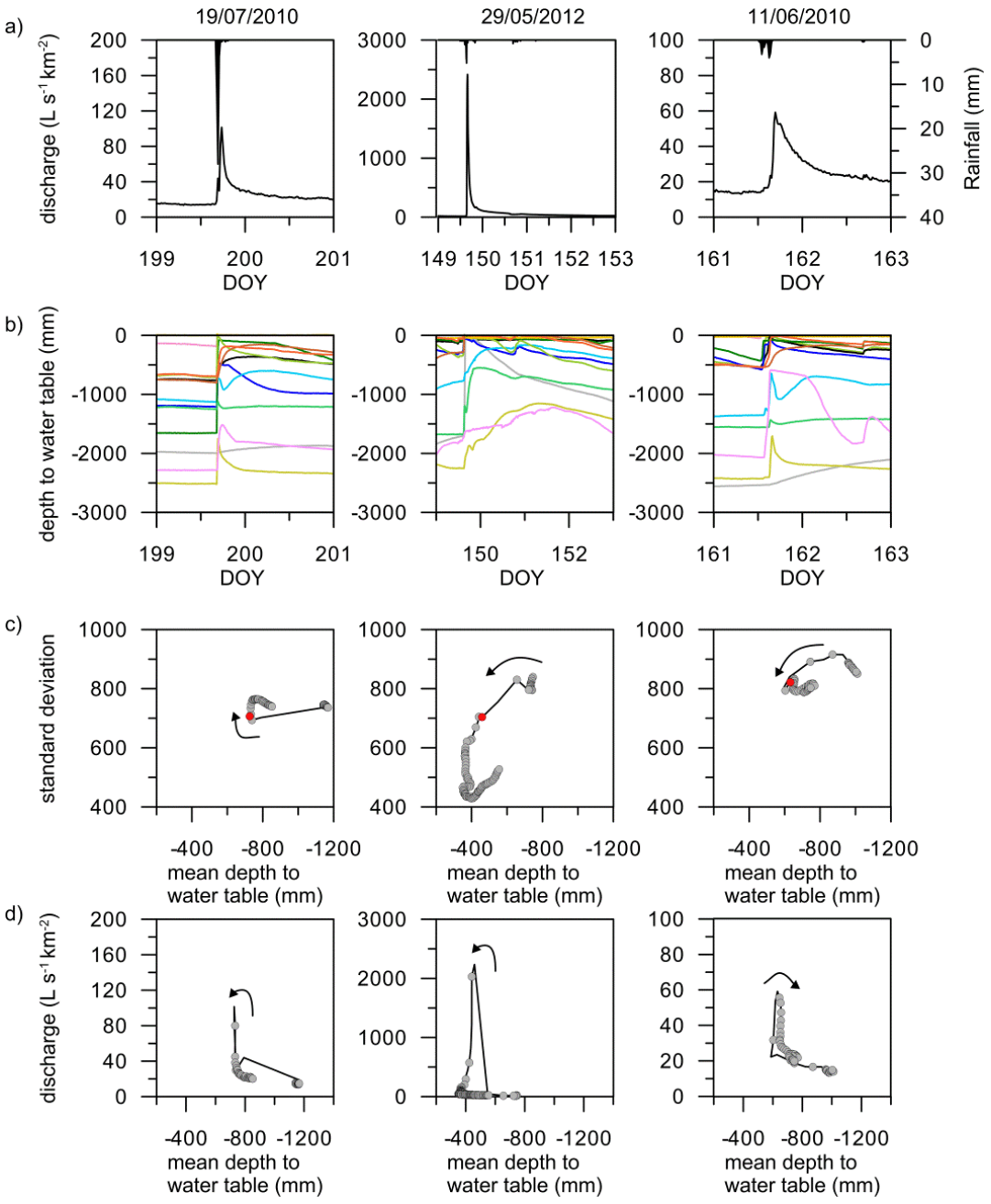

Fig. 3 (a) Rainfall and discharge and (b) depth to water table in the 13 piezometer locations, observed during three floods with similar antecedent wetness conditions. (c) Relationship between the mean depth to water table and its standard deviation (red dot correspond to the time of peak discharge). (d) Relationship between the mean depth to water table and discharge (one hour time step).

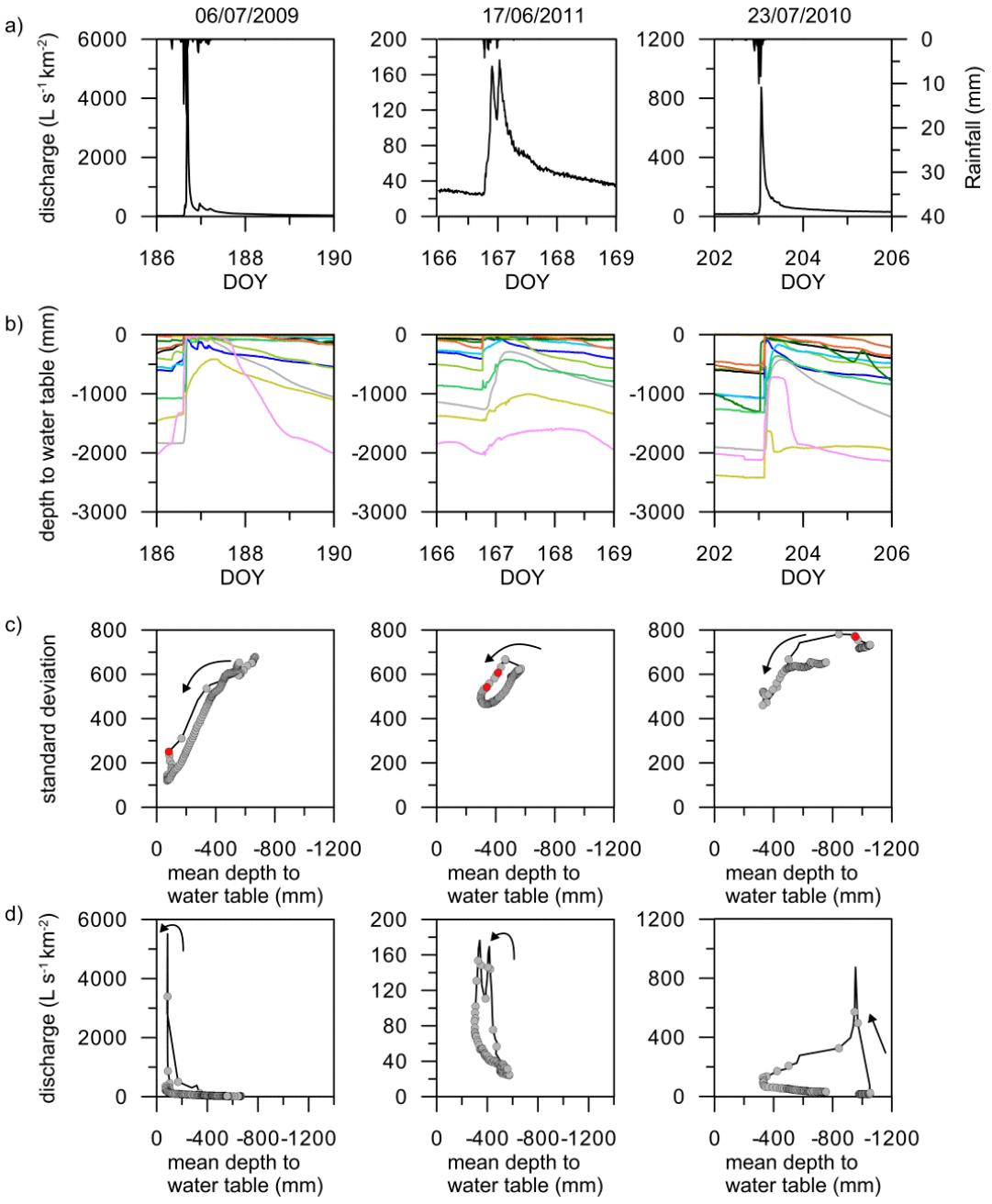

Fig. 4 (a) Rainfall and discharge and (b) depth to water table in the 13 piezometer locations, observed during three floods with similar antecedent wetness conditions. (c) Relationship between the mean depth to water table and its standard deviation (red dot correspond to the time of peak discharge). (d) Relationship between the mean depth to water table and discharge (one hour time step).

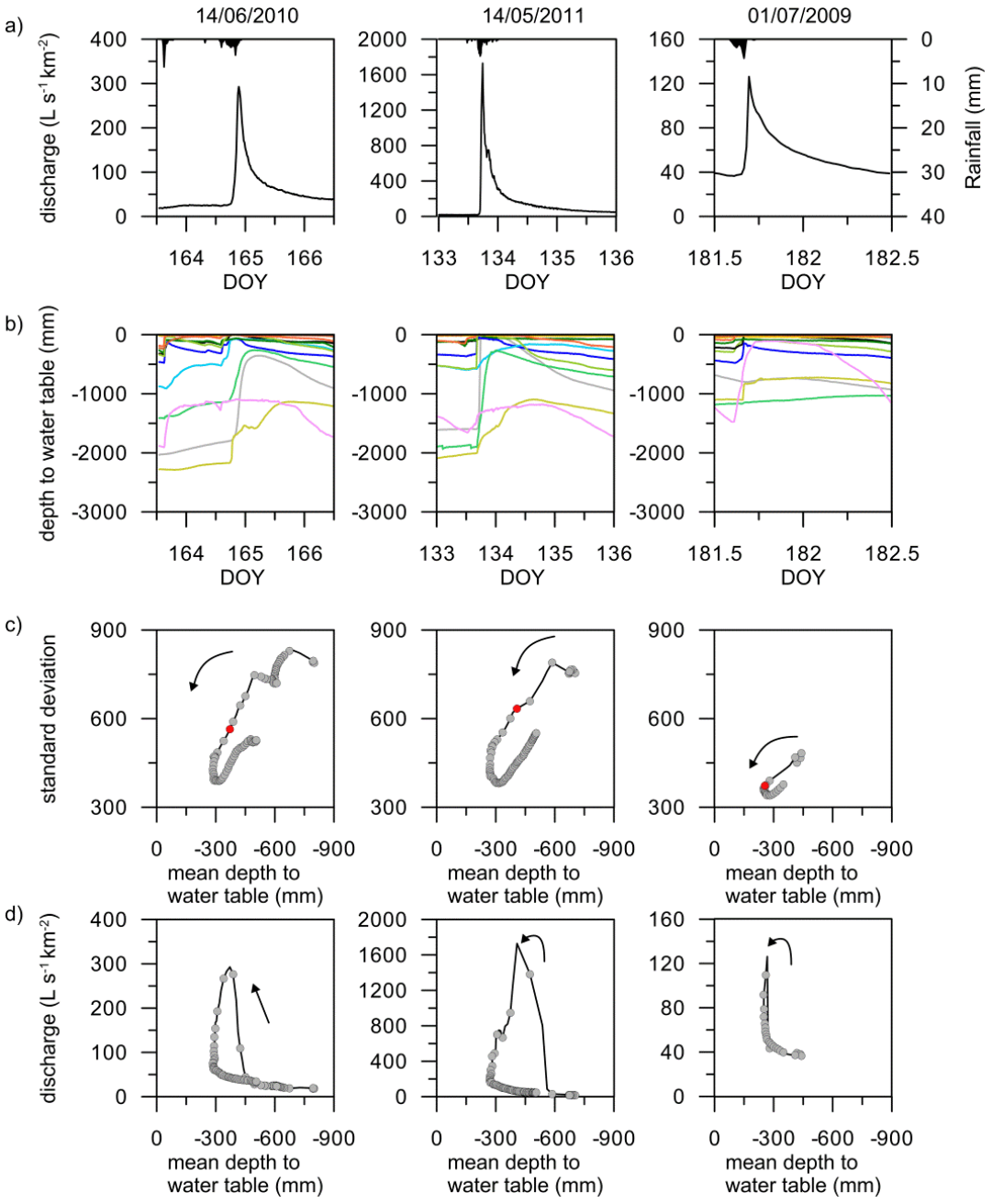

Fig. 5 (a) Rainfall and discharge and (b) depth to water table in the 13 piezometer locations, observed during three floods with similar antecedent wetness conditions. (c) Relationship between the mean depth to water table and its standard deviation (red dot correspond to the time of peak discharge). (d) Relationship between the mean depth to water table and discharge (one hour time step).

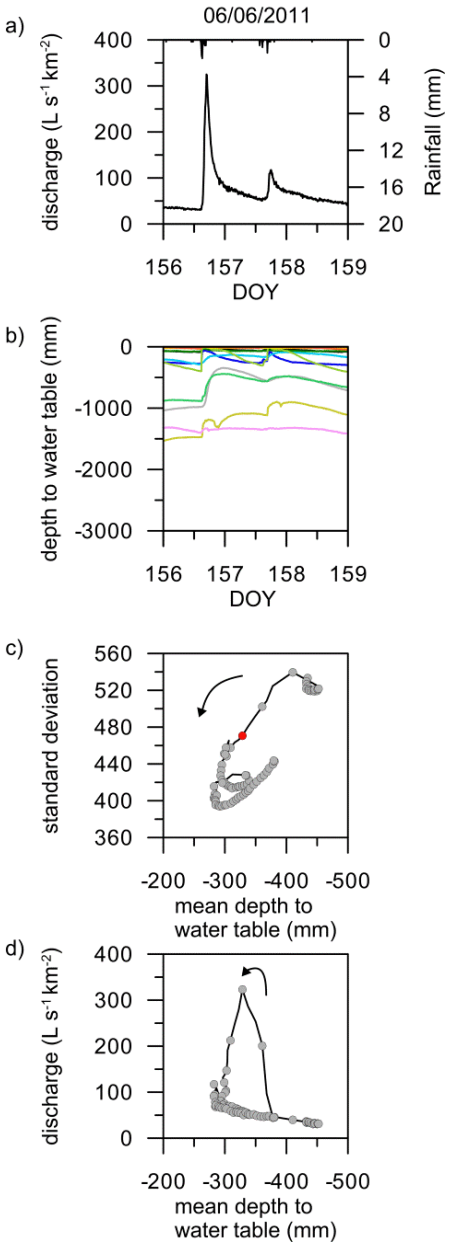

Fig. 6 (a) Rainfall and discharge and (b) depth to water table in the 13 piezometer locations, observed during a flood. (c) Relationship between the mean depth to water table and its standard deviation (red dot correspond to the time of peak discharge). (d) Relationship between the mean depth to water table and discharge (one hour time step).

APPENDIX C. COMPLEMENTARY INFORMATION OF CHAPTER 3

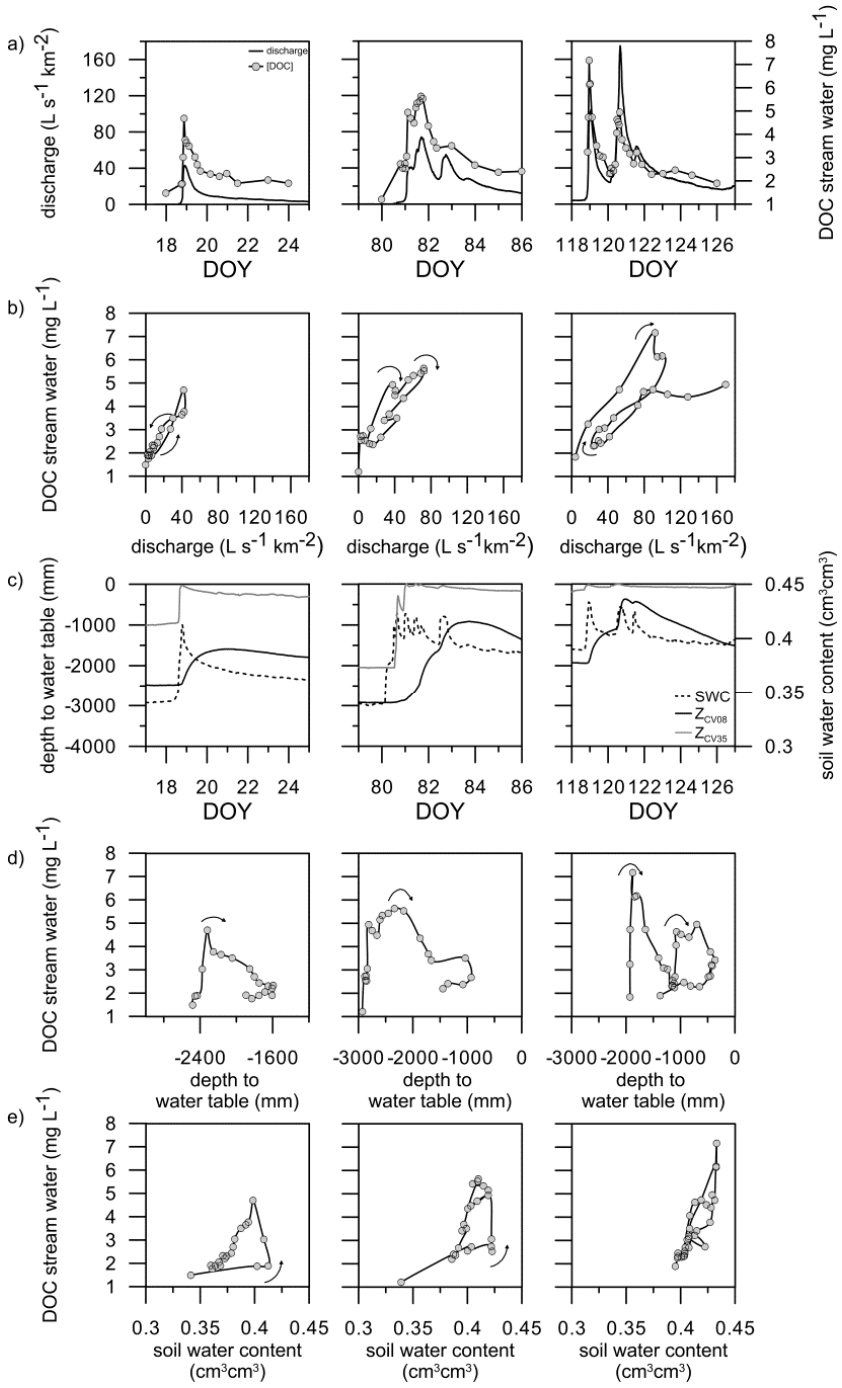

Fig.1 (a) Discharge and DOC concentration in stream water during three floods (19 January 2013, 22 March 2012 and 30 April 2012). (b) Relationship between discharge and DOC concentration in stream water during the event. (c) Soil water content (SWC at 0-90cm depth) and depth to the water table (piezometers Z_{CV08} and Z_{CV35}) during the event. (d) Relationship between the depth to the water table at Z_{CV08} and DOC concentration in stream water during the event. (e) Relationship between the soil water content (0-90cm) and DOC concentration in stream water during the event. In (b), (d) and (e), arrows indicate the directions of the hysteresis for each flood peak.

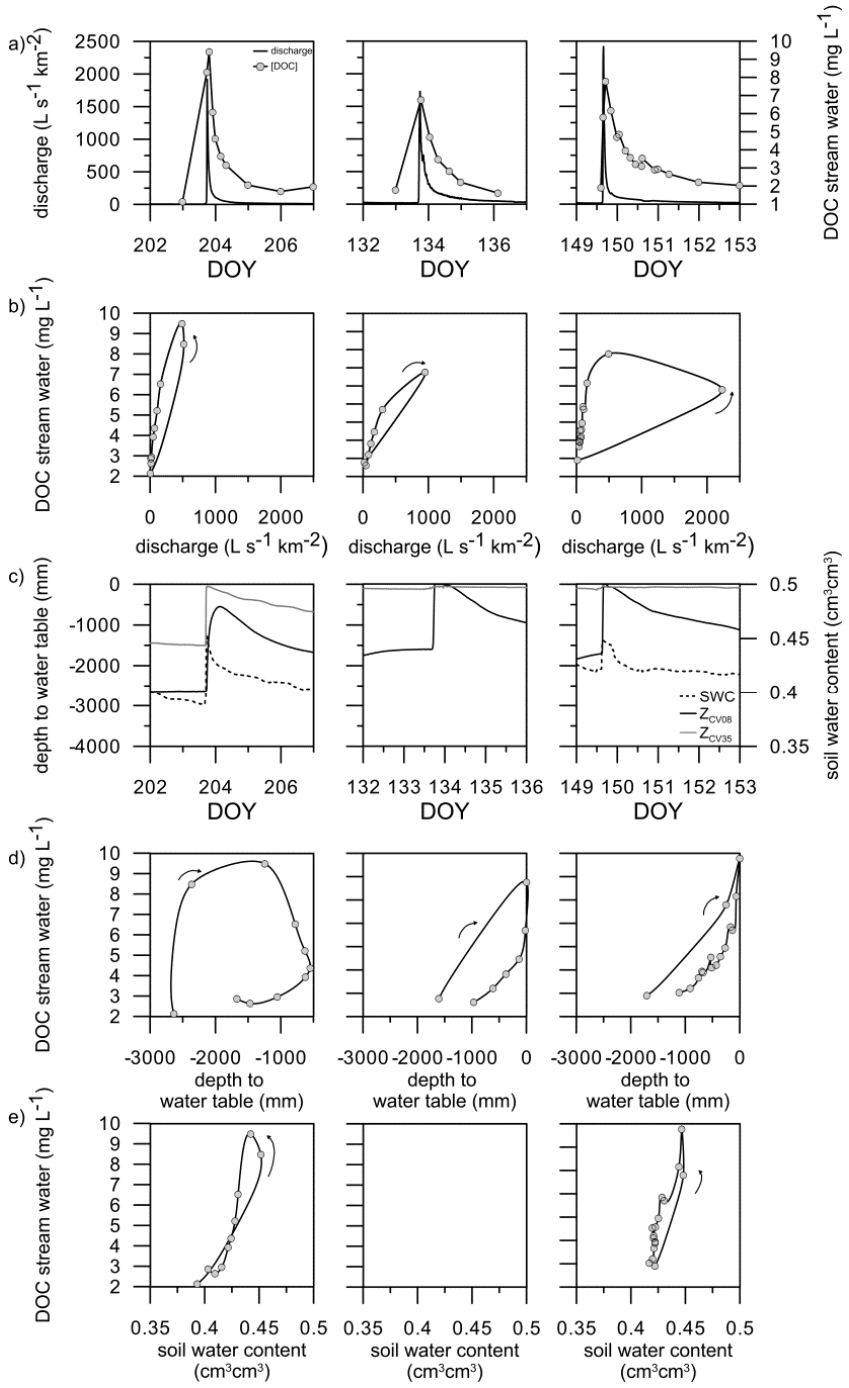

Fig. 2 (a) Discharge and DOC concentration in stream water during three floods (23 July 2013, 14 May 2011 and 29 May 2012). (b) Relationship between discharge and DOC concentration in stream water during the event. Soil water content (SWC at 0-90cm depth) and depth to the water table (piezometers Z_{CV08} and Z_{CV35}) during the event (c). (d)Relationship between the depth to the water table at Z_{CV08} and DOC concentration in stream water during the event. (e)Relationship between the soil water content (0-90cm) and DOC concentration in stream water during the event. In (b), (d) and (e), arrows indicate the directions of the hysteresis for each flood peak. Note the lack of SWC data in flood 14 May 2011.

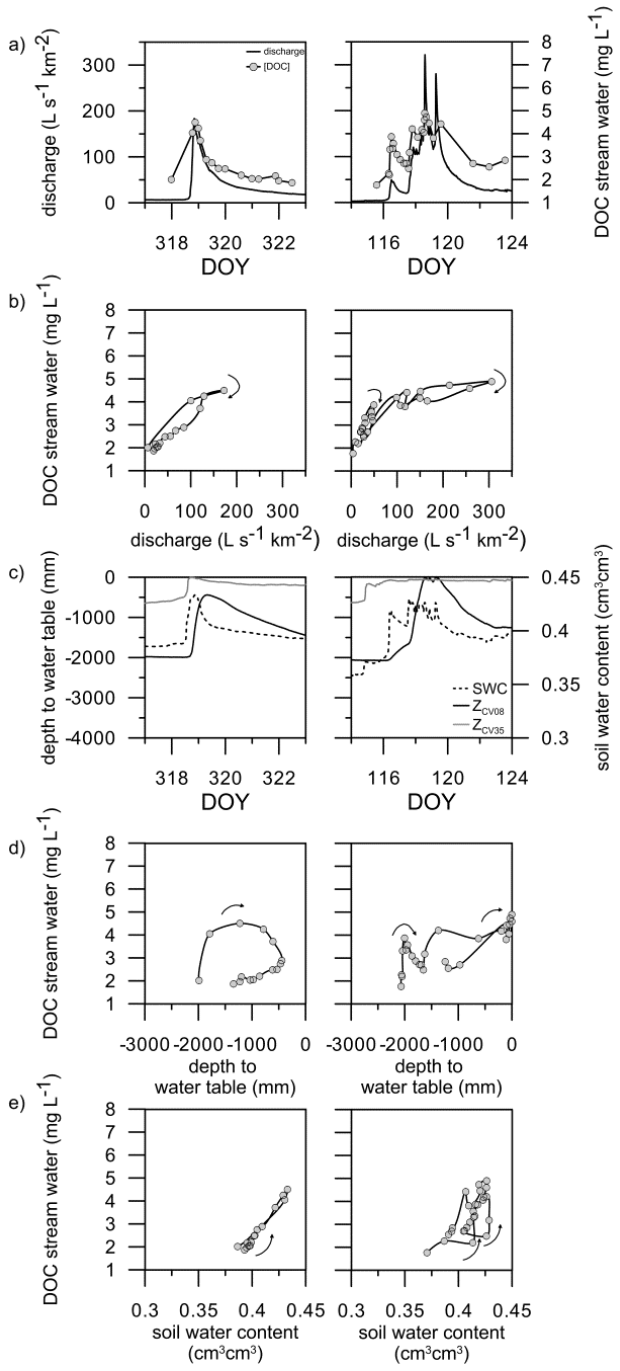

Fig.3. (a) Discharge and DOC concentration in stream water during two floods (15 November 2011 and 29 April 2013). (b) Relationship between discharge and DOC concentration in stream water during the event. (c) Soil water content (SWC at 0-90cm depth) and depth to the water table (piezometers Z_{CV08} and Z_{CV35}) during the event. (d) Relationship between the depth to the water table at Z_{CV08} and DOC concentration in stream water during the event. (e) Relationship between the soil water content (0-90cm) and DOC concentration in stream water during the event. In (b), (d) and (e), arrows indicate the directions of the hysteresis for each flood peak.

APPENDIX D. COMPLEMENTARY INFORMATION OF CHAPTER 4

Table 1. Mean δ18O and δ2H concentration (‰, ± standard deviation) measured in rainwater, stream water, spring water and groundwater over the whole study period, and during the spring, summer, autumn and winter periods. n is the number of samples.

	Rainwater		Stream water		Spring water		Groundwater	
	$\delta^{18}O$	$\delta^{2}H$	$\delta^{18}O$	$\delta^{2}H$	$\delta^{18}O$	$\delta^{2}H$	$\delta^{18}O$	$\delta^{2}H$
Total	-7.0 ± 3.3	-42.8 ± 26.7	-7.2 ± 0.2	-43.9 ± 1.6	-7.5 ± 0.2	-46.1 ± 1.4	-7.0 ± 0.5	-42.7 ± 3.5
	n = 66	n = 66	n = 109	n = 109	n = 68	n = 68	n = 70	n = 70
Spring	-6.9 ± 3.1	-42.8 ± 24.9	-7.3 ± 0.2	-44.4 ± 1.2	-7.5 ± 0.2	-45.7 ± 1.4	-7.2 ± 0.5	-42.8 ± 3.9
	n = 24	n = 24	n =34	n = 34	n = 19	n = 19	n = 21	n = 21
Summer	-4.4 ± 1.8	-22.9 ± 14.2	-7.1 ± 0.3	-43.0 ± 2.1	-7.5 ± 0.3	-46.7 ± 1.4	-6.9 ± 0.5	-41.6 ± 4.0
	n = 15	n = 15	n = 26	n = 26	n = 18	n = 18	n = 18	n = 18
Autumn	-7.9 ± 2.7	-46.5 ± 20.8	-7.2 ± 0.2	-43.9 ± 1.4	-7.4 ± 0.2	-45.6 ± 1.3	-6.9 ± 0.4	-42.4 ± 2.1
	n = 16	n =16	n = 25	n = 25	n = 17	n = 17	n = 17	n = 17
Winter	-9.7 ± 3.5	-64.4 ± 33.8	-7.2 ± 0.2	-43.9 ± 1.0	-7.6 ± 0.2	-46.6 ± 1.3	-7.1 ± 0.4	-44.3 ± 3.4
	n = 11	n = 11	n = 24	n = 24	n = 14	n = 14	n = 14	n =14

Table 2. Tritium content (TU) ± standard errors in springs, streams and wells of Cal Rodó catchment. Data from the nineties are from Herrmann et al. (1999).

	Location	26/07/1996	02/10/1996	12/05/1997	13/03/1998	25/06/1998	3/09/2013
Springs	Sp5	10.0 ± 1.00	11.5 ± 1.00	10.3 ± 0.60	9.4 ± 0.50	9.1 ± 0.95	
	Sp6	14.5 ± 1.25	14.1 ± 075	12.6 ± 0.70	12.7 ± 0.80	11.6 ± 0.85	
	Sp12	10.6 ± 1.15	11.3 ± 0.65	9.9 ± 0.55	9.0 ± 0.80	9.0 ± 0.85	5.127 ± 0.093
Streams	St1	9.3 ± 0.90	10.7 ± 0.95	10.5 ± 0.65	9.4 ± 0.55	8.7 ± 0.95	5.384 ± 0.097
	St2	12.3 ± 1.05	14.2 ± 1.20	11.9 ± 0.65	10.6 ± 0.55	11.0 ± 0.85	
	St3	10.3 ± 1.05	11.7 ± 1.15	9.3 ± 0.55	8.9 ± 0.70	9.6 ± 1.00	
	St4	11.0 ± 1.3	12.0 ± 1.15	9.9 ± 0.60	8.3 ± 0.50	9.7 ± 0.85	5.376 ± 0.097
	St8	10.8 ± 1.00		10.5 ± 0.60	10.6 ±0.70	11.4 ± 0.90	
	St10		15.8 ± 0.85	12.5 ± 0.65	11.0 ± 0.85		
	St11	9.8 ± 0.95			10.2 ± 0.80		
	St16			8.9 ± 0.55	6.8 ± 0.70		
	St17	9.4 ± 0.95	10.8 ± 0.80	9.2 ± 0.55	9.0 ± 0.75	11.3 ± 0.90	
	St21	7.9 ± 1.20	9.9 ± 0.70				
	St22	10.1 ± 1.00	10.8 ± 0.65	10.2 ± 0.60	8.8 ± 0.90	9.1 ± 0.90	
	St23	10.4 ± 1.05	11.6 ± 0.75	9.0 ± 0.60	8.0 ± 0.80	8.7 ± 0.75	
Wells	Gw7	8.5 ± 1.15	7.9 ± 0.55	7.1 ± 0.60	6.9 ± 0.60	8.7 ± 0.95	
	Gw9	11.5 ± 1.00	11.7 ± 0.65	10.6 ± 0.60	10.5 ± 0.85	11.0 ± 0.85	
	Gw13	6.6 ± 1.05	9.8 ± 0.60	8.5 ± 0.60	7.0 ± 0.75	10.2 ± 1.10	
	Gw14	9.4 ± 1.10	8.8 ± 0.60	7.2 ± 0.50	8.1 ± 0.85	7.2 ± 0.80	
	Gw15	8.7 ± 1.20	8.4 ± 0.60				
	Gw18	8.7 ± 1.20	8.2 ± 0.60	7.7 ± 0.55	6.8 ± 0.85	7.4 ± 1.00	6.171 ± 0.110

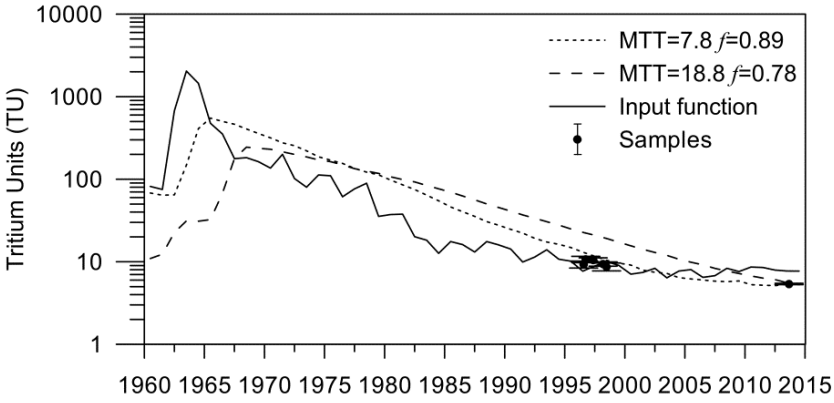

Fig.1 Temporal series (1960-2015) of tritium input in rainfall and of the two model simulations using the stream water samples (St1). Black dots with the error bars show the tritium values in the samples.

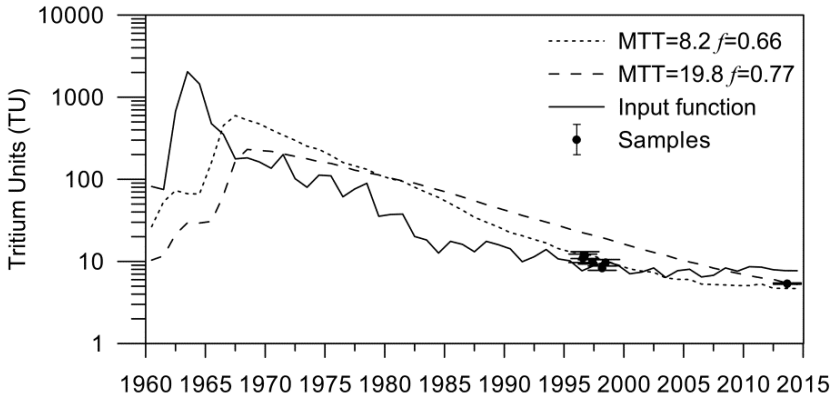

Fig. 2 Temporal series (1960-2015) of tritium input in rainfall and of the two model simulations using the stream water samples (St4). Black dots with the error bars show the tritium values in the samples.

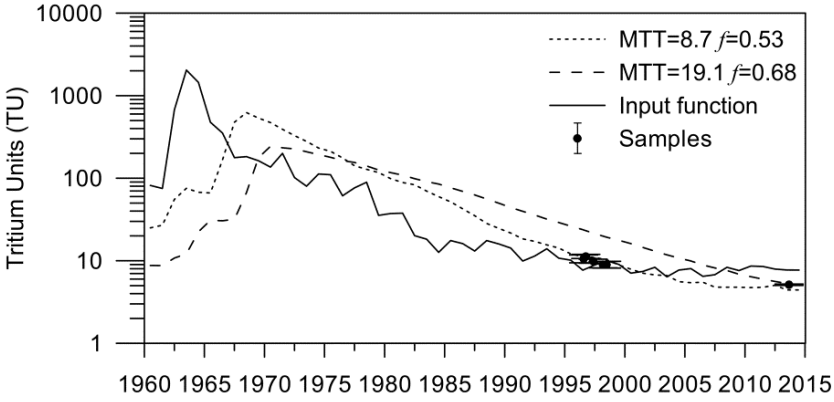

Fig. 3 Temporal series (1960-2015) of tritium input in rainfall and of the two model simulations using the spring water samples (Sp12). Black dots with the error bars show the tritium values in the samples.

LIST OF PUBLICATIONS

Publications

Roig-Planasdemunt, M., Llorens, P., Latron, J., in prep. Spatial and temporal variability of depth to water table during rainfall-runoff events in a Mediterranean mountain catchment (Vallcebre, Eastern Pyrenees). Journal of Hydrology.

Latron, J., Roig-Planasdemunt, M., Gallart, F., Llorens, P., in prep. Combining stable isotopes and hydrometric data to investigate the stormflow response of a Mediterranean mountain catchment (Vallcebre Research Catchments, Spain).

Gallart, F., Roig-Planasdemunt, M., Stewart, M., Llorens, P., Morgenstern, U., Stichler, W.,Pfister, L., Latron, L., In review. A glue framework to improve the analysis of catchment baseflows: a proof-of-concept study relying on tritium and tracer analytical errors. Hydrological Processes.

Roig-Planasdemunt, M., Llorens, P., Latron, J., accepted. Seasonal and strom dynamics of Dissolved Organic Carbon in a Mediterranean mountain catchment (Vallcebre, Eastern Pyrenees). Hydrological Science Journal.

Latron, J., Llorens, P., Garcia-Estringana, P., Roig-Planasdemunt, M., Gallart, F., 2014. Estudio y modelización de la dinámica hidrológica de un ambiente Mediterráneo de montaña. Síntesis de los resultados obtenidos a lo largo de 25 años de investigaciones en las cuencas de Vallcebre (Pirineo Oriental). In: Arnáez, J., González Sampériz, P., Lasanta, T., Valero Garcés, B. (Eds.), Geoecología, cambio ambiental y paisaje: Homenaje al Professor José María García Ruiz, Instituto Pirenaico de Ecología (CSIC) y Universidad de La Rioja, pp. 183-193.

Conferences

Roig-Planasdemunt M., Llorens P., Latron J., (2016) Spatio-temporal variability of shallow groundwater during rainfall-runoff events in a Mediterranean mountain catchment (Vallcebre Research Catchments, Spain). EGU General Assembly. Vienna (Austria). 18/04/16. Poster

Gallart F., Roig-Planasdemunt M., Stewart M., Llorens P., Morgenstern U., Stichler W., Pfister L., Latron J. (2016). Implementing a GLUE-based approach for analysing the uncertainties associated with the modelling of water mean transit times using tritium. EGU General Assembly. Vienna (Austria). 20/04/16. Oral.

Roig-Planasdemunt. M., Llorens. P, Latron. J (2016). Shallow groundwater dynamics during storm events (Vallcebre research catchments). 4th JIPI. Barcelona (España).02/02/2016. Poster

Roig-Planasdemunt M., Gallart F., Stewart M., Llorens P., Morgenstern U., Stichler W., Pfister L. and Latron J. (2015). Mean transit time estimation using tritium in a Mediterranean mountain catchment. 1rst Meeting of young researchers from IDAEA-CSIC. Barcelona (Spain). 22/10/2015. Oral

Roig-Planasdemunt M., Stewart M., Latron J., Llorens P., Morgenstern U. (2015). Transit time estimation using tritium and stable isotopes in a Mediterranean mountain catchment. EGU General Assembly. Vienna (Austria). 14/04/2015. Oral.

Latron J., Roig-Planasdemunt M., Llorens P., Gallart F. (2015). Combining stable isotopes and hydrometric data to investigate the stormflow response of a Mediterranean mountain catchment (Vallcebre Research Catchments, Spain). EGU General Assembly. Vienna (Austria). 13/04/2015. Oral.

Roig-Planasdemunt M, Stewart M., Latron J., Llorens P. (2015). How old is the water in Mediterranean mountain catchment?. 3rd JIPI. Barcelona (Spain). 05/02/2015. Oral.

Roig-Planasdemunt M., Stewart M., Latron J., Llorens P., Morgenstern U. (2014). Transit time determination using tritium at Vallcebre research catchment (NE Spain). Water Symposium. Blenheim (New Zealand). 29/11/2014. Oral.

Latron J., Roig-Planasdemunt M., and Llorens P. (2014). Combining stable isotopes and hydrometric data to investigate the stormflow response of a Mediterranean mountain catchment (Vallcebre Research Catchments, Spain). 15th Biennial Conference ERB 2014. Coimbra (Portugal). 10/09/2014. Oral.

Roig-Planasdemunt M., Llorens P. and Latron J. (2014). Seasonal and storm dynamics of Dissolved Organic Carbon in a Mediterranean mountain catchment (Vallcebre Research Catchments, Spain). 15th Biennial Conference ERB2014. Coimbra (Portugal). 10/09/2014. Poster.

Latron J., Roig-Planasdemunt M. and Llorens P. (2014). Understanding the changing behaviour of a Mediterranean mountain catchment using stable isotopes and hydrometric data. EGU General Assembly. Vienna (Austria). 01/05/2014. Poster.

Roig-Planasdemunt M., Llorens P. and Latron J. (2014). Dissolved Organic Carbon dynamics in a Mediterranean mountain catchment. EGU General Assembly. Vienna (Austria). 29/04/2014. Oral.

Latron J., Llorens P., Garcia-Estringana P., Pérez-Gallego N., Roig-Planasdemunt M. and Gallart F. The "changing hydrology" of Mediterranean mountain areas. EGU General Assembly. Vienna (Austria). 08/04/2013. Oral.

Roig-Planasdemunt M., Latron J. and Llorens P. (2012). Characterization of hydrological processes in a Mediterranean mountain research catchment combining distributed hydrological measurements and environmental tracers. Jornada Instituto de Diagnóstico Ambiental y Estudios del Agua (CSIC). Roquetes (España). 15/05/2012. Oral.

ABOUT THE AUTHOR

Maria Roig Planasdemunt was born the 16th of October 1987 in Barcelona, Spain. She studied Environmental Sciences at the University of Barcelona (2005-2010). During this study she specialized in waste management. Her final graduation project was a research about "the effect of soil on compost". She also obtained an Erasmus scholarship to study Environmental Sciences courses at the University of Copenhagen. Thereafter, she rendered services as an Enviromental consultant in companies and institutions, both public and private (SmaSolucions Medioambientals, EMSHTR-Area Metropolitana de Barcelona, Deplan, etc.).

In September 2010 Maria started working as technician at the Institute of Environmental Sciences and Water Research (IDAEA) of the Spanish National Research Council (CSIC). One year later, she had the opportunity to start a PhD on hydrology named "Characterization of hydrological processes in a Mediterranean mountain research catchment by combining distributed hydrological measurements and environmental tracers", supervised by Dr. Jérôme Latron and Dr. Pilar Llorens Garcia at the Surface Hydrology and Erosion group of IDAEA-CSIC. This PhD was carried out with a FPI scholarship. During the PhD: she studied some Master courses in Environmental Engineering at the Polytechnic University of Catalonia; she carried out field work (hydrometric monitoring and water sampling) in the Vallcebre Research Catchment; and laboratory analyses. In 2012 she obtained a scholarship to stay and collaborate, during three months, with the research group within Environmental Research and Innovation Department (ERIN) at the Luxembourg Institute of Science and Technology. In 2014 she obtained a scholarship to stay and collaborate, during three months, with the Hydrogeology research group at the GNS Science, New Zealand.

Maria published the results of her research in international journals, such as Hydrological Science Journal, Hydrological Processes, etc. She also presented her research at International and national conferences such as the EGU General Assembly, ERB conferences and Water Symposium of Blenheim, etc.